Metallocalix[*n*]arenes in catalysis: a 13-year update

Orlando Santoro and Carl Redshaw*

Plastics Collaboratory, Department of Chemistry, The University of Hull, Cottingham Rd, Hull, HU6 7RX, U.K.

* C.Redshaw@hull.ac.uk

Abstract: Aside from their applications in the fields of ion extraction, gas storage and molecular sensors, calixarenes have been extensively employed as ligands for metal complexation. Moreover, metallocalix[*n*]arenes have shown interesting catalytic activity in a plethora of reactions proving, in many cases, superior to other systems bearing different ligand scaffolds. In this review, we summarize the latest advances (post-2008) in the field, categorizing the complexes by metal center.

Keywords: Calixarene, catalyst, metal, activity, structure.

1. Introduction

During the past three decades, calixarenes have emerged as an important class of molecules, having a plethora of applications such as molecular sensors [1], selective ion extraction [2] and gas storage systems [3]. Moreover, these molecules have been extensively used as ligands for metal complexes [4-12]. The interest in the use of these ligands is justified by the ready availability of the parent calix[*n*]arene (n = 4, 6 or 8) and on their tremendous tunability (Figure 1); the odd numbered calix[*n*]arenes (n = 5, 7 or 9) are far less accessible [13]. In fact, both the upper and lower rims can be readily functionalized allowing for a virtually infinite number of structures.

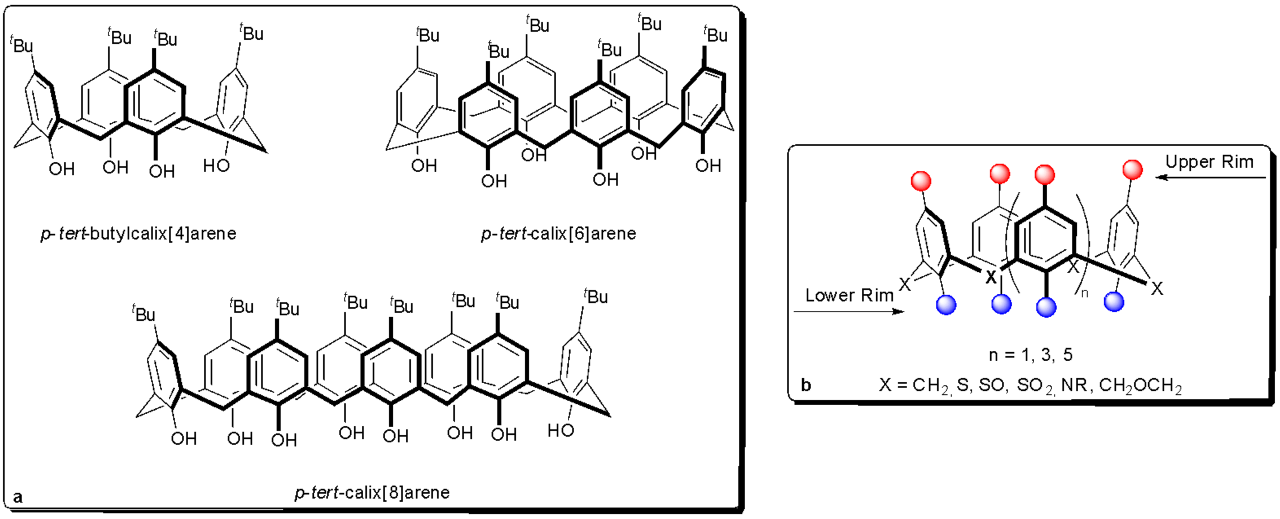

Figure 1. (a) Readily available calix[*n*]arene (n = 4, 6, 8) precursors; (b) Sites of the calixarene scaffold available for modification.

Remarkably, metal complexes of calix[*n*]arene have been widely employed as catalysts in numerous chemical transformations, and such applications prior to 2007 have been comprehensively reviewed [14]. With this review, we intend to provide a 13-year update on the use of metallocalix[*n*]arenes in catalysis, presenting the material by categorizing *via* the catalytic metal center employed. As highlighted in Chart 1, most of the research is focused on Ti-, Rh- and Pd-based catalyst systems. However, complexes of other early- and late transition metals, as well as main-group elements have been employed, albeit less extensively.

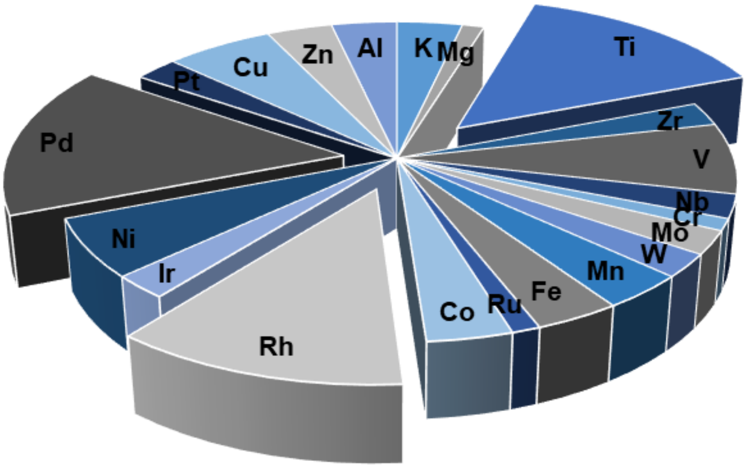

Chart 1. Breakdown of the metals employed in the metallocalix[*n*]arene-catalyzed reactions described in this review.

2. Alkali Metals

2.1 Lithium

2.1.1 Ring Opening Polymerization of Cyclic Esters

Very recently, our group disclosed the synthesis and structural characterization of lithiated calix[4]arenes with different bridging units, namely -CH_2-, -S-, -SO-, -SO_2- or -CH_2OCH_2- and various lower/upper rim substituents [15]. These species were tested as catalysts in the Ring Opening Polymerization (ROP) of several cyclic esters, namely ε-caprolactone (ε-CL), δ-valerolactone (δ-VL) and *rac*-lactide (*r*-LA), under solvent-free conditions. In all cases, the dimethyleneoxa-bridged derivative outperformed the other systems, allowing for complete monomer conversion (100 equiv. with respect to the Li center) within minutes at 130 °C with moderate control. In fact, the M_w/M_n span from 1.6 to 1.8, suggesting the occurrence of transesterification, allegedly due to the forcing reaction conditions employed. The detected M_n values were generally higher than the calculated ones (*i.e.* 27 *vs* 11 kDa for *poly*-caprolactone), suggesting a concentration of active species lower than expected [16]. The higher activity of the dimethylenoxy-bridged catalyst was thought to be due to the higher flexibility of the -CH_2OCH_2- bridge allowing better access to the metal center(s) and/or to stabilizing effects excreted by the oxygen atoms of said bridge.

Concomitantly, we have also explored the use of larger calix[*n*]arenes (n = 6, 8) [17]. The interaction of these pre-ligands with different metal sources, namely LiO*t*Bu and $LiOH{\cdot}H_2O$, led to the isolation of a series of novel multi-nuclear Li complexes. Interestingly, one structure featured a carbonate unit, allegedly derived from the adventitious incorporation of atmospheric CO_2, as previously observed in metal-phenolate chemistry [18]. These complexes were tested in the ROP of ε-CL, δ-VL and *r*-LA, with monomer:Li ratios as high as 1000. Regardless of the monomer, the best performances were achieved in the presence of a mixed lithium/aluminium complex of p-*tert*-butylcalix[8]arene. Moderate to good conversions were obtained after 8-24 hours, affording low molecular weight products (5-10 kDa) with good control (M_w/M_n spanning from 1.09 to 1.82). In the case of *r*-LA, all catalysts produced heterotactic polymers ($0.45 < P_r < 0.46$).

2.2 Potassium

2.2.1 Synthesis of O,O-dialkyl-Se-aryl phosphoroselenoates

Recently, Qiu *et al* reported the synthesis of *O*,*O*-dialkyl-Se-aryl phosphoroselenoates catalyzed by KOH assisted by the calix[4]arene derivative **1** (Scheme 1) [19]. By reacting diphenyl diselenide with different dialkylphosphonates, a slight drop of conversion was observed upon increasing the size of the R-group. A similar trend was obtained when using Me- and Cl-*para* substituted diaryl diselenides. Interestingly, the calixarene could be recovered and reused up to 5 times without any significant loss of activity.

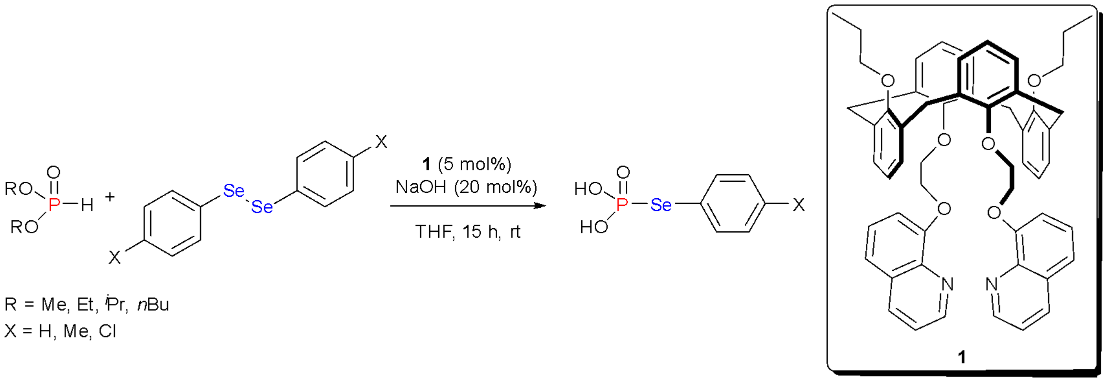

Scheme 1. KOH/calix[4]arene catalyzed synthesis of *O*,*O*-dialkyl-Se-aryl phosphoroselenoates [19].

Eventually, ^{1}H NMR spectroscopy experiments suggested that the catalytically active species could be an *in-situ* generated potassium complex of type **2** (Figure 2).

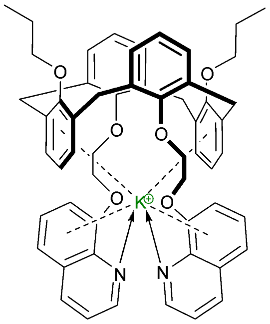

2

Figure 2. Plausible active species for the catalytic synthesis of *O*,*O*-dialkyl-Se-aryl phosphoroselenoates [19].

2.2.2 Ring Opening Polymerization of Cyclic Esters

In 2016, Li *et al* synthesized and fully characterized four novel K-calix[4]arene complexes (**3**-**6**, Figure 3) [20]. Furthermore, the activity of these compounds as promoters in the ROP of *rac*-lactide (*r*-LA) was investigated (Table 1).

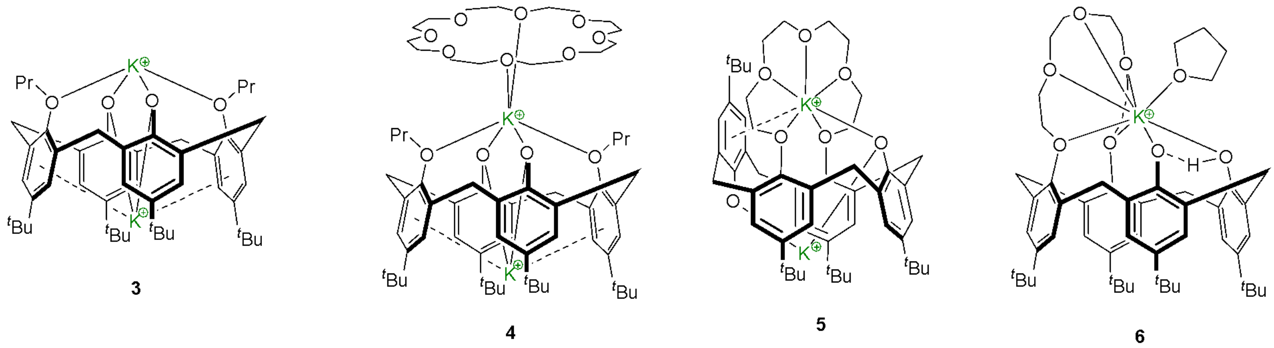

3 **4** **5** **6**

Figure 3. Calix[4]arene potassium complexes **3**-**6** [20].

Almost complete monomer conversion was achieved within 4 minutes by using complex **3** in combination with BnOH as co-initiator. The polymer molecular weight was found to be close to the calculated value, albeit with broad polydispersity (run 1). This was attributed to the possible formation of multiple active species. In fact, complex **3** was shown to form aggregates in solution. A similar outcome was obtained when using complex **4** under the same reaction conditions and with the same LA:cat:BnOH ratios of 200:1:2, albeit with better control (run 2). Interestingly, by using only 1 equivalent of BnOH, the resulting polymer M_n was found to be significantly lower than the calculated value (run 3). This was attributed to the occurrence of cyclization side-reactions. However, this phenomenon could be suppressed by introducing a higher amount of co-activator (2 and 5 equiv., runs 4 and 5, respectively). By performing a "second feed" experiment (run 6), a polymer with M_n close to the calculated value was obtained, suggesting that the polymerization might proceed in an *immortal* fashion. The complexes bearing calix[4]arene with a fused crown ether moiety, namely **5** and **6**, were next investigated. By using **5** in the presence of LA:cat:BnOH in the ratio 200:1:2, 89% conversion was achieved after 5.5 h (run 7). The polymer M_n was found to be *ca*. half of the theoretical value, suggesting the occurrence of undesired side-reactions. Also, in this case, these were suppressed by using a higher amount of BnOH (10 equiv., runs 8-10). Under the optimized reaction conditions (LA:cat:BnOH ratio 200:1:2), low activity was exhibited by complex **6**. In fact, 89% conversion was obtained after 4.5 h. (run 11). This was attributed to the presence of intramolecular hydrogen bonding partially inhibiting the activation of the complex with BnOH. The isotactic bias was determined by analysis of all of the tetrad signals in the methine region of the homonuclear-decoupled ^{1}H NMR spectrum. In all cases, moderate isoselectivity ($0.5 < P_m < 0.6$) was observed.

Table 1. ROP of *rac*-lactide (*r*-LA) catalyzed by **3-6** [20].

Run	**Catalyst**	**$[LA]_0/[Cat]_0/[BnOH]_0$**	**t** (min)	**Conv.** (%)^a	**$M_{n(obs)}$**^{b,c} (Da)	**$M_{n(calc)}$**^{d} (Da)	**M_w/M_n**^{b}	**P_m**^{e}	**TOF** (s^{-1})
1	**3**	200:1:2	4	95	13,400	13,800	1.42	0.60	0.79
2	**4**	200:1:2	3	93	13,400	13,500	1.21	0.63	1.03
3	**4**	200:1:1	5	95	16,200	27,400	1.26	0.65	0.63
4	**4**	500:1:2	4	95	30,100	34,300	1.19	0.65	1.98
5	**4**	500:1:5	3	96	12,600	14,000	1.32	0.65	2.67
6	**4**	200(200):1:2	3(3)	96	25,400	27,800	1.22	0.65	1.07
7	**5**	200:1:2	330	89	6,200	12,900	1.17	0.52	0.01
8	**5**	200:1:10	10	98	2,700	2,900	1.08	0.60	0.33
9	**5**	400:1:10	24	96	5,400	5,600	1.07	0.62	0.27
10	**5**	1000:1:10	240	98	14,300	14,200	1.20	0.59	0.07
11	**6**	200:1:10	270	89	2,800	2,700	1.06	0.60	0.01

Reaction conditions: $[cat]_0$ = 2 mM, toluene 5 mL, rt. ^{a} Determined by ^{1}H NMR spectroscopy. ^{b} From GPC. ^{c} Values corrected using the Mark-Houwink factor of 0.58 from PS standards in THF. ^{d} Calculated from $M_{w(LA)} \times [LA]_0/[BnOH]_0 \times$ conversion $+ M_{W(BnOH)}$. ^{e} Isotactic bias; determined by analysis of all of the tetrad signals in the methine region of the homonuclear-decoupled ^{1}H NMR spectrum.

Very recently, a fused crown-5-calix[4]arenes was shown to be an efficient promoters of nucleophilic fluorination using KF [21]. However, a stoichiometric amount of the compound is required in order to achieve complete substrate conversion.

3. Alkaline Earth Metals

3.1 Magnesium

3.1.1 Ring Opening Polymerization of Cyclic Esters

In 2014, our group disclosed the synthesis of the Mg-calix[4]arene complexes **7** and **8** (Scheme 2) [22]. The heterobimetallic Li/Mg compound was obtained by treating the corresponding 1,3-substituted calix[4]arene precursor with *n*BuLi and further reaction with *n*BuMgBr, while its monometallic congener was synthesized upon reacting the tri-substituted calixarene pre-ligand with $n\text{Bu}_2\text{Mg}$.

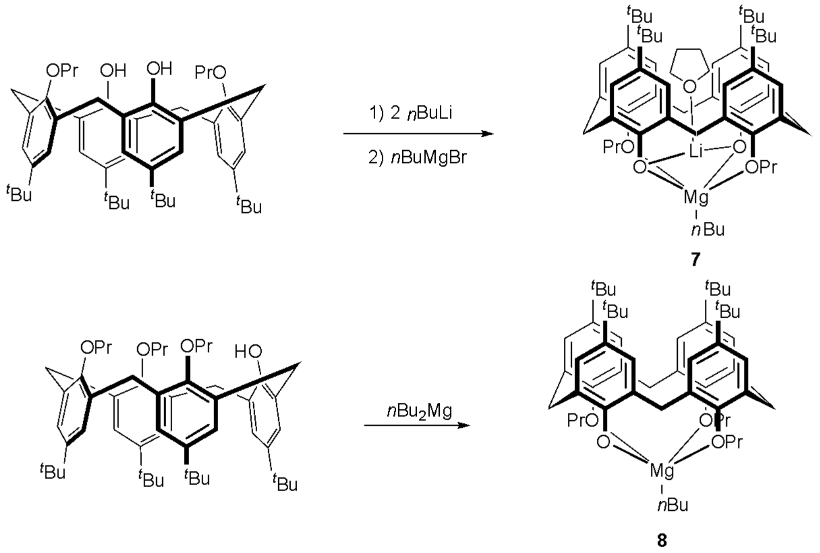

Scheme 2. Synthesis of Mg-calix[4]arene complexes **7** and **8** [22].

Both complexes were tested as catalysts in the ROP of *r*-LA (Table 2). Complex **7**, in combination with an equimolar amount of MeOH, proved poorly active in toluene and THF (runs 1 and 2, respectively). Higher conversion (55%) was achieved in CH_2Cl_2 in 60 minutes (run 3), affording a polymer with M_n higher than the expected value. This was attributed to the degradation of the Mg-butyl species in CH_2Cl_2 generating MgCl- moieties incapable of ROP, leading to a higher than expected LA:Mg ratio. However, the catalyst deactivation in the chlorinated solvent could be overcome by using a greater amount of MeOH (4 equiv., run 4). Notably, only 9% conversion was achieved upon replacing MeOH with BnOH (run 5). In all cases, the polymerization was rather well controlled, with polydispersity values spanning from 1.09 to 1.22. Complex **8** was found to be more active in toluene than in CH_2Cl_2 or THF (*cf.* runs 6-7 with 8). Unlike its bimetallic counterpart, **8** proved to be better performing in combination with BnOH instead of MeOH. Indeed, while only 61% conversion was observed after 2 h in toluene in the presence of MeOH, almost full monomer consumption was achieved in 5 minutes by using BnOH under the same reaction conditions (runs 8 and 9, respectively). The use of additional benzyl alcohol acted as chain transfer agent to control the resultant chain length and gave the catalytic system an *immortal character* (runs 10 and 11) [16]. Compared to the catalyst **7**, lower control was achieved with **8**, with polydispersities spanning from 1.44 to 1.98, depending on the reaction conditions.

Table 2. ROP of *r*-LA catalyzed by complexes **7** and **8** [22].

Run	Cat.	Solvent	LA:ROH	t	Conv.	$M_{n(obs)}^{b,c}$	$M_{n(calc)}^{d}$	M_w/M_n^{b}	P_r^{e}	TOF

				(min)	(%)	(kDa)	(kDa)			(s^{-1})
1	**7**	Toluene	100:1 (MeOH)	60	9.4	-	-	-	-	-
2	**7**	THF	100:1 (MeOH)	60	35	2.33	5.08	1.09	-	-
3	**7**	CH_2Cl_2	100:1 (MeOH)	60	55	15.4	7.96	1.22	-	-
4	**7**	CH_2Cl_2	100:4 (MeOH)	120	94	1.79	3.40	1.19	0.42	-
5	**7**	CH_2Cl_2	100:1 (BnOH)	60	8.8	-	-	-	-	-
6	**8**	CH_2Cl_2	100:1 (MeOH)	120	55	15.5	7.96	1.12	0.49	-
7	**8**	THF	100:1 (MeOH)	120	65	12.4	9.40	1.44	0.73	-
8	**8**	Toluene	100:1 (MeOH)	120	61	11.7	8.82	1.98	0.30	-
9	**8**	Toluene	100:1 (BnOH)	5	94	10.5	13.5	1.54	0.35	0.31
10	**8**	Toluene	100:2 (BnOH)	5	99	6.17	7.20	1.54	0.35	0.33
11	**8**	Toluene	100:4 (BnOH)	5	99	3.57	2.82	1.50	0.36	0.33

Reaction conditions: Polymerization performed by using 60 μM of catalyst at 20 °C, [LA] = 0.6 M, 10 mL of solvent, ROH taken from a ROH/Toluene solution. [a] Determined by ^1H NMR spectroscopy. [b] From GPC. [c] Values corrected using the Mark-Houwink factor of 0.58 from PS standards in THF. [d] Calculated from $M_{w(LA)} \times [LA]_0/[BnOH]_0 \times$ conversion + $M_{W(BnOH)}$. [e] Syndiotactic bias; determined by 2D J-resolved ^1H NMR spectroscopy.

The syndiotactic bias (P_r) was determined by 2D J-resolved ^1H NMR spectroscopy [23]. Both catalysts afforded atactic polymers when CH_2Cl_2 was used (P_r 0.42-0.49, runs 4 and 6 for **7** and **8**, respectively). Interestingly, complex **8** displayed either *iso*- or *heteroatactive* selectivity depending on the solvent. Indeed, while an heteroatactive polymer was isolated by performing the reaction in THF (P_r = 0.73, run 7), syndiotactic PLAs were obtained upon using toluene (P_r 0.30-0.36, runs 8-11) [24].

4. Early Transition Metals

4.1 Titanium

The topics of sections *4.1.1* and *4.1.2* will only be briefly discussed, since they have been extensively treated in a recent review [25].

4.1.1. Ethylene Polymerization

Based on the seminal works of Ladipo [26] and Frediani [27], in 2010 Taoufik, Bonnamour *et al* studied the efficiency of the titanocalix[4]arene complexes **9-16** (Figure 4) in the polymerization of ethylene [28]. Complexes **9-12**, activated by MAO, exhibited rather low productivity (14-21 kg_{PE}. mol_{cat}^{-1} h^{-1}) regardless of the size of the 1,3-dialkyloxy R groups (methyl, ethyl, *n*-propyl and *i*-butyl). Catalysts based on 1,2- and 1,3-depleted calix[4]arenes, obtained from the corresponding proximal- and distal diethyl phosphate precursors by reductive cleavage of the phosphate groups with K/NH_3, were also investigated. Under the same reaction conditions, higher activities were observed by using the 1,3-depleted complex **13** (185 kg_{PE}. mol_{cat}^{-1} h^{-1}) and the 1,2-*O*-substituted compounds **15** and **16** (83 and 113 kg_{PE}. mol_{cat}^{-1} h^{-1}, respectively). All catalysts were outperformed by the 1,2-depleted complex **14** (productivity 350 kg_{PE}. mol_{cat}^{-1} h^{-1}). This data suggested that in both proximal and distal titanocalix[4]arene complexes increasing the number of ether oxygens bound to the Ti center has a detrimental effect on the productivity of the polymerization. Notably, the samples isolated with complexes **9-12** had M_w values consistent with Ultra High Molecular Weight (UHMW) PE (2.3 – 3.2 $\times 10^6$ g mol^{-1}).

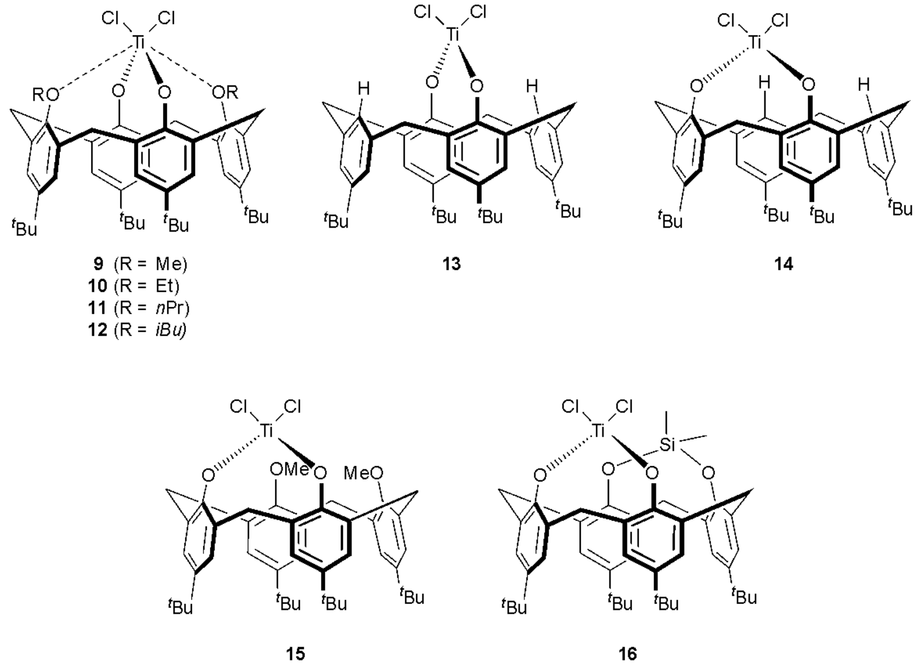

9 (R = Me)
10 (R = Et)
11 (R = *n*Pr)
12 (R = *iBu)*

13

14

15

16

Figure 4. Titanocalix[4]arene pre-catalysts used in the polymerization of ethylene [28].

In 2009, Capacchione *et al. s*tudied the efficiency of the Ti-thiacalix[4]arene complexes **17** and **18** (Figure 5), activated by MAO, as catalysts for ethylene polymerization [29]. Both complexes exhibited maximum activity at 25 °C, while significantly lower productivities were achieved by performing the reaction either at 0 or 50 °C. This was explained assuming incomplete catalyst activation and its partial decomposition at low and high temperature, respectively. The 1,2-alternate complex **18** was shown to be less active than its cone analogue, possibly due to the *t*Bu groups inhibiting the insertion of the monomer. In all cases, highly linear PEs were obtained, as observed by ^{13}C NMR spectroscopy.

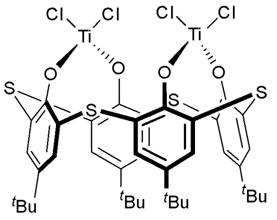

17

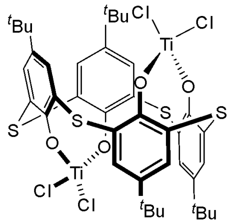

18

Figure 5. Titanium-thiacalix[4]arene pre-catalysts used for ethylene polymerization [29].

4.1.2. Ring Opening Polymerization of Cyclic Esters

The first report concerning the use of titanocalixarene complexes in the ROP of cyclic esters dates back to 2008, when Frediani, Sémeril *et al.* tested the efficiency of complex **19** (Figure 6) as catalyst for the ROP of *L*-lactide (*L*-LA) [30]. The catalyst proved to be active in the absence of a co-activator, affording high molecular weight *poly*-lactide (up to 40 kDa) with productivities (*ca.* 90 $kg_{(pol)} \times mol^{-1}{}_{(Ti)} \times h^{-1}$) that are higher than those observed for other Ti-Cl complexes. In spite of the presence of two active sites allowing for undesired intramolecular transesterifications, the polymerization was rather well controlled, with polydispersities spanning from 1.2 to 1.4. Moreover, the use of *n*BuOH as co-activator proved to enhance the catalytic performances of the complex.

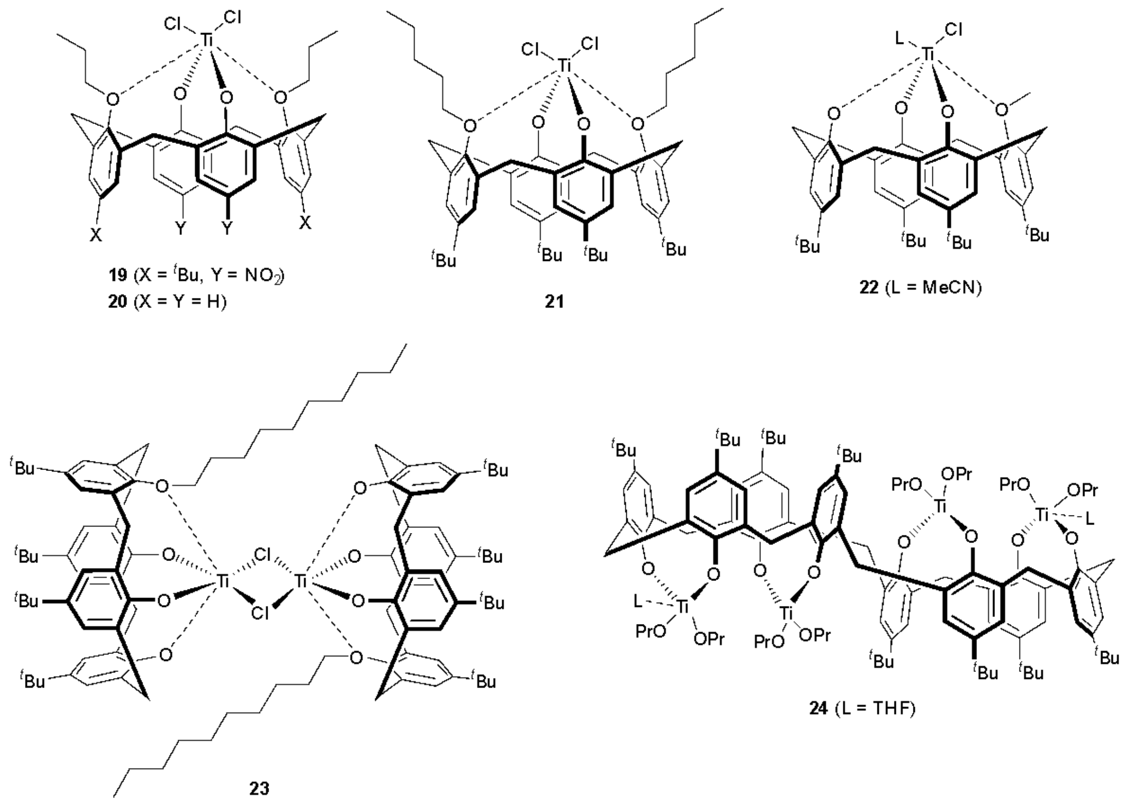

19 (X = ^{t}Bu, Y = NO_2)
20 (X = Y = H)

21

22 (L = MeCN)

23

24 (L = THF)

Figure 6. Titanocalix[4]arenes used in the ROP of cyclic esters [30-34].

Later, the same group reported the use of complex **20** for the ROP of *rac*-lactide (*r*-LA) under both thermal and microwave heating conditions [31]. While the conventional heating allowed for better control of the polymer M_n and molecular weight distribution, the use of microwave irradiation increased the reaction rate. Noteworthy, the polymers exhibited a partial isotactic-stereoblock microstructure, allegedly controlled by a chain-end mechanism.

Very recently, we have disclosed the use of complexes **9**, **11** and **21-23** isolated as MeCN solvates (Figure 6), in combination with BnOH, as catalysts for the ROP of various cyclic esters [32]. In the case of ε-caprolactone (ε-CL), δ-valerolactone (δ-VL) and *rac*-lactide (*r*-LA), the monochloride complex **22** outperformed its dialkoxy congeners, both in terms of activity and polymer M_n. This was thought to be due to the liability of the metal-bound MeCN under ROP conditions. Remarkably, the process could be carried-out in air without significant loss of activity. Amongst all complexes investigated, only compound **22** proved to promote the ROP of the larger monomer ω-pentadecalactone (ω-PDL) [33]. Finally, the activity of this complex in the ROP of several monomers under various reaction conditions were compared to that of benchmark catalysts, such as **19**, $[\mathrm{Ti}(\mathrm{O}i\mathrm{Pr})_4]$ and a dichlorotitanium di-phenolate species. Although **19** outperformed **22** in most of the cases, both complexes resulted to be much more active than the other systems. This suggested that the presence of a calixarene scaffold has a positive effect on the catalytic activity of the complexes.

With respect to Ti-based complexes supported by larger calix[*n*]arene ligands, complex **24** (Figure 6), bearing a *p*-*tert*-butylcalix[8]arene scaffold was reported by McInstosh *et al.* [34] The compound was tested as catalyst for the ROP of *r*-LA at 130 °C with a LA/Ti ratio of 100:1. Complete monomer conversion was achieved after 16 h, affording *n*PrO-terminated polymers whose molecular weights were lower than the expected values. This suggested the occurrence of undesired intramolecular transesterification processes.

In this field, we have recently synthesized a library of new titanocalix[*n*]arene (n = 6, 8) complexes by treating the corresponding pre-ligand with TiX_4 (X = F, Cl, Br and I) [35]. While bimetallic species were isolated in the case of *p*-*tert*-butylcalix[6]arene, tri- and tetranuclear compounds were synthesized with the larger pre-ligand. Interestingly, the structures of the compounds obtained upon using TiF_4 contained Na- and Ca ions, thought to be derived from the drying agent used for the solvents (Na/benzophenone and CaH_2). In spite of their interesting structural features, these species proved poorly active in the ROP of cyclic esters. In particular, the tetranucluear complexes were found completely inactive, regardless of the halide ancillary ligand, suggesting that for this particular catalyst system, the presence of multiple metal centers might be detrimental for the polymerization process. These tetrametallic species have also been tested in the ring opening co-polymerization of CO_2 and propylene oxide to afford cyclic polycarbonates [36]. Turn Over Numbers spanning from 2 to 6 g/g_{cat} were observed at 90 °C at a CO_2 pressure of 6 MPa after 5 h; the catalyst activity proved dependent on the nature of the halide ligand (Cl > Br > I) present.

Finally, we have recently disclosed the synthesis of rare titanium complexes bearing $–CH_2OCH_2$- and –N(R)-bridged calix[*n*]arenes (n = 4, 6) [37]. In the presence of BnOH as chain transfer, all species proved moderately active in the ROP of ε-CL, δ-VL and *r*-LA at 130 °C over 24 h. Turn over numbers as high as 800 were observed with moderate to good control (M_w/M_n spanning from 1.12 to 1.74), while the M_n were generally lower than the expected values (*i.e.* 10 *vs* 30 kDa, for PCL). A significant drop of activity and better control were observed when the process was carried out in the absence of exogeneous alcohol. In terms of structure/activity relationships, the methyleneoxa-bridged species were found to be more active than the azacalixarene-derivatives; this was accounted to the arrangement of, and the distance between, the Ti centers. The virtual inactivity of the larger calix[6]arene-based complexes was attributed to their poor solubility in the reaction medium. Moreover, Cl- and Br-containing species were more active than their F-bearing congeners, possibly because of the higher liability of the former ancillary ligands.

4.1.3 Olefin epoxidation

Ti-based complexes supported by multidentate ligands have been extensively used as catalysts in the epoxidation of olefins (Scheme 3) [38-41].

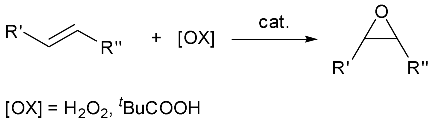

Scheme 3. Metal-catalyzed olefin epoxidation (cat. = [Ti(O*i*Pr)$_4$]) [38].

In this scenario, Vigalok *et al.* recently reported the successful epoxidation of cyclohexene with *tert*-butyl hydroperoxide (TBHP) catalyzed by two novel *N*,*O*-type calixarene Ti complexes **25** and **26** (Figure 7) [42].

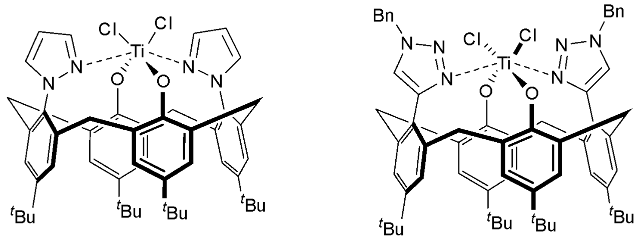

25 **26**

Figure 7. Ti complexes bearing *N*,*O*-type calixarene ligands used in the cyclohexene epoxidation [42].

Both complexes proved to be active in CH_2Cl_2 at room temperature with a 1 mol% catalyst loading. However, while the substrate was completely converted into cyclohexene oxide (CHO) in the presence of **25** after 7 h, only 45% conversion was observed upon using its triazole-analogue. Interestingly, under the same reaction conditions, complex **22** was found to be even less active (27% conversion).

In the field of heterogeneous catalysis, Katz *et al* reported moderate activity for the supported version of complex **22** in the epoxidation of cyclohexene with hydrogen peroxide [43]. In fact, only

33 and 42% conversion was achieved after 6 h at 45 and 65 °C, respectively. Later, the same group disclosed the impact of the nature of the support on the activity of the catalyst. Indeed, complex **22** was grafted on crystalline- and amorphous silicates and the obtained catalysts were tested in the cyclohexene epoxidation with TBHP [44]. Interestingly, the compound bearing a crystalline support proved to be 5 times more active than its amorphous counterpart. Such a difference was explained by considering the differences in the proximal organization of surface silanol groups and their framework location relative to the active centers [45]. Finally, silica supporter tetrameric titanocalix[4]arene complexes **27** and **28** (Figure 8) were employed in the epoxidation of 1-octene [46]. Complex **28** and the supported version of **22** were found to be equally performing, with TOFs of 9 and 45 h^{-1} at 50 and 80 °C, respectively. On the other hand, complex **27**, bearing a shorter alkyl chain (X = 5) was more reactive, allowing for TOFs of 12 and 50 h^{-1} at 50 and 80 °C, respectively. The enhanced reactivity of **27** over **28** and **22** was explained considering a high site density due to the short branching chain. Such site density was thought to be responsible for a microsolvation environment favorable for catalysis.

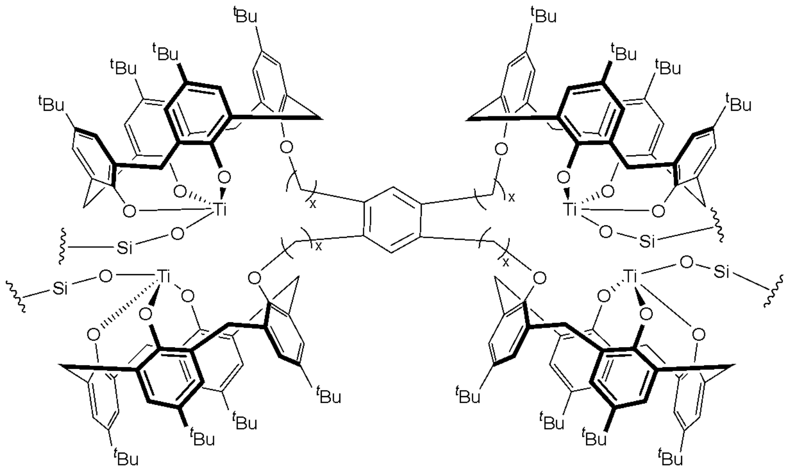

27 (X= 5)
28 (X=10)

Figure 8. Silica supporter tetrameric titanocalix[4]arene complexes [46].

4.1.4 Photocatalytic reactions

Very recently, Ti_4 and Ti_6 clusters based on thiacalix[4]arene scaffolds have been tested in the visible-light photocatalytic production of hydrogen [47]. The water splitting experiments were carried out in the presence of triethanolamine (TEOA) as sacrificial electron-donor with wavelengths higher than 420 nm. Although the two species exhibited similar light absorption properties, the Ti_4 cluster proved *ca*. 5 time more efficient than its hexanuclear analogue, generating 365.3 and 65.4 μmol/g of gas, respectively, after 5 h under similar reaction conditions.

Finally, polyoxotitanate clusters bearing calix[8]arene scaffolds have been recently disclosed by Yi, Liu *et al*. [48, 49]. These species displayed remarkable H_2 evolution ability, with the highest rate being 415.11 μmol/h/g. Related compounds proved really active in the photocatalytic conversion of CO_2 to HCOO- in water and in the presence of sacrificial triethanolamine (TEOA) [50].

4.2 Zirconium

4.2.1 Ring Opening Polymerization of Cyclic Esters

Reports concerning the use of Zr complexes bearing calixarenes are scant. In 2018, Bounerba, Talotta *et al* reported the synthesis of the dinuclear 1,5-*m*-xylene-diyl-bridged calix[8]arene zirconium complex **29** (Figure 9) [51]. The compound was tested as catalyst in the ROP of *r*-LA, ε-CL and β-butyrolactone (β-BL). With respect to *r*-LA, the catalyst activity proved to increase with the temperature, allowing for complete monomer conversion in 30 minutes at 100 °C with a LA/catalyst ratio of 100:1. The polymer M_n were found to be lower than the calculated values, suggesting the occurrence of transesterification reactions. In spite of that, the polymerization was rather controlled (M_w/M_n 1.1 – 1-3). MALDI-TOF analysis of the polymers showed confirmed the presence of cyclic and liner species in a 7:3 ratio. Moreover, the average monomer lenght was found to be 7 and 7.5 for the cyclic and the linear compounds, respectively. The preference towards generating macrolactones was thought to be due to cooperative effects between the two Zr centres. In order to corroborate this assumption, a mononuclear Zr species (**30**, Figure 9) mimicking the sectioned half complex **29** was synthesized and tested in the ROP of *r*-LA. As expected, linear polymers were predominantly obtained (cyclic/ liner ratio 3:97), as observed by MALDI-TOF. Computational studies also confirmed the occurrence of cooperative effects of the two metal centres favouring the backbiting of the growing polymer chain leading to macrolactones. Also in the case of ε-CL and β-BL, cyclic species were isolated upon using **29**.

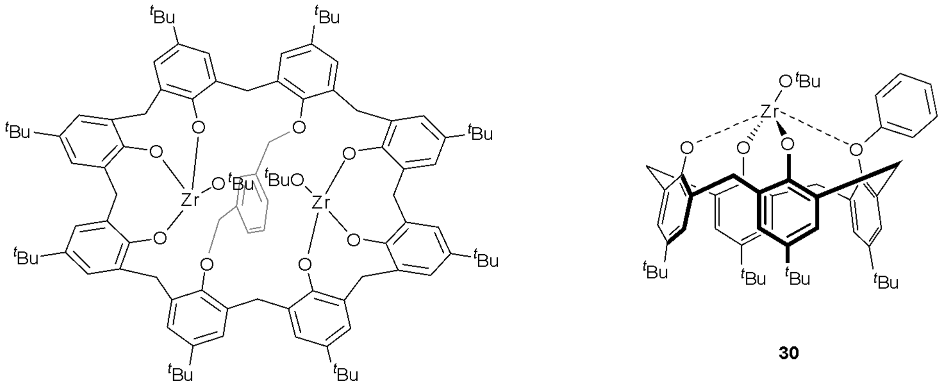

29

30

Figure 9. Di- and mononuclear calix[*n*]arene (n = 8, 4) Zr complexes used in the ROP of lactones [51].

4.2.2 Alkene Epoxidation

In terms of heterogeneous catalysts, silica supported Zr-calixarene complexes have been employed in the epoxidation of cyclohexene to cyclohexene oxide (CHO) with H_2O_2 [43]. Moderate conversion (33%) was observed at 65 °C after 6 h, albeit with good selectivity (74%) towards the epoxide over the other possible oxidation products (diol, enol and enone).

4.3 Vanadium

4.3.1 Olefin polymerization

In 2011, our group studied the behavior the vanadium complexes **31**-**33** bearing sulfur-bridged calix[4]arenes (Figure 10) as catalysts in ethylene polymerization [52]. All catalysts were tested in combination of either dimethylaluminium chloride (DMAC) or methylaluminium dichloride (MADC) as co-catalyst and in the presence of ethyl trichloroacetate (ETA) as reactivator (Table 3). For all complexes, optimization of the reaction conditions revealed that the best [Al]/[V] ratio was be of 6,000. In fact, higher or lower ratios led to a decrease of activity. In turn, the catalytic performances proved to improve upon increasing the temperature (*cf.* Run 1 and 3, 6 and 7, 9 and 10 for **31**, **32** and **33**, respectively). Interestingly, the type of co-catalyst dramatically affected the process.

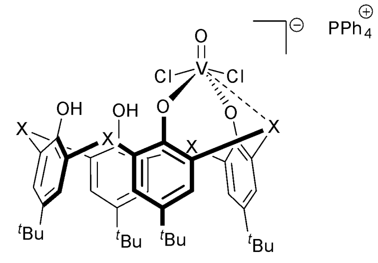

31 (X = S)
32 (X = SO)
33 (X = SO_2)

Figure 10. Vanadium complexes bearing S-containing calix[4]arenes [52].

Table 3. Ethylene polymerization catalyzed by **31**-**33**/Me_nAlCl_{3-n} (n = 1, 2) [52].

Run	Pre-catalyst	Co-catalyst	[Al]/[V]	T (°C)	Activity[a]
1	**31**	DMAC	6,000	20	12.0
2	**31**	MADC	6,000	20	19.2
3	**31**	DADC	6,000	60	13.8
4	**31**	MADC	6,000	60	26.1
5	**32**	DMAC	6,000	20	0.2
6	**32**	MADC	6,000	20	27.5
7	**32**	MADC	6,000	80	37.4
8	**33**	DMAC	6,000	20	20.1
9	**33**	MADC	6,000	20	27.9
10	**33**	MADC	6,000	80	37.4

Reaction conditions: Ethylene 1 bar, toluene (250 mL), 15 min., in the presence of ETA (0.05 mL). [a] g/(mmol.h.bar) (×10^3). DMAC = dimethylaluminium chloride; MADC = methylaluminium dichloride; ETA = ethyl trichloroacetate.

Indeed, **31**-**33** were found to be more active when combined with MADC rather than DMAC. In fact, for **31**, the activity observed upon using MADC was about double the values achieved in the presence of the monochloride congener, regardless of the temperature employed (*cf.* runs 1/2 and 3/4). Remarkably, while **32** was completely inactive in the presence of DMAC, activities of 28 and 37 kg/(mmol h bar) were observed with MADC at 20 and 80 °C, respectively (runs 6 and 7). Finally, **33**/MADC was only moderately more active than the system obtained with the monochloride co-catalyst (runs 8 and 9). The higher efficiency of MADC was explained considering the nature of a catalytically active species featuring multiple V-Al-Cl bridges, as proposed by Gambarotta [53]. The formation of this species would be more readily formed in the presence of multiple chlorides available in MADC compared to DMAC. Overall, the activity trend was found to be **33** > **32** > **31**, suggesting that the presence of oxygen atoms in the calixarene bridge is beneficial. This was confirmed by comparing the performances of **31**-**33** to that of a previously reported V-oxacalix[4]arene complex, namely [V(O)*p*-*tert*-butylhexahomooxacalix[3]arene(O)$_3$] [54], whose activity was shown to be in between those of **33** and **32**. Although the nature of the active species remain unclear, EPR studies performed on similar catalytic systems suggested the involvement of V(IV) intermediates [55].

We also developed a series of vanadium complexes based on depleted 1,3-calix[4]arene ligands (**34**-**47**, Figure 11) [56]. These species, activated by either MADC or DMAC, were tested as catalysts in the polymerization of ethylene. Pre-catalysts **34** and **35** proved equally performing regardless of the co-catalyst employed; in turn, the activity improved upon increasing the temperature, reaching a maximum at 80 °C. Similar results were observed in the presence of the *tert*-butyl derivative **36**, whose thermal stability was lower than its *n*-propyl analogue. In fact, the highest activity was obtained at 40 and 60 °C upon using DMAC and MADC, respectively. The tetrametallic species **37** was also shown to be thermally stable, exhibiting maximum activity at 80 °C. Overall, the activity trends were found to be **37** ≈ **34** > **35** > **36** and **37** > **34** ≈ **35** > **36** with DMAC and MADC, respectively.

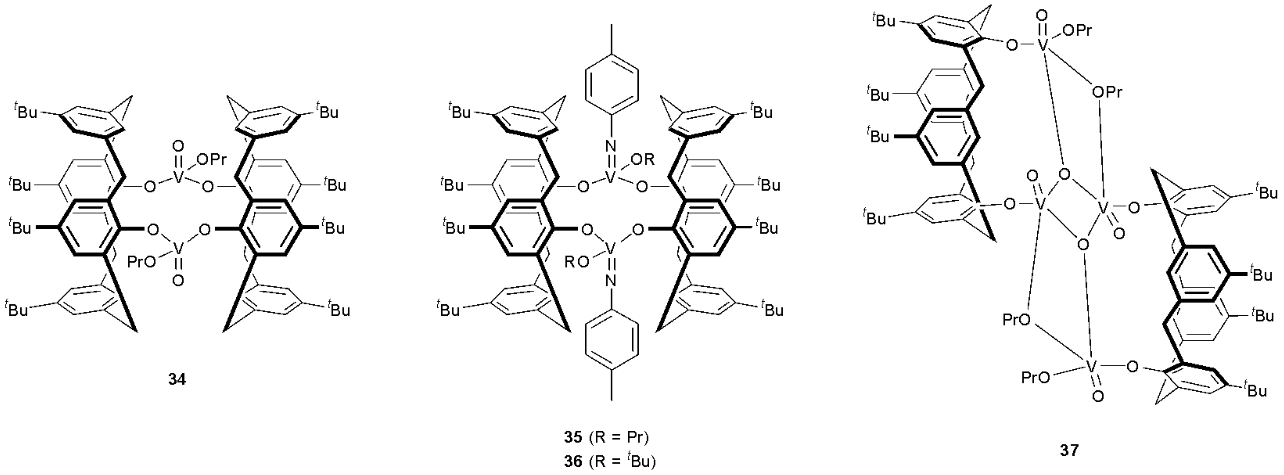

34

35 (R = Pr)
36 (R = ^{t}Bu)

37

Figure 11. Vanadium complexes bearing depleted 1,3-calix[4]arenes [56].

In terms of larger calix[*n*]arene pre-ligands, we have synthesized a set of vanadium complexes (**38**-**40**) by treating *tert*-butyl-calix[8]arene with the heterobimetallic species [MVO(O*t*Bu)$_4$] (M = Na, K) [57]. The molecular structures of such species are shown in Figure 12. When activated by DMAC or MADC in the presence of ETA, high activity (up to 136 Kg(mmol(V) h)$^{-1}$) was exhibited by all complexes, affording high molecular weight liner polymers. Interestingly, **38** proved more active than the benchmark catalyst [VO(OEt)Cl$_2$] under the same reaction conditions. In the case of ethylene/propylene co-polymerization, the propylene incorporation was spanning from 7 to 11%.

Although these values were consistent with that observed in the presence of [$VO(OEt)Cl_2$], the activities of the calixarene-based complexes were somewhat lower.

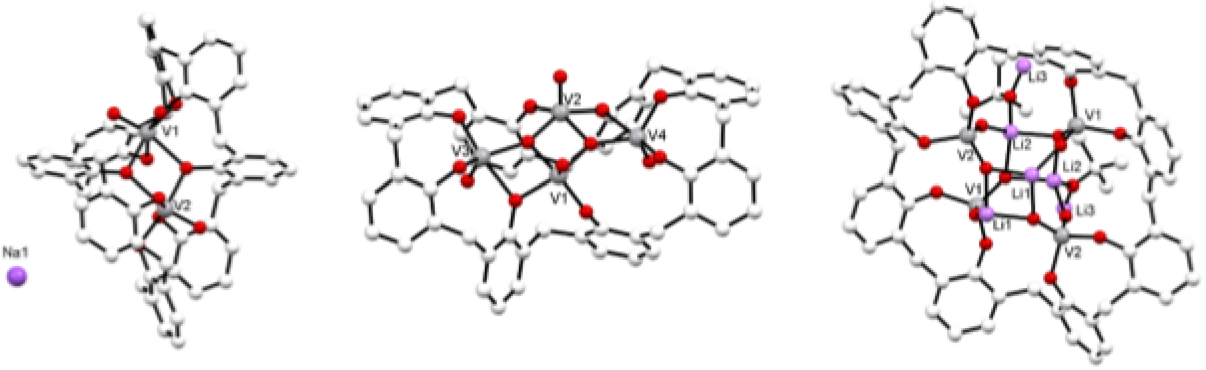

Figure 12. Molecular structures of complexes **38** (left), **39** (center) and **40** (right) [57]. Hydrogen atoms, solvent molecules and *p-tert*-butyl groups omitted for clarity.

Finally, our group recently isolated the vanadium oxacalix[6]arene complexes **41**-**45**, bearing different *para*-substituents at the arylimido moiety [58]. When activated by Me_2AlCl and in the presence of ETA, compound **42** proved almost inactive towards the polymerization of ethylene, whilst the reactivity trend of the other species was found to be **41** ~ **43** > **44** > **45**. Linear PEs were isolated in all cases, with M_n spanning from 74 to 120 kDa and M_w/M_n in the 2.2-2-5 range.

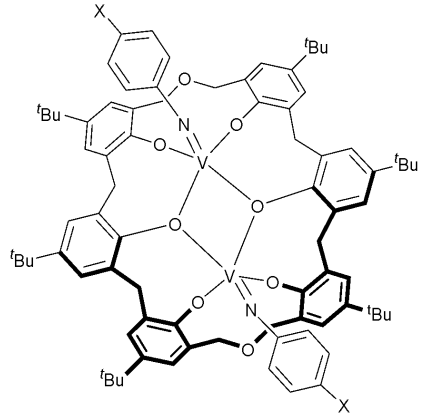

41 (X = Me)
42 (X = OMe)
43 ($X = CF_3$)
44 (X = Cl)
45 (X = F)

Figure 13. Vanadium-oxacalix[6]arene complexes **41-45** [58].

4.3.2 Ring Opening Polymerization of Cyclic Esters

The sulfur-containing V-calixarene complexes **31-33** (Figure 10) were also tested in the ROP of ε-caprolactone [52]. Unfortunately, all complexes were found to be inactive, regardless of the reaction conditions employed (CL:V 400:1; 25−80 °C; 20 mL of toluene; 0 - 5 equiv. of benzyl alcohol). The depleted 1,3-calixarene complexes **34-36** (Figure 11) were also tested [56]. By using a CL/V ratio of 400 and 5 equiv. of BnOH, almost complete monomer conversion (94%) was achieved in the presence of **34** at 80 °C after 72 h. Under the same reaction conditions, lower conversions were obtained with the other two catalysts (46 and 20% for **35** and **36**, respectively). In all cases, PCLs with M_n lower than the expected values were isolated, albeit with good control (polydispersity spanning from 1.1 to 1.3).

The oxacalix[6]arene complexes **41**-**45** (Figure 13) also proved active in the ROP of ε-CL at 130 °C in the absence of a co-activator with monomer:V ratios as high as 500 [58]. After 24 h, almost complete monomer conversion was achieved with all catalysts, following the trend **43** > **44** > **45** > **42** > **41**. Although the Me-substituted compound was the least active of the series, it allowed for better control compared to its congeners. M_n values were significantly lower than the calculated values, suggesting the occurrence of transesterification. Under the same reaction conditions, the ROP of δ-VL was also achieved. While the reactivity trend was similar to that of ε-CL, better control was observed with the Cl-substituted complex **44**. All complexes promoted CL/VL co-polymerization; complex **42** exhibiting a preference towards the incorporation of VL over the other co-monomer, while the opposite was observed with the other catalysts. None of the compounds proved active in the ROP of *r*-LA. Finally, complex **41** was also poorly active in the synthesis of cyclic polycarbonates by the ring opening co-polymerization of CO_2 with propylene oxide [36].

4.3.3 Alkene Epoxidation

Silica supported calix[4]arene vanadium species were also reported to catalyze the oxidation of cyclohexene with H_2O_2 [43]. Both the overall substrate conversion and the selectivity towards the formation of cyclohexene oxide (CHO) over the other oxidation products (diol, enol, enone) decreased upon increasing the temperature. In fact, while 60% conversion and 6% CHO selectivity were achieved at 45 °C, only 40% conversion and <0.1% selectivity were obtained at 65 °C. Polyoxo-vanadium clusters supported by calix[4] have also shown oxygen activation potential [59].

4.4 Niobium

4.4.1 Olefin Epoxidation

Recent reports concerning the use of Nb-calixarene complexes in catalysis are rather scant. In 2015, Thornburg *et al.* investigated the efficiency of Si-supported compounds in the epoxidation of cyclohexene to cyclohexene oxide with H_2O_2 [43]. The catalyst proved very active, allowing for 84 and 78% substrate conversion at 45 a 65 °C, respectively as well as high selectivity towards the epoxide product (up to 97%). Such a result was remarkable, since the Nb-based catalyst proved to be better performing than related group IV metal species (*cf. sections 4.1.1* and 4.2 for Ti- and Zr, respectively). In light of these findings, the same group lately compared the efficiency of the catalysts derived from Nb-calixarene complexes to that of species obtained by direct grafting of commercially available metal precursors, namely $NbCl_5$, $Nb(Cp)Cl_4$, $Nb(DMA)_5$ and $Nb(OEt)_5$ [60]. For each set of catalysts, different specific surface loadings of the metal (spanning from 0.07 to 1.6 Nb groups nm^{-2}) were considered. In all cases, the calixarene derivatives outperformed the other catalysts, regardless of the surface metal density, suggesting that the presence of a bulky calixarene groups allows for a larger fraction of kinetically relevant active sites which dramatically increase the activity of the catalyst.

4.5 Tantalum

4.5.1 Olefin Epoxidation

In 2010, Morlanés and Notestain studied the heterogeneous epoxidation of alkenes (cyclohexene and cyclootene) catalyzed a Ta-calix[4]arene complex [61]. The catalysts were generated by the reaction *p*-*tert*-butylcalix[4]arene with $TaCl_5$ followed by grafting on SiO_2. The further calcination of this compound led to the loss of the organic fragment affording a pure Ta-oxide species. The calixarene-containing catalyst proved more active than its calcinated counterpart in the epoxidation of cyclohexene with H_2O_2 in acetonitrile. In fact, after 2h the TONs were found to be 105 and 83, respectively. Moreover, the calixarene derivative displayed high selectivity towards the desired epoxide than to other side-products (*i.e.* diol), while side reactions took place to a larger extent with the calcinated compound.

Lately, the same group also studied heterogeneous catalysts derived from other calixarene precursors, namely *p*-*tert*-butylthiacalix[4]arene, 1,3-dimethoxy-*p*-*tert*-butylcalix[4]arene and *p*-*tert*-butylcalix[6]arene [62]. Amongst the series, the S-containing species proved the most performing in the epoxidation of cyclohexene and cyclooctene with H_2O_2, while comparable activity was exhibited by the other two species.

4.6 Chromium

4.6.1 Ethylene Polymerization

In 2009, our group synthesized novel Cr(III) complexes bearing *tert*-butylcalix[*n*]arene ligands (n = 4, 6) [63]. The molecular structures of some of these species (**46**-**49**) is shown in figure 14. In spite of their interesting structural features, all complexes were found to be poorly active for ethylene polymerization (Table 4).

Table 4. Ethylene polymerization catalyzed by Cr-calixarene complexes **46-49** [63].

Run	**Catalyst**	**Co-catalyst** ([Al]/[Cr])	Activity (g $mmol^{-1}$ hr^{-1} bar^{-1})
1	**46**	DMAC (400)	1
2	**47**	DMAC (400)	0.2
3	**48**	DMAC (400)	0.3
4	**49**	DMAC (400)	1

Reaction conditions: [Cr] 20 µmol, toluene 40 mL, T = toluene,400 equiv., 60 min.

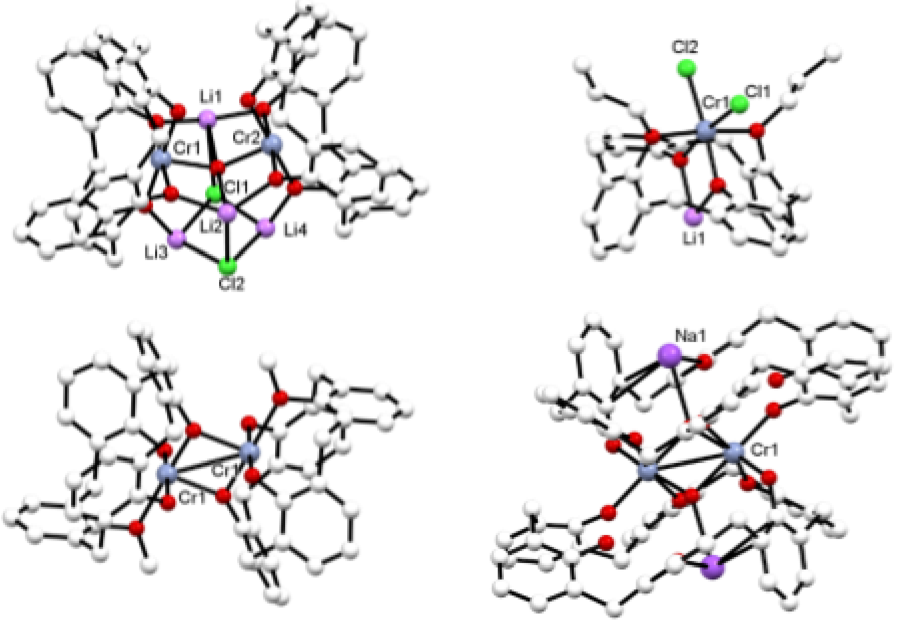

Figure 14. Molecular structure of the Cr-calix[*n*]arene (*n* = 4, 6) complexes **46** (top left), **47** (top right), **48** (bottom left) and **49** (bottom right) [63]. Hydrogen atoms, solvent molecules and *p*-*tert*-butyl groups omitted for clarity.

4.7 Molybdenum

4.7.1 Olefin Epoxidation

A limited number of reports concerning the catalytic applications of Mo-based calixarene complexes are found. In this scenario, the styrene epoxidation with TBHP catalyzed by the Mo(IV) calix[4]arene salt (**50**) was recently disclosed by Acharya and Hanna (Scheme 4) [64]. High substrate conversion (84%) and good selectivity towards the desired 1,2-(epoxyethyl)benzene (49%) were obtained within 8 hours at 80 °C in the presence of 0.5 mol% of catalyst in neat conditions. Interestingly, no reaction occurred upon addition of toluene as solvent. Similarly, the use pyridine to reduce the formation of diol side-product completely inhibited the reaction. The catalyst was also inactive in the epoxidation of other substrates, namely 1-octene, cyclohexene, and 3,3-dimethyl-1-butene.

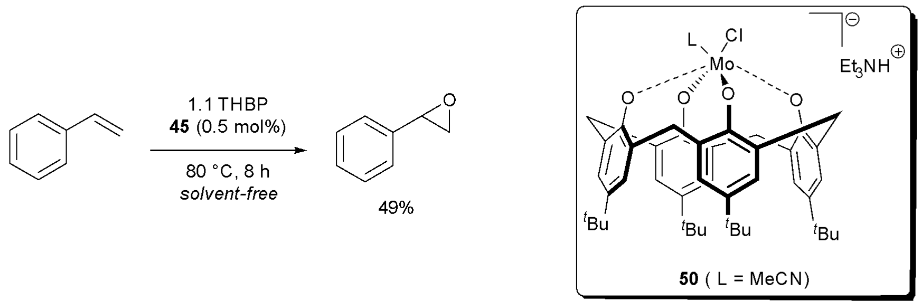

Scheme 4. Styrene epoxidation catalyzed by Mo-based complex **50** [64].

4.7.2 Ring Opening Polymerization of Cyclic Esters

The oxo-molybdenum calix[4]arene complex **51** (Figure 15) was tested as catalyst for ROP of cyclic esters [65]. In the case of ε-CL, complete monomer conversion was observed after 24h at 130 °C with a CL:Mo ratio of 250:1, affording oligomers ($M_n \approx$ 5,000 Da) with good control (M_w/M_n 1.21). Similar results were achieved in the case of δ-VL, albeit with lower conversion (80%). The catalyst was inactive in the ROP of the more challenging monomer ω-pentadecalactone (ω-PDL).

4.8 Tungsten

4.8.1 Ring Opening Polymerization of Cyclic Esters

Tungsten(VI) complexes bearing a *p-tert*-butylcalix[4]arene scaffold (**52-54**, Figure 15) have been recently synthesized by our group and tested in the ROP of ε-CL, δ-VL (Table 5) [65]. The oxo- and dichloride derivatives **52** and **53** allowed for complete conversion of ε-CL in 48 h with a CL:W ratio of 250 at 130 °C (runs 1 and 2). On the other hand, only 40% conversion was achieved in the presence of their alkoxy-congener **53** (run 3). A similar trend was observed in the ROP of δ-VL (runs 4-6).

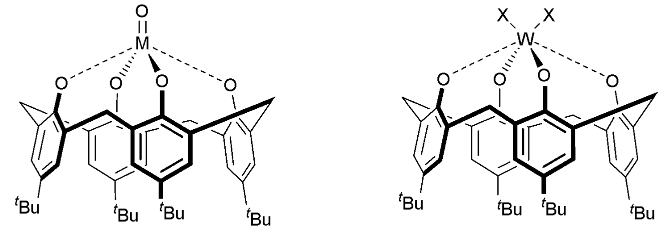

51 (M = Mo)
52 (M = W)

53 (X = Cl)
54 (X = O^{t}Bu)

Figure 15. Mo- and W-calix[4]arene complexes employed in the ROP of cyclic esters [65].

In all cases, the M_n of the polymers were much lower than the expected values. Low control was observed with **53** with both monomers (M_w/M_n 1.6 and 1.7 for PCL and PVL, respectively). Rather broad polydispersity was obtained with δ-VL in the presence of complex **52**. Similar to their Mo-based analogue **51**, none of the catalysts proved active in the ROP of the larger monomer ω-PDL.

Table 5. ROP of cyclic esters catalyzed by W-calixarene complexes **52-54** [65].

Run	**Monomer**	**Catalyst**	**Conversion**[a] (%)	$M_{n(obs.)}$[b, c] (kDa)	$M_{n(calc.)}$[d] (kDa)	M_w/M_n[b]	**TOF** (h^{-1})
1[e]	ε-CL	**52**	95	5.0	23.0	1.10	4.95
2[e]		**53**	99	3.6	28.3	1.61	5.16
3		**54**	40	5.3	11.1	1.10	4.17
4	δ-VL	**52**	98	4.6	24.4	1.56	10.2
5		**53**	83	4.9	20.8	1.73	8.64
6		**54**	46	3.2	11.5	1.15	4.79

Reaction conditions: $[\text{Monomer}]_0:[\text{W}]_0$ = 250, toluene, T = 130 °C, 24 h. [a] Determined by ^{1}H NMR spectroscopy. [b] From GPC. [c] For PCL, the values are corrected using the Mark-Houwink factor of 0.56 from PS standards in THF. [d] Calculated from $M_{w(\text{Monomer})} \times [\text{Monomer}]_0[\text{W}]_0 \times$ conversion. [e] 48 h.

Compounds bearing larger calixarene scaffolds have also been explored. In this scenario, our group reported the synthesis of three ethylene glycol tungsten complexes obtained by treating $[W(eg)_3]$ (eg = 1,2-ethanediolato) with *p*-*tert*-butylcalix[6]arene or *p*-*tert*-butyltetrahomodioxacalix[6]arene (**55**-**57**, Figure 16) [66]. All complexes, activated by BnOH, proved to be active in the ROP of ε-CL at 110 °C with CL:W:BnOH ratio of 400:1:1. High molecular weight and narrow polydispersities were observed in all cases. No beneficial effect deriving from the presence of a dimethyleneoxa ($-CH_2OCH_2-$) bridge in **57** over the methylene ($-CH_2-$) of **55** and **56** was detected. NMR spectroscopic analysis of the polymers revealed the presence of both benzyloxy- and $-CH_2OH$ end-groups, suggesting that the polymerization is initiated by the insertion of a CL moiety into the $W-OCH_2Bn$ group. Interestingly, analogues complexes supported by the larger *p*-*tert*-butylcalix[8]arene were inactive. This was attributed to the increased conformational flexibility of the ligand which somehow inhibits the ROP process.

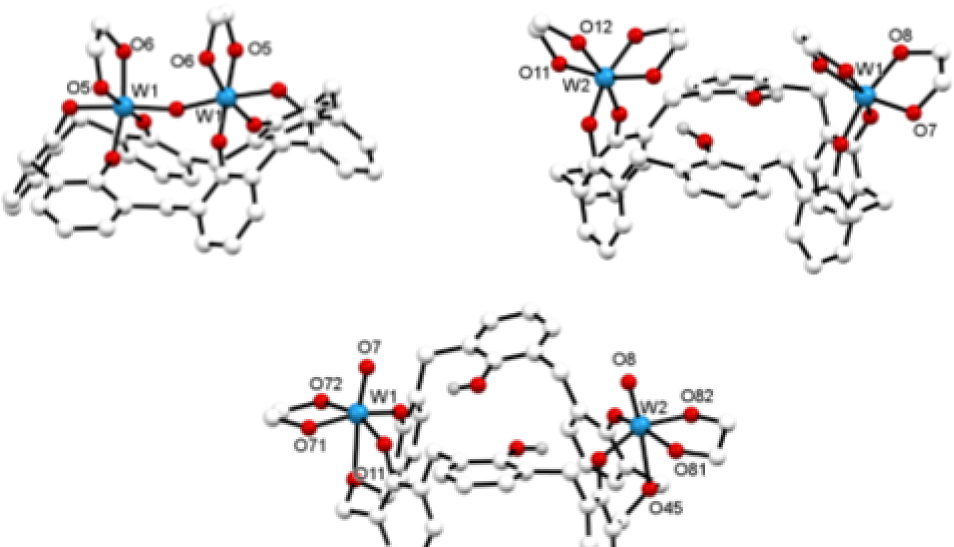

Figure 16. Molecular structure of the W-calix[6]arene complexes **55** (top left), **56** (top right) and **57** (bottom) [66]. Hydrogen atoms, solvent molecules and *p-tert*-butyl groups omitted for clarity.

4.9 Manganese

4.9.1 Olefin Epoxidation

Manganese-calixarene complexes have been reported as efficient catalysts for the epoxidation of alkenes. In this scenario, Lang *et al.* recently isolated a Mn^{III}-superoxo species bearing a zwitterionic calix[4]arene ligand (**58**, Figure 17) [67]. Aside from the interesting structural features, the complex also exhibited high activity in the epoxidation of cyclohexene with O_2/isobutyraldehyde. Indeed, complete conversion of the substrate and 99% selectivity towards the epoxide were achieved in 5 h at 20 °C. The rate increased at higher temperature (40 - 60 °C), albeit with a decrease of selectivity. Isotopic labelling experiments confirmed that the “O” of the superoxo-group was not involved in the reaction and the *external* gaseous oxygen is responsible for the oxidation of the substrate. Remarkably, the catalyst proved efficient also in the selective epoxidation of other cyclic and linear alkenes. Subsequently, Mn^{III} complexes of calix[4]arene-(salen) ligands were isolated by Sciotto, Tomaselli *et al* (**59** and **60**, Figure 17) [68]. These species were employed as catalysts in the enantioselective epoxidation of aryl-(Z)-aryl alkenes with NaClO/4-phenyl-pyridine N-oxide (4-PPNO) system. In all cases, complex **59** was found to be better performing than its larger analogues **60**, both in terms of substrate conversion and enantioselectivity. Finally, Mn^{II} complexes bearing calix[4]arene-Schiff bases scaffolds (**61** and **62**, Figure 17) have been employed in the catalytic epoxidation of cyclohexene and styrene with iodosylbenzene (Table 6) [69].

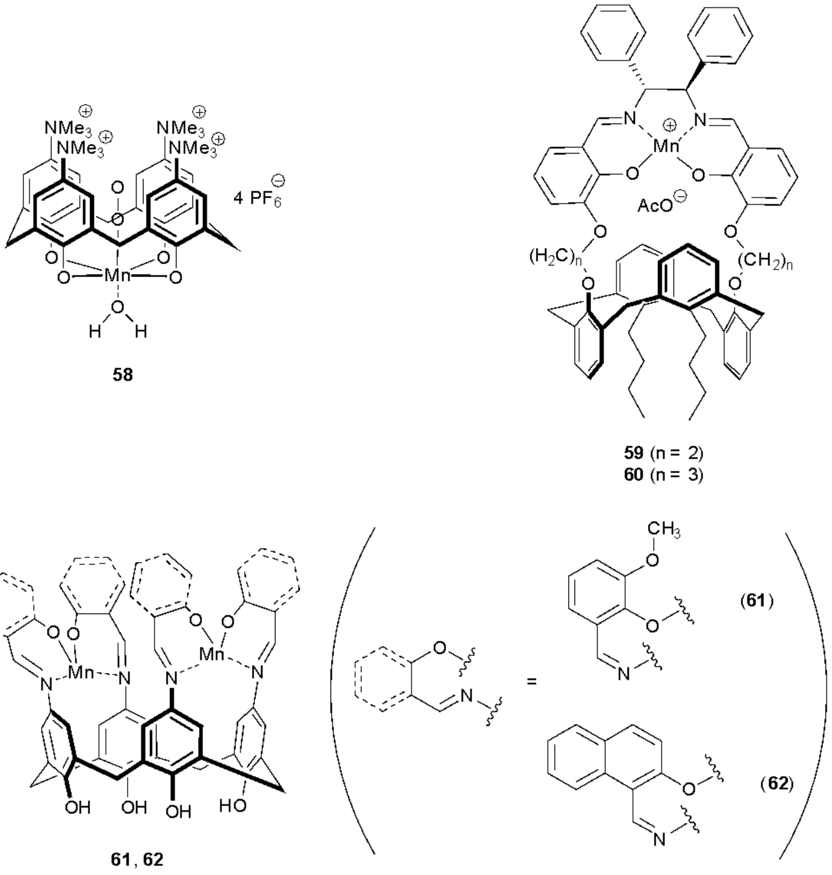

Figure 17. Mn-based calixarene complexes employed in the catalytic epoxidation of alkenes [67-68].

Good conversions were achieved for both substrates; nevertheless, cyclohexane was more reactive than styrene. In turn, complex **61** proved more efficient than its bulkier congener, both in terms of activity and selectivity.

Table 6. Epoxidation of alkenes with iodosylbenzene (PhIO) catalyzed by **61** and **62** [69].

Run	Catalyst	Substrate	Product	Conversion[a]	Yield[b]	Selectivity[c]	TOF[d]
1	**61**	Styrene	Styrene Oxide	78	77	99	0.70
2	**62**			72	71	96	0.73
3	**61**	Cyclohexene	CHO	94	85	90	1.23
4	**62**			88	74	84	0.90

Reaction conditions: [Mn] 0.01 mmol, PhIO 0.1 mmol, Substrate 2.5 mmol, room temperature, 4 h. [a] Determined by GC with internal standard. [b] Epoxide isolated yield. [c] Calculated by the expression [yield (%)/conversion (%)] × 100. [d] Calculated by the expression [product]/[catalyst] × time s^{-1}. CHO = Cyclohexene oxide.

5. Late Transition Metals

5.1 Iron

5.1.1 Ring Opening Polymerization of Cyclic Esters

In 2010, our group disclosed the synthesis of a family of heteromultimetallic Fe(III) complexes obtained by treating the Fe(II) precursors $[MFe(OtBu)_3(THF)]_2$ (M = Na, K) either with: a) conventional methylene-bridge calix[*n*]arenes (n = 4, 6 and 8) or b) the dimethyleneoxa-bridged ($-CH_2OCH_2-$) *p-tert*-butyltetrahomodioxacalix[6]arene and *p-tert*-butylhexahomotrioxacalix[3]arene [70]. In spite of their anionic nature and the presence of alkali metals (favorable in the polymerization process) [71], these complexes proved poorly active in the ROP of ε-CL. In fact, complete monomer conversion was achieved only after 40 h at room temperature with a CL/Fe ratio of 700, in the presence of BnOH as activator. Moreover, the polymer M_n were much lower than the calculated values, suggesting the occurrence of intensive backbiting reactions. Broad polydispersities, spanning from 1.7 to 2.0, were also observed.

5.1.1 Olefin Polymerization

Poor catalytic performances were exhibited by the mixed Fe/Li calix[4]arene compound **63** (Figure 18), recently synthesized by Crochet and Fromm [72]. In fact, the complex proved inactive in the polymerization of styrene and other smaller monomers. This was explained considering the absence of accessible coordination sites for the monomer molecules.

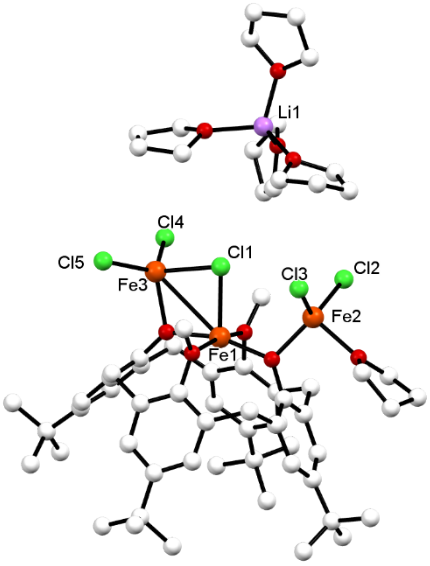

Figure 18. Molecular structure of the mixed Fe/Li calixarene complex **63**. Hydrogen atoms omitted for clarity [72].

5.1.2 Mannich-type reaction

Sayin and Yilmaz recently reported the grafting of calix[4]arene-based Lewis acid-type **64** and **65** onto epoxyl-functionalized silica-coated Fe_3O_4 magnetic nanoparticles, affording their corresponding calixarene-based magnetic nanoparticles **64-Fe/Si** and **65/Si** (Scheme 5) [73]. These compounds, as well as their corresponding calixarene precursors, were employed in the three-component Mannich-type reaction of benzaldehyde, aniline and acetophenone (Table 7).

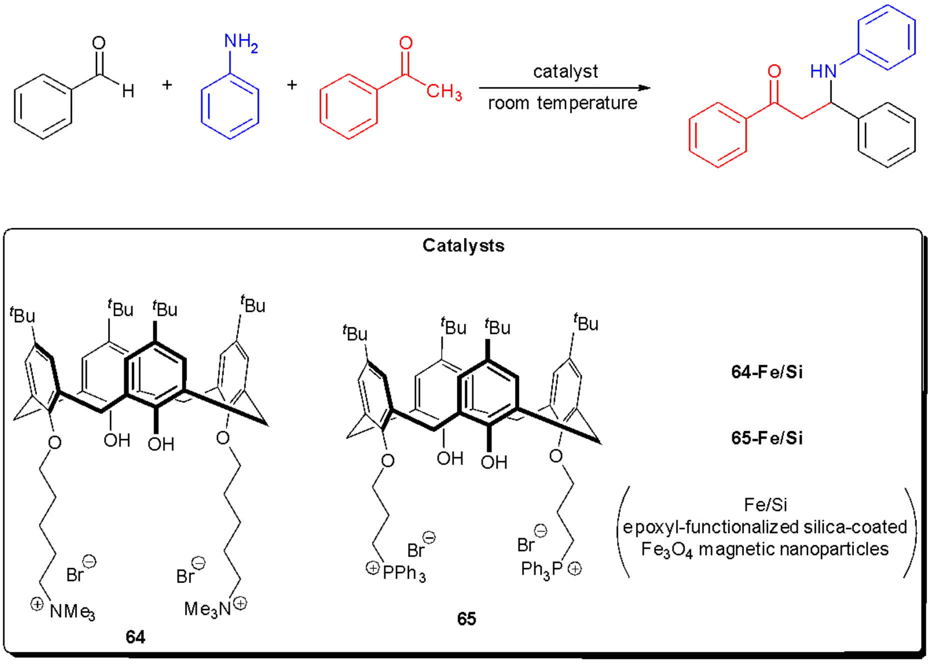

Scheme 5. Three-component Mannich-type reaction catalyzed by Fe/Si-supported calixarenes [73].

The Lewis acidic calixarene precursors were found to promote the reaction at catalyst loadings as low as 2 mol% in 3.5 mL of water (runs 1 and 2). However, compound **64** proved more efficient than **65**, affording the reaction product in higher yield (69 and 43%, respectively). In the presence of the Fe-containing species, excellent yields (>99%) were achieved within 72 h in 1 mL of water (runs 4 and 6). Finally, both catalysts were shown to be reusable up to three times without loss of activity (runs 3 and 5).

Table 7. Fe-calixarene catalyzed Mannich reaction [73].

Run	**Catalyst**	**Catalyst Loading**	**H_2O** (mL)	**Time** (h)	**Isolated Yield** (%)

1	**64**	2 mol%	3.5	6	69[a]
2	**65**	2 mol%	3.5	6	43[a]
3	**64-Fe/Si**	5 mg	1	6	68,[b] 68,[c] 68[d]
4	**64-Fe/Si**	5 mg	1	72	>99[b]
5	**65-Fe/Si**	5 mg	1	6	62,[b] 62,[c] 62[d]
6	**65-Fe/Si**	5 mg	1	72	>99[b]

Reaction conditions: [a] Benzaldehyde (0.23 g, 2.19 mmol), aniline (2.19 mmol), acetophenone (2.19 mmol), NaOH (11 mmol). [b] Benzaldehyde (51 mL, 0.5 mmol), aniline (0.5 mmol), acetophenone (1.0 mmol). [c] Second reuse of the catalyst. [d] Third reuse of the catalyst.

5.2 Ruthenium

5.2.1 Metathesis Reactions

Water soluble calix[*n*]arenes [n = 4, 6, 8] **66-74** (Figure 19) have been used as supramolecular additives in the Ru-catalyzed ring closing metathesis (RCM) cross metathesis (CM) reactions in water [74]. For this purpose, the commercially available Grubbs [75] and Hoveyda [76] catalysts have been employed (Scheme 6). The use of these additives allows one to overcome the main issues of conducing metathesis reaction in aqueous media, namely catalyst decomposition and low substrate solubility. In particular, *p*-sulfonatecalix[*n*]arenes **66-68** were shown to be highly efficient in RCM using the standard Grubbs-II catalyst.

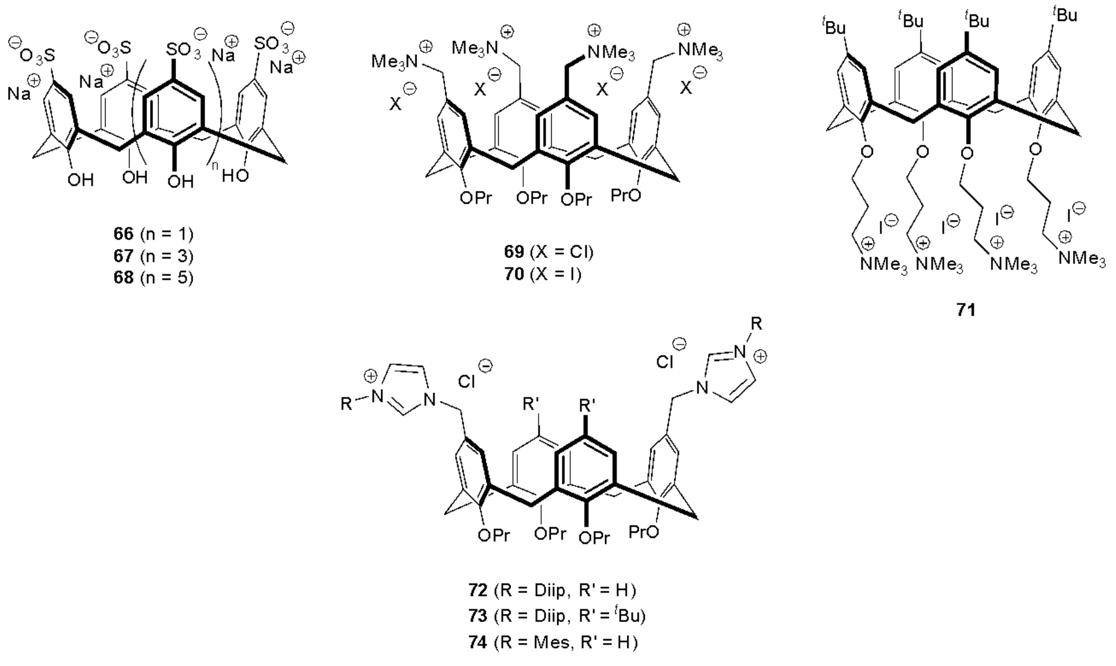

Figure 19. Calixarene additives used in Ru-catalyzed RCM and CM in water [74]. (Diip = 2,6-diisopropylphenyl; Mes = 1,3,5-trimethylphenyl).

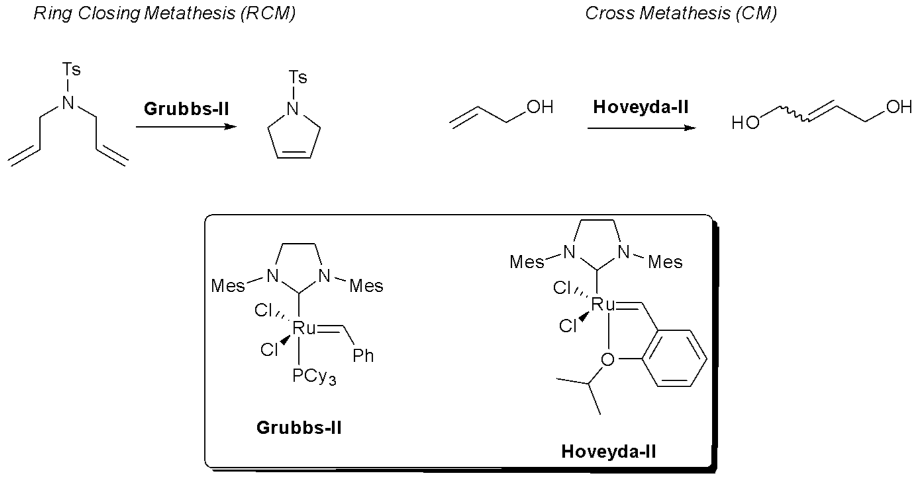

Scheme 6. Commercially available Ru-catalysts for metathesis reactions [74-76].

5.2.2 Water Oxidation

Very recently, Noll and Würthner reported on the synthesis of a dinuclear ruthenium complex bearing a functionalized calix[4]arene-based scaffold [77]. This species proved highly active in the photocatalytic water oxidation, with an unprecedented turn over frequency of 15.5 s^{-1}.

5.3 Cobalt

5.3.1 Olefin Epoxidation

Bimetallic Co^{II} complexes bearing calix[4]arene-(salen) ligands have been successfully employed as catalysts in the epoxidation of styrene and cyclohexene with PhIO (Figure 20) [78]. Concerning the first substrate, higher yield was achieved in the presence of complex **75**, while both catalysts exhibited same selectivity towards the epoxide product (99%). With respect to cyclohexene, compound **76** proved less performing than its less sterically demanding congener, both in terms of yield and selectivity. This is in line with what observed in the same reaction catalyzed by their Mn^{III}-based analogues **61** and **62** [69].

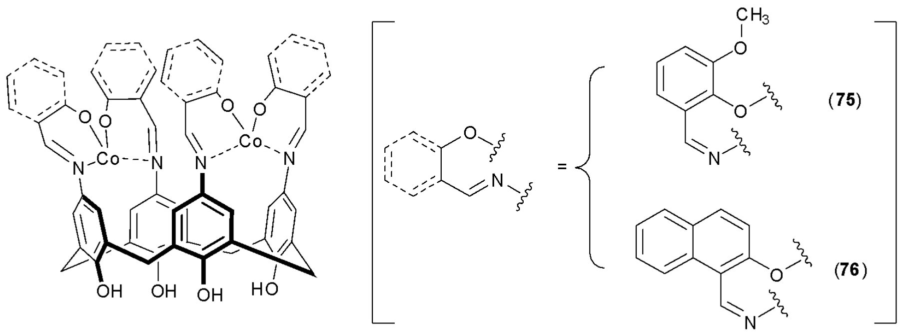

Figure 20. Bimetallic calix[4]arene-(salen) Co^{II} used in the catalytic olefin epoxidation with PhIO [78].

Moreover, the Co complexes were shown to be reusable up to four time without significant loss of activity. The reaction was thought to proceed according to an *oxygen rebound* mechanism of the Co^{II} complex, as depicted in scheme 7.

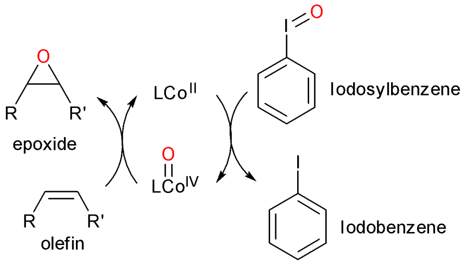

Scheme 7. Proposed catalytic cycle for the Co-catalyzed olefin epoxidation with PhIO [78].

With respect to compounds based on larger calixarenes, the catalytic hydrolysis of several terminal *meso* epoxides was successfully achieved in the presence of a benzyloxycalix[8]arene-supported cobalt-salen complex [79]. Since the process afforded enantio-enriched diols, it could be considered as an elegant example of Hydrolytic Kinetic Resolution (HKR) of epoxides. The mechanism was thought to be facilitated by the cooperation of multiple Co- centers. In fact, the conformational flexibility of the calix[8]arene scaffold would allow for two (or more) metal centres to be close to each other. The complex could also be reused up to three times without any loss of activity/selectivity. Moreover, almost no leaching of the catalyst was observed, enabling the recovery of the reaction products without prior purification.

Finally, we have recently prepared novel heterometallic Co/Li complexes of p-*tert*-butylcalix[6 and 8]arenes [80]. These compounds have been either generated *in-situ* by treating the ligand precursors with a lithium reagent (*n*BuLi or *t*BuOLi) and further reaction with $CoBr_2$ or via the addition of the *in-situ* formed $Li[Co(OtBu)_3]$ to p-*tert*-butylcalix[*n*]arene. Although the X-ray analysis of these complicated multinuclear species was somewhat problematic (due to partial occupancy issues), the atom connectivity could be sensibly assigned. These systems have been tested in preliminary screening for electrochemical water oxidation, displaying good activity. This process is accompanied with an irreversible calixarene-H_2O exchange with consequent precipitation of Co hydroxide.

5.4 Rhodium

5.4.1 Olefin Hydroformylation

The rhodium-catalyzed olefin hydroformylation with CO/H_2 is currently the main synthetic route to linear C_3-C_{18} aldehydes (Scheme 8) [81]. The main issue of such transformations is the undesired formation of branched aldehydes; hence the development of catalytic systems exhibiting high selectivity towards the linear product has been extensively investigated. In this regard, Rh-calixarene catalysts have been considered.

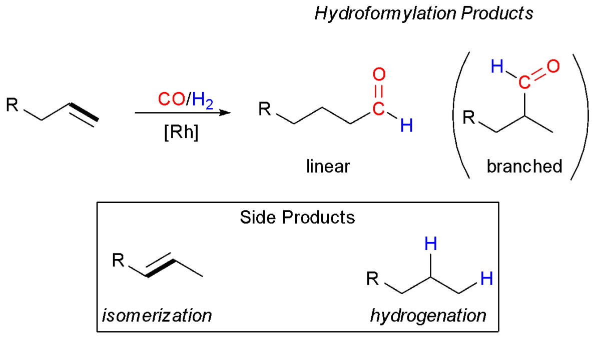

Scheme 8. General scheme for the Rh-catalyzed olefin hydroformylation [81].

Based on their preliminary work dating back to 2006 [82], Sèmeril, Matt *et al.* studied the hydroformylation of several alkenes in the presence of Rh complexes of the calix[4]diphosphites **77-83** (Figure 21) [83]. The catalysts were generated *in-situ* upon treating $[Rh(acac)(CO)_2]$ (acac = acetylacetonate) with a 10-fold excess of the ligand. The excess of ligand was required in order to avoid the formation of "naked" metal causing a drop of selectivity [84].

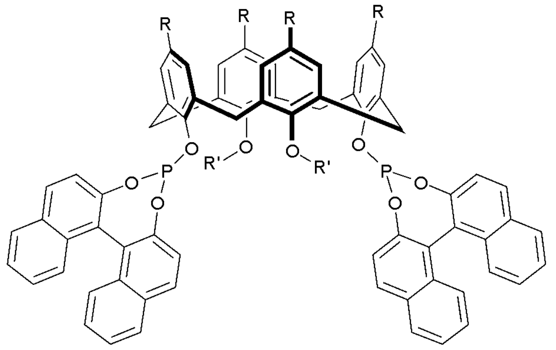

77 (*S*,*S*), R = H, R' = *n*Pr
78 (*S*,*S*), R = ^{t}Bu, R' = *n*Pr
79 (*R*,*R*), R = ^{t}Bu, R' = *n*Pr
80 (*S*,*S*), R = ^{t}Bu, R' = Bn
81 (*R*,*R*), R = ^{t}Bu, R' = Bn

82 (*S*,*S*), R = ^{t}Bu, R' =

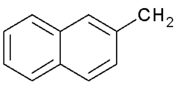

83 (*S*,*S*), R = ^{t}Bu, R' =

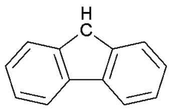

Figure 21. Calix[4]diphosphites employed in the Rh-catalyzed olefin hydroformylation [83].

When 1-octene was used as substrate, a drop of conversion was obtained upon increasing the size of the 1,3-*O*-substituents on the calixarene. On the other hand, the opposite trend was observed with respect to reaction selectivity. In fact, the linear/branched ratio increased with the size of the substituents. However, no simple size-selectivity correlation was drawn, since a dramatic drop of selectivity was obtained in the presence of **83**, bearing two fluorenyl groups. Remarkably, no significant different was observed in the presence of either the (*R*,*R*) or (*S*,*S*) isomers. Although no hydrogenation products were recovered, internal alkene deriving from isomerization reactions were detected. This suggested that the complexes could act also as isomerization catalysts. Indeed, by using *trans* 2-octene as substrate in the presence of the [Rh]/**82** system, a moderate amount (25%) of linear aldehyde was isolated. Interestingly, the hydroformylation of styrene with **77**-**82** afforded mainly linear aldehyde, unlikely the common Rh/PPh_3 catalysts that favor the formation the branched product [85]. Remarkably, complex **83** afforded mainly the branched product. The low selectivity of this catalyst was lately explained by means of high-pressure NMR spectroscopy studies [86]. Indeed, it was shown that temporary ligand dissociation might occur upon treating the complex with CO, affording a poorly defined and less selective species. Finally, the systems proved active also in the hydroformylation of allyl benzyl ether and norbornene. In the latter case, optical active products were obtained, with enantio-selectivity increasing with the bulkiness of the *O*-substituents of the calixarene. In particular, the highest enantiomeric excess (*ee* = 61) was achieved on the presence of the fluorenyl derivative **83**.

Concomitantly, Kamer, van Leeuwen *et al.* studied the 1-octene hydroformylation catalyzed by a Rh complex bearing a calix[4]quinoline-based *P,N*-ligand [87]. The pre-catalyst was prepared *in-situ* by treating a toluene solution of the ligand with [Rh(acac)$(CO)_2$]. Complete substrate conversion was achieved within 2 h, with a linear/branched ratio of 1.4 and *ca.* 13% of isomerization. High-pressure NMR spectroscopy studies suggested the formation of multiple catalytically active species, in which the metal is bond to the calixarene-*P,N*-containing ligand only by the phosphorus atom.

Lately, the performances of the well-defined complexes **84**, in combination with upper-rim sulfonated calix[4]arene surfactants (Figure 22) in the olefin hydroformylation in aqueous medium were tested [88]. In the case of 1-octene, good substrate conversion (62%) and a high linear/branched ratio (63) was achieved in the presence of surfactant **86** bearing *n*-butyl groups at the lower rim. A drop of performance, both in terms of conversion and selectivity, was observed upon using additives with either longer substituents at the lower rim (**87** and **88**) or free hydroxy groups (**85**). Interestingly, the reaction occurred also in the absence of surfactant, albeit with lower conversion and selectivity. Noteworthy, addition of excess ligand **80** (10 equiv. with respect to the **84**) improved the overall performances of the catalyst. A similar trend was also observed when 1-hexene was used as substrate, albeit with lower selectivity (linear/branched ratio of 11). With respect to styrene, the best results were achieved in the presence of the surfactant bearing *n*-octyl groups (**88**). Nevertheless, both conversion and linear/branched ratio (38% and 2, respectively) were lower than those observed in the case of aliphatic substrates. The possibility to perform olefin hydroformylation in aqueous media has been also investigated by Pringle and Cobley, who reported on the hydroformylation 2-methylpentenoate in water/toluene mixtures promoted by a water soluble Rh-calix[4]arene complexes [89]. Poor selectivity was generally observed; in fact, only branched aldehydes were obtained. Moreover, one of the branched products was also shown to undergo selective hydrogenation affording its lactone derivative.

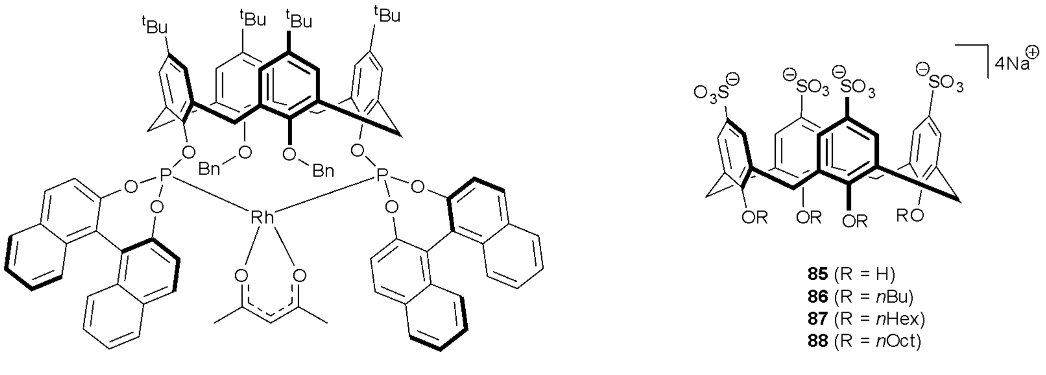

84 (*S*,*S*)

85 (R = H)
86 (R = *n*Bu)
87 (R = *n*Hex)
88 (R = *n*Oct)

Figure 22. Rh catalyst (**84**) and calixarene-based surfactants (**85-88**) used in the olefin hydroformylation in water [88].

With respect to tests performed in other protic solvents, Vatsouro *et al.* recently described the synthesis of the polyfunctional phosphorus-containing calixarenes **89** and **90** (Figure 23) and their use as ligands in the olefin hydroformylation in ethanol [90]. In this case, $[Rh(cod)_2]BF_4$ (cod = cyclooctadiene) was selected as metal precursor. Preliminary NMR spectroscopic studies in deuterated methanol were carried out in order to identify the possible catalytically active species. By treating **89** or **90** with the Rh precursor, broad signals compatible with the oxidized form of the ligands as well as the diagnostic resonance of free cod, were observed. Concurrently, the formation of a precipitate occurred. It was then suggested that complexation took place, with the solid being oligomeric/polymeric Rh-complexes insoluble in the alcoholic medium. Addition of deuterated sulfuric acid to the reaction significantly reduced the amount of insoluble material; in turn, ^{1}H- and ^{31}P NMR spectroscopy suggested the formation of cationic species featuring P-Rh^{+} bonds. Based on these findings, the hydroformylation of 1-octene in ethanol was carried out at 80 °C both in the presence and in the absence of sulfuric acid with a ligand/Rh ratio of 2. In the presence of the acid, full conversion of the substrate was achieved: moreover, undesired hydrogenation reactions were significantly reduced, compared to the run performed in the absence of H_2SO_4.

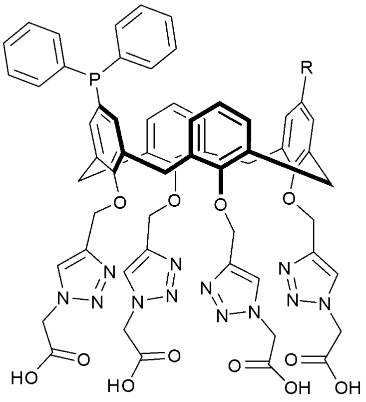

89 (R = H)
90 (R = PPh$_2$)

Figure 23. Polyfunctional phosphorus-containing calixarenes ligands [90].

Finally, Sémeril, Matt *et al.* synthesized a Rh complexes supported by a calix[4]arene-fused phosphole ligand (**91**, Figure 24) and tested it in the hydroformylation of vinyl-arenes (Table 8) [91]. When styrene was used as substrate, good conversion was achieved after 7 h (run 1). However, an improvement was observed upon adding 1 equiv./Rh of free ligand (run 2). The TOF determined after 1 h was two-fold higher than that achieved upon using PPh_3 under the same reaction conditions (160 and 75 h^{-1}, respectively). On the other hand, a significant drop of conversion was obtained by using and additional equivalent of ligand (run 3). Finally, full styrene consumption was achieved after 22 h in the presence of **91**/ligand (1:1 ratio, run 4). Under the same reaction conditions, the catalytic system proved to be active also in the hydroformylation of *para*-substituted substrate, namely 4-F-Styrene and 4-*t*Bu-Styrene (runs 5 and 6, respectively). In all cases, the branched aldehyde was the main product, with conversion spanning from 94 to 97%.

Table 8. Hydroformylation of vinyl arenes catalyzed by **91** [91].

Run	Substrate	Time (h)	Conversion (%)[a]	TOF (h^{-1})	Linear aldehyde (%)[a]	Branched aldehyde (%)[a]
1	Styrene	7	69	98.6	5.0	95.0
2[b]		7	82	117.1	4.8	95.2
3[c]		7	47	67.1	3.2	96.8
4[b]		22	>99	45.4	5.8	94.2
5[b]	4-F-Styrene	22	>99	45.4	3.7	96.3
6[b]	4-^{t}Bu-Styrene	22	>99	45.4	5.4	94.6

Reaction conditions: 91 (2 µmol), substrate (2 mmol), toluene/*n*-decane (20 mL/0.25 mL), P(CO/H_2) = 30 bar (CO/H_2, 1:1 v/v), T = 60 °C. [a] Determined by GC using decane as an internal standard. [b] Addition of 1 equiv./Rh of free ligand. [c] Addition of 2 equiv./Rh of free ligand.

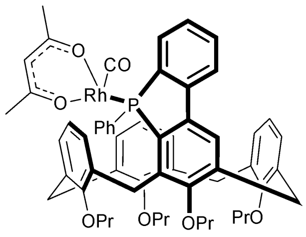

91

Figure 24. Rh(I) complex bearing a calix[4]arene-fused phosphole [91].

5.4.2 Alkene hydrogenation

Aside from being an undesired side-reaction often occurring during hydroformylation reactions, alkene hydrogenation is a useful synthetic tool. In particular, its enantioselective version could be used to achieve optical active molecules from pro-chiral substrates [92-94]. With respect to calixarene chemistry, Liu and Sandoval described the enantioselective hydrogenation of dehydroamino acid derivatives catalyzed by Rh-calix[4]arene-diphosphite complexes (Scheme 9) [95]. The catalysts were generated *in-situ* by treating $[Rh(cod)_2]BF_4$ with several chiral calix[4]arene-based diphosphite ligands; nevertheless, the best results were achieved in the presence of the previously encountered **78** and **80** (see Figure 21).

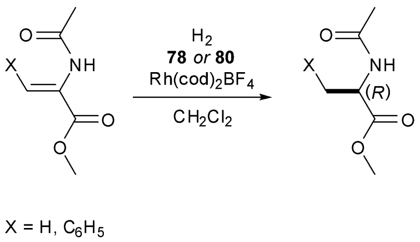

Scheme 9. Rh-catalyzed enantioselective hydrogenation of methyl-(*Z*)-2-(acetamido)acrylate (X = H) and methyl-(*Z*)-2-(acetamido)cinnamate (X = C_6H_5) [95].

The catalytic systems proved very efficient, allowing for complete conversion of the substrates within 12 h at 30 °C in CH_2Cl_2, affording the products as (*R*)-isomer in high enantiomeric excess (*ee* >95%). Interestingly, the enantio-selectivity was high from the early stages of the transformation and proved to be slightly dependent on the pressure of hydrogen. Indeed, higher H_2 pressures caused a drop of *ee* (from 97% to 93%, for 5 and 16 bar, respectively). Similarly, the drop of *ee* was observed upon increasing the temperature from 30 to 50 °C (97 and 94%, respectively). Eventually, the use of non-halogenated solvents (protic and aprotic) was detrimental for the reaction, both in terms of conversion and enantio-selectivity.

Harvey, Jugé *et al.* studied the hydrogenation of several pro-chiral alkenes in the presence of the well-defined Rh species **92** (Scheme 10) [96]. The complex is based on a P-chirogenic aminophosphane-phosphinite group bound to the upper rim of a calix[4]arene scaffold. Unlike the previous case, the catalyst exhibited its best performances in aprotic non-halogenated solvents, such as benzene or toluene. Low yields and poor selectivity were also observed in alcoholic media. In the majority of the cases, the hydrogenated products were recovered as (*R*)-isomers. Also, in this case, the selectivity dropped upon increasing the pressure of H_2. By employing catalysts bearing groups other than the calixarene, namely 3,5-dimethyl-4-propoxyphenyl or 3,5-dimethylphenyl, significant loss of activity and selectivity were observed in all cases. This suggested that the calixarene scaffold might play a crucial role on the catalytic performance of the complex. Although the molecular structure of **92** (Figure 25) clearly shows the Rh-center outside of the calixarene pocket, computational models indicated the possible conformers for the active species, in which the metal is either inside (*inner*) or outside (*outer*) of the calixarene pocket. The coordination of the substrate forces the species to adopt preferentially the outer configuration, leading to the formation of only one enantiomer of the product.

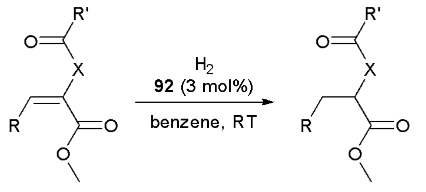

R = H, Ph, Me
R' = CH_3, CH_3O
X = NH, CH_2, $N(CH_2)_3$

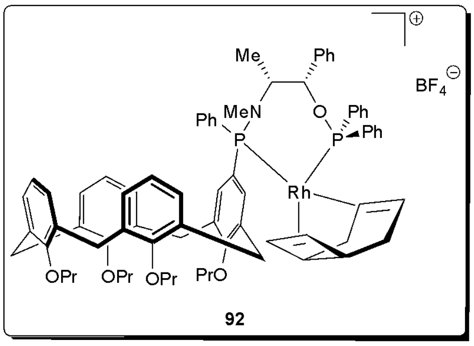

92

Scheme 10. Asymmetric hydrogenation of alkenes catalyzed by **92** [96].

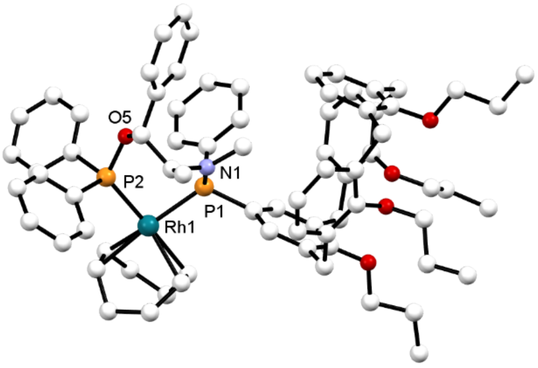

Figure 25. Molecular structure of the cation of complex **92** showing the Rh center outside of the calix[4]arene cavity [96].

In terms of non-stereoselective applications, Sémeril, Matt *et al.* have tested complex **93** (Figure 26), bearing a 1,3-P^{III}-upper-rim functionalized calix[4]arene, in the hydrogenation of terminal- and internal alkenes [97]. With 1 mol% catalyst loading and 5 bar of H_2, complete conversion of 1-octene and allyl benzyl ether was obtained in 5 h. A shorter reaction time (4 h) was required by styrene and cyclooctene. Eventually, the catalyst was tested in the hydrogenation of a terminal alkyne, namely 1-pentyne. Under the optimized reaction conditions, the complete hydrogenation of the substrate to pentane was achieved after 24 h.

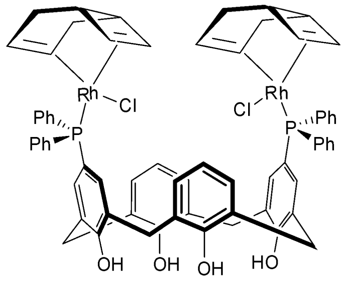

93

Figure 26. Dinuclear Rh-calixarene complex used in the hydrogenation of terminal- and internal alkenes [97].

5.5 Iridium

5.5.1 Ethylene Hydrogenation

Examples concerning the iridium-calixarene complexes in catalysis are limited. Recent reports by the group of Katz describe the behavior of the Si-supported multinuclear species **94** and **95** (Figure

27) in hydrogenation reactions [98, 99]. With respect to the tetrairidium cluster **94**, ^{13}C NMR spectroscopic analysis at variable temperature assessed that no scrambling of the carbonyl ligands occurs, suggesting the existence of distinct sites for CO bonding [98]. This was confirmed *via* oxidative decarbonylation with trimethylamine *N*-oxide (TMAO) monitored by IR spectroscopy. When the reaction was performed under an argon atmosphere, bridging CO ligands at the basal plane of the cluster were selectively removed. On the other hand, by conducting the treatment in the presence of ethylene, carbonyl groups at the apical Ir center were removed, generating Ir-ethyl groups. Both decarbonylated clusters, supported on silica, proved active in the ethylene hydrogenation; however, the species with the open sites at the apical position granted the best performances.

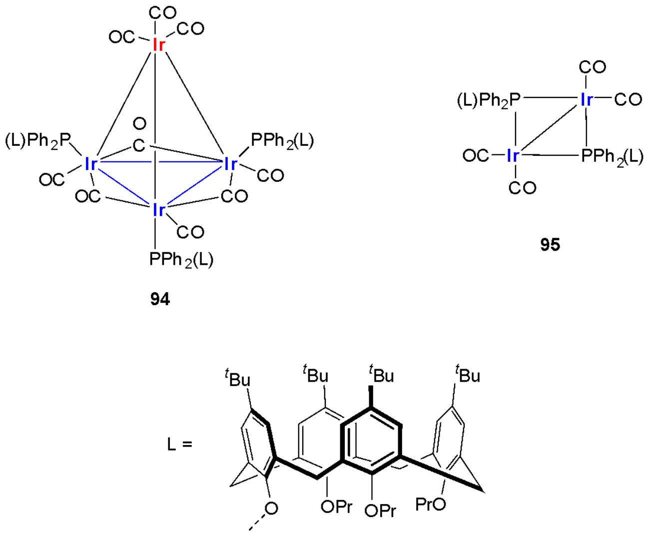

Figure 27. Multinuclear Iridium carbonyl complexes supported by a calix[4]arene-phosphine scaffold [98, 99].

Similarly, complex **95** was supported on dehydroxylated silica as well as on a crystalline zeolitic silicate material [99]. Both heterogeneous catalysts were efficient in the ethylene hydrogenation, exhibiting stable turnover and activities higher than those of conventional hydrogenation catalysts. This superior activity was accounted to the effect of the calixarene scaffold, thought to prevent the aggregation of the metal on the supports, hence allowing the presence of multiple active sites.

5.6 Nickel

5.6.1 Cross-Coupling Reactions

Nickel complexes bearing calixarene-based ligands have been mainly employed as catalysts for cross-coupling reactions, with the majority of the studies being carried out by the group of Sémeril and Matt. In 2009, they tested a Ni-complex bearing a “1,3-calixdiphosphine” ligand in the Kumada-Tamao-Corriu (KTC) coupling of PhMgBr with various aryl bromides (Scheme 11) [100]. Initial optimization of the reaction conditions was performed with 4-bromoanisole in refluxing 1,4-dioxane. In order to achieve complete substrate conversion, 2 equiv. of Grignard reagent were required. Moreover, the catalyst needed pre-activation (heating in dioxane at reflux for 1 h) to exhibit the best performances. Under these reaction conditions, homo-coupling side-products were recovered in less than 3%.

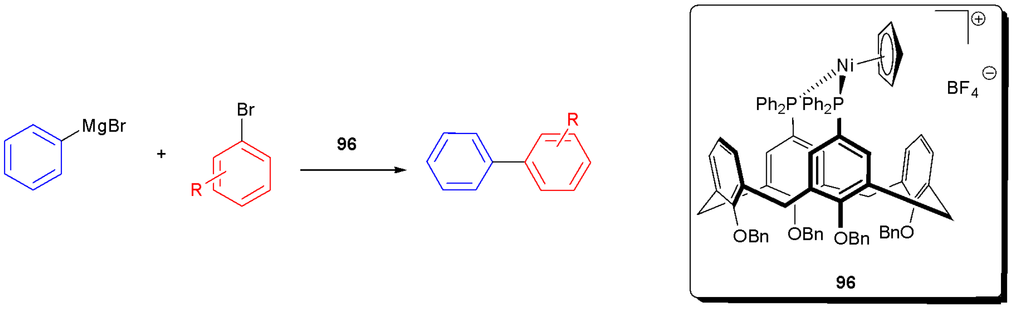

Scheme 11. Kumada-Tamao-Corriu (KTC) coupling catalyzed by Ni-complex **96** [100].

Activated bromoaryls, *i.e.* 4-bromotoluene and 1-bromonaphthalene, were completely converted into the coupling products within 1 h, with catalyst loadings as low as 0.02%. More challenging substrates, such as chloroaryls were also reactive, although with lower activities. Noteworthy, **96** outperformed the benchmark catalyst $[NiCl_2(dppp)]$ (dppp = 1,3-bis(diphenylphosphino)propane). The high catalytic efficiency of the complex was attributed to the intrinsic dynamics of the calixarene moiety, thought to favor the reductive elimination step by temporary increasing the bite angle, thus enhancing the steric pressure on the aryl groups bound to the Ni center. Interestingly, in a later contribution the authors proved that Ni-complexes supported by mono-phosphine calix[4]arene ligands **97** and **98** (Figure 28) were *ca.* 20% more efficient than their di-phosphine analogues [101]. In this case, the formation of a transient [Ni(π-ArX)(calix-phosphine)] intermediate, having the coordinated ArX entrapped in the calixarene cavity, was proposed. The orientation of the Ni-P bond towards the calixarene axis would increase the steric bulk around the metal center favoring the formation of a mono-coordinated Ni^0 intermediate.

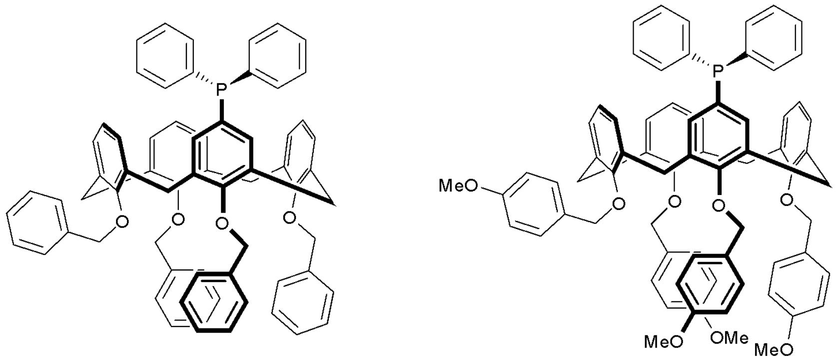

97 **98**

Figure 28. Calix[4]arene-monophosphine ligands **97** and **98** [101].

Lately, Ni-catalysts bearing by the calix[4]arene-iminophosphoranes **99-101** (Figure 29) were also tested in the Kumada-Tamao-Corriu (KTC) coupling under the same reaction conditions used for **96** (Table 9) [102]. The complexes were generated *in-situ* be reacting $[Ni(cod)_2]$ with the pre-ligands in refluxing dioxane for 1 h before addition of the reactants. The reaction proved highly substrate-dependent. Indeed, *p*ara-substituted bromoaryl were found more reactive than their *ortho*-analogues (cf. runs 1-2 and 5-6), while the highest conversions were achieved in the case of naphthalene-derivatives (runs 3 and 4). No clear correlation between the structure of the ligand and the catalytic performances of the catalysts could be found. Turn Over Frequencies (TOF) as high as 390000 h^{-1} were obtained. Remarkably, these values were up to 60-fold higher than those achieved, under the same reaction conditions, with Ni catalysts based on *o*-MeO-C_6H_4-NH_2 (TOF = 6310 h^{-1}).

Table 9. Ni-catalyzed KTC coupling in the presence of **99-101** [102].

Run	**Substrate**	**Ligand**	**Conversion** (%)[a]	**TOF** (h^{-1})
1	4-bromoanisole	**99**	37.9	37900
		100	46.1	46100
		101	42.6	42600
2	2-bromoanisole	**90**	20.8	20800
		100	32.7	32700
		101	23.9	23900
3	2-bromo-6-methoxynaphthalene	**99**	68.8 30.4[b]	68800 304000[b]
		100	60.7 17.3[b]	60700 173000[b]
		101	68.7 29.7[b]	68700 297000[b]
4	1-bromonaphthalene	**99**	77.7 34.4[b]	77700 344000[b]

		100	85.6	85600
			38.1[b]	381000[b]
		101	85.5	85500
			39.0[b]	390000[b]
5	2-bromotoluene	**99**	19.5	19500
		100	20.5	20500
		101	22.4	22400
6	4-bromotoluene	**99**	49.3	49300
		100	45.7	45700
		101	45.5	45500

Reaction conditions: [Ni(cod)$_2$] 10 ppm, ligand 20 ppm, ArBr 0.5 mmol, PhMgBr 1 mmol, 1,4-dioxane 1.5 mL, 100 °C. [a] Determined by GC, using decane as internal standard. [b] [Ni(cod)$_2$] 1 ppm, ligand 2 ppm

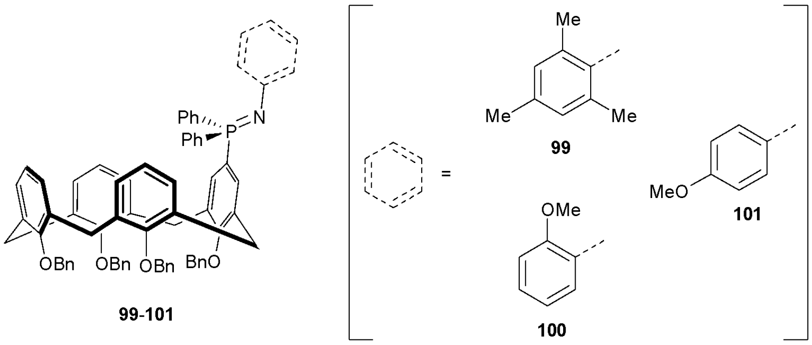

Figure 29. Calix[4]arene-iminophosphoranes ligands **99-101** [102].

Catalysts based on the calix[4]arene phosphanes **97** and **98** proved also efficient in the Suzuki-Miyaura coupling of bromo- and chloroaryl with phenylboronic acid (Scheme 12) [103].

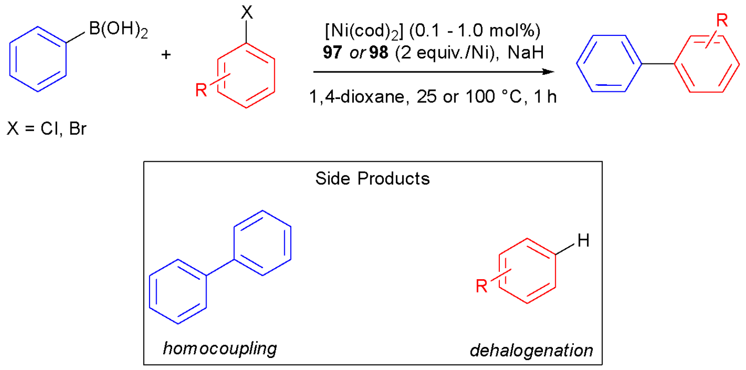

Scheme 12. Ni-catalyzed Suzuki-Miyaura coupling in the presence of **97-98** [103].

By using 0.1 mol% of Ni-precursor and 2 equiv./Ni of pre-ligand, good to moderate conversion were achieved for several arylbromides. Methoxy-substituted compounds were more efficiently converted in the presence of **97** rather than **98**, while the opposite was observed in the case of methyl-containing substrates, regardless of the position (*ortho*, *meta* or *para*) of the substituent. In all cases, an amount of ArX spanning from 20 to 40% was converted into the corresponding dehalogenated product. Good conversions were also obtained with more challenging ArCl substrates. However, a 10-fold higher catalyst loading (1 mol%) was required. The amount of dehalogenated product was dependent on the substrate; for chloroaryl bearing electron-withdrawing groups (*i.e.* NO_2, CN) less than 10% side-product was obtained. On the other hand, substrates with electron-donating groups (Me, OMe) were less reactive and provided higher amounts (up to 30%) of dehalogenated product. Remarkably, Ni/**97** systems proved better performing than benchmark catalysts based on other phosphines such as PPh_3, P(*o*-tolyl)$_3$ and the Buchwald-type phosphane *o*-biph-PPh_2.

With respect to larger calixarene platforms, Ni complexes of *N*-heterocyclic carbenes (NHCs) bound to a calix[6]arene scaffold were recently disclosed by Chetcuti e*t al.* (Figure 30) [104]. These compounds were tested in the Suzuki-Miyaura coupling of $PhB(OH)_2$ with 4-X-acetophenone (X = Cl, Br) in toluene at 100 °C in the presence of K_3PO_4 as a base. The influence of the substituent of the imidazole moiety was first investigated. Complex **102**, bearing a mesityl group, was found to be more active than its congeners **105** and **106**, bearing a 2,6-diisopropyl and methyl group, respectively. In terms of the length of the spacer between the NHC and calix[6]arene groups, the activity trend was **102** > **103** > **104**, suggesting a shorted Ni-calixarene distance is beneficial for the reaction. These trends hold for both the Br- and Cl-substrates, although the differences are more pronounced in the latter case.

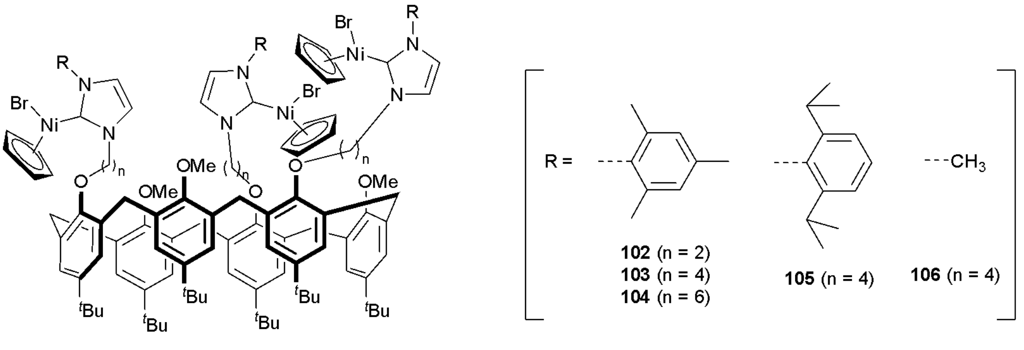

102-106

Figure 30. Ni complexes supported by NHC-functionalized calix[6]arenes [104].

5.6.2 Electrocatalytic CO_2 Reduction and VGO Hydrocracking

Recently, Reyes-Mata and Castillo reported on the synthesis of Ni complexes of a phenanthroline-functionalized calix[8]arene bearing either Cl- or acetate ancillary ligands [105].

The Cl-adduct was shown to promote the electrocatalytic reduction of CO_2 in a CH_3CN/THF (95:5) mixture by using water as a source of proton, with catalytic performance comparable to that of Ni-neocuproine complexes. On the other hand, its AcO-containing congeners proved completely inactive, indicating that the acetate counterions hinders the reactivity of the metal center.

Nickel complexes have also been used in the Vacuum Gas Oil (VGO) hydrocracking of heavy oils to provide high-value lighter petroleum products [106]. Indeed, when combining a Ni-calix[4]arene- based species with a commercial first-stage hydrocracking supported catalyst, enhanced hydrogen activity and reduced coke- and gas formation were observed. In particular, upon using the Ni cocatalyst, the coke yield decreased from 36 to 14%, hence affording cleaner naphtha and distillate fractions. Modelling of the reaction kinetics indicated a drop of the activation energy of the distillate (from 65 to 57 kcal/mol) in the presence of the Ni-calix[4]arene cocatalyst.

5.7 Palladium

5.7.1. Cross-coupling reactions

In 2009, Schatz *et al.* synthesized the *trans*- and *cis* isomers of a Pd complex supported by a bis-NHC-calix[4]arene ligand (**107** and **108**, respectively, Figure 31) [107]. Both compounds were tested in the Suzuki-Miyaura coupling of phenylboronic acid and 4-chlorotoluene in 1,4-dioxane in the presence of Cs_2CO_3 as a base. The same substrate conversion was achieved, regardless of the isomer (30 and 27% for **107** and **108**, respectively), suggesting that both compounds generate the same catalytically active species, allegedly a complex having only one NHC moiety coordinated to the metal center. This assumption was corroborated by employing a mono-NHC-calixarene complex whose catalytic activity was found to be similar to that of **107** and **108**.

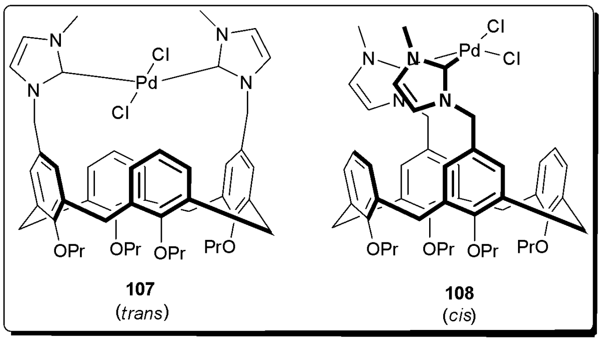

Figure 31. *trans*- and *cis*-isomers of bis-NHC-calix[4]arene Pd complex [107].

Based on these findings, the activity of Pd complexes bearing mono-NHC was next investigated (Figure 32) [108,109].

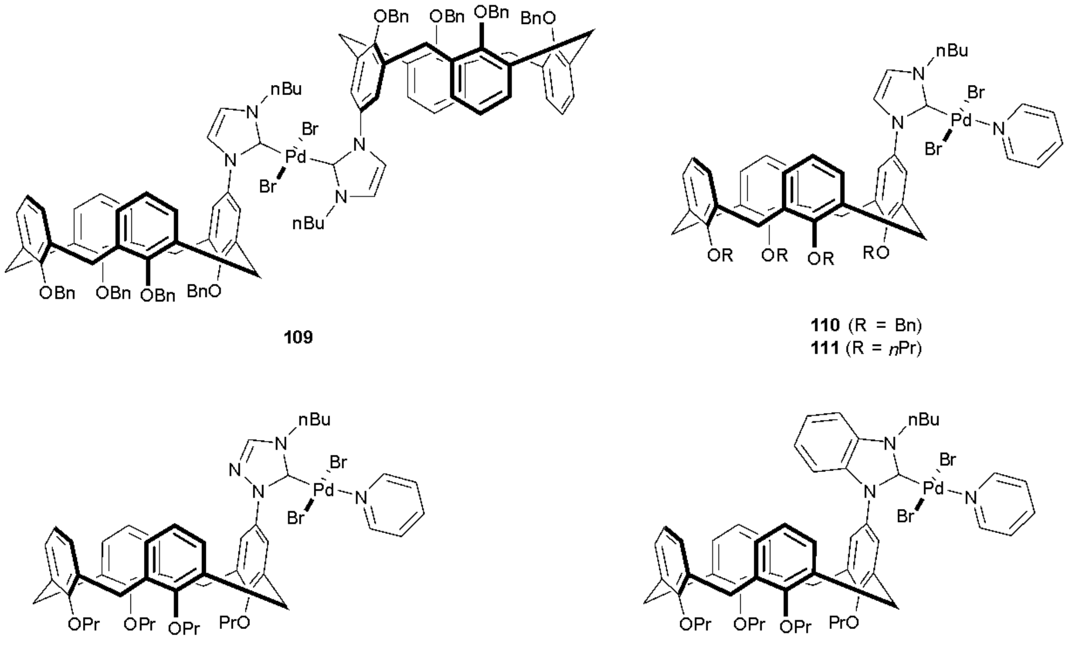

109

110 (R = Bn)
111 (R = *n*Pr)

112

113

Figure 32. Pd complexes supported by mono-NHC-calix[4]arene ligands [108,109].

Complexes **109** and **110** displayed good activities in the Suzuki-Miyaura coupling of phenylboronic acid with 4-Br-toluene, allowing for complete substrate conversion within 2 h with 0.1 mol% of Pd [108]. By halving the catalyst loading, both complexes were still highly active, although higher conversion was obtained with **109** compared to its mono-calixarene derivative **110** (92 and 87% conversion, respectively). Moderate conversions were obtained also in the case of the more challenging substrate 4-Cl-toluene, in the presence of a 10-fold higher catalyst loading (1 mol%). Noteworthy, the presence of two NHC moieties did not significantly affect the catalytic activity of **109**, compared to that of the pyridine-containing complex **110**. The nature of NHC group proved to significantly impact the catalytic activity of complexes **111-113** [107]. In fact, when tested in the coupling of bromobenzene and 4-methoxyphenylboronic acid, the activity trend was found to be **113** > **111** > **112**. The highest performance of **113** was attributed to the stronger σ-donor and weaker π-acceptor features of the benzimidazolyl moiety compared to that of imidazolyl- and triazolyl groups of **111** and **112**, respectively. Finally, the tetrakis(*p*-(palladium NHC)) mesityl calix[4]arene species **114** was synthesized by Willans *et al* by carbene transfer to Pd from the corresponding Cu(I) complex (Figure 33) [108]. Complex **114**, was tested as catalyst in the Suzuki-Miyaura reaction of phenylboronic acid and 4-Br-toluene, exhibiting inverse concentration-activity effect, with activity increasing at lower catalyst loadings. This was attributed to the 1,3-alternate conformation of the calix[4]arene scaffold, thought to be unable to prevent the aggregation of inactive Pd^0 nanoclusters at high catalyst concentration. Interestingly, the catalyst generated *in-situ* by reacting the pre-ligand with $Pd(OAc)_2$ was found to be more active than the pre-formed complex. This was in contrast with the results obtained in the case of Pd-NHC-calixarene species in the cone-conformation [107].

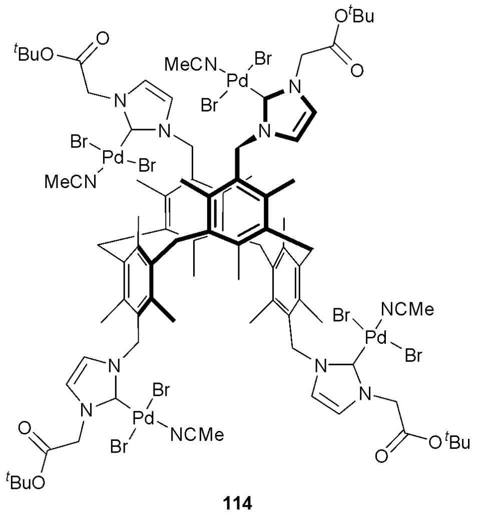

114

Figure 33. Tetranuclear Pd complex supported by a *p*-NHC-mesityl calix[4]arene ligand [110].

Lately, *in-situ* generated Pd complexes of calix[4]arene-monophosphine ligands (**97-98** and **115-117**, figures 28 and 34, respectively) were tested as catalysts in the Suzuki-Miyaura coupling of phenylboronic acids and various ArylX (X = Cl, Br) [111]. After an initial screening for the optimal reaction conditions, $Pd(OAc)_2$ and NaH were selected as metal precursor and base, respectively.

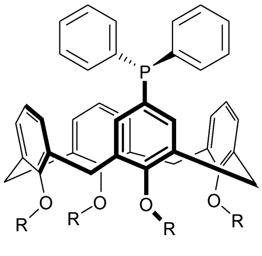

115 (R = 2-methoxybenzyl)
116 (R = *n*Pentyl)
117 (R = OH)

Figure 34. Lower rim-functionalized calix[4]arene-monophosphine ligands **115-117** [111].

As shown in table 10, no correlation between ligand structure and catalyst efficiency could be drawn, as the reaction proved very substrate-dependent. In fact, while **97** was very efficient in the case of 4-bromoanisole and 4-bromotoluene (runs 1, and 6, respectively), only 27% conversion was achieved with their 2-substituted analogues (runs 2 and 5, respectively). On the other hand, high conversions were observed with **116** and **117** with all substrates aside from 2-bromotoluene. Remarkably, the activity of these complexes was found to be comparable to that of Buchwald-type catalysts (2-diphenylphosphanyl-2'-methylbiphenyl) and *ca*. three times higher than those achievable with bulky phosphine ligands, such as $P(o\text{-tolyl})_3$. Finally, all systems proved active also in the reaction of the more challenging ArCl substrates, albeit with lower efficiency. In fact, the highest conversion (49%) was achieved with Pd/**98** for 4-Cl-nitrobenzene.

With respect to the use of calixarene-based diphosphines, Tanaka, Hattori *et al*. recently reported five novel Pd complexes, whose molecular structures are shown in figure 35 [112]. Amongst the series, complex **118** is the only compound featuring two metal centers and the calix[4]arene moiety in a 1*,3-alternate* conformation, while the cationic species **119** and **120** only differ in the nature of the counterion (Cl^- and BF_4^-, respectively). The dicationic complex **121** was obtained upon treating the parental monocationic compound with $AgBF_4$. Finally, **122** is a neutral monometallic compound featuring the calix[4]arene scaffold in *cone* conformation.

Table 10. Suzuki-Miyaura coupling of $PhB(OH)_2$ and ArBr with Pd/**97**, **98**, **115**-**117** catalysts [111].

Run	Substrate	Ligand	Conversion (%)[a]	TOF (h^{-1})
1	4-bromoanisole	**97**	95.4	95400
		98	49.8	49800
		115	89.4	89400
		116	99.7	99700
		117	94.4	94400
2	2-bromoanisole	**97**	27.1	27100
		98	40.4	40400
		115	42.0	42000
		116	80.3	80300
		117	98.8	98800
3	2-bromo-6-methoxynaphthalene	**97**	94.7	94700
		98	47.6	47600
		115	99.3	99300
		116	95.0	95000
		117	98.8	98800
4	1-bromonaphthalene	**97**	48.7	48700
		98	91.4	91400
		115	96.2	96200
		116	>99	100000
		117	>99	100000
5	2-bromotoluene	**97**	26.7	26700
		98	99.2	99200
		115	58.5	58500
		116	49.1	49100
		117	26.4	26400
6	4-bromotoluene	**97**	>99	100000
		98	99.2	99200
		115	>99	100000
		116	97.9	97900
		117	92.0	92000

Reaction conditions: $[Pd(OAc)_2]$ 10 ppm, ligand 20 ppm, ArBr 0.5 mmol, $PhB(OH)_2$ 1.0 mmol, NaH 1.0 mmol, 1,4-dioxane 1.5 mL, 100 °C, 1 h. [a] Determined by GC, using decane as internal standard

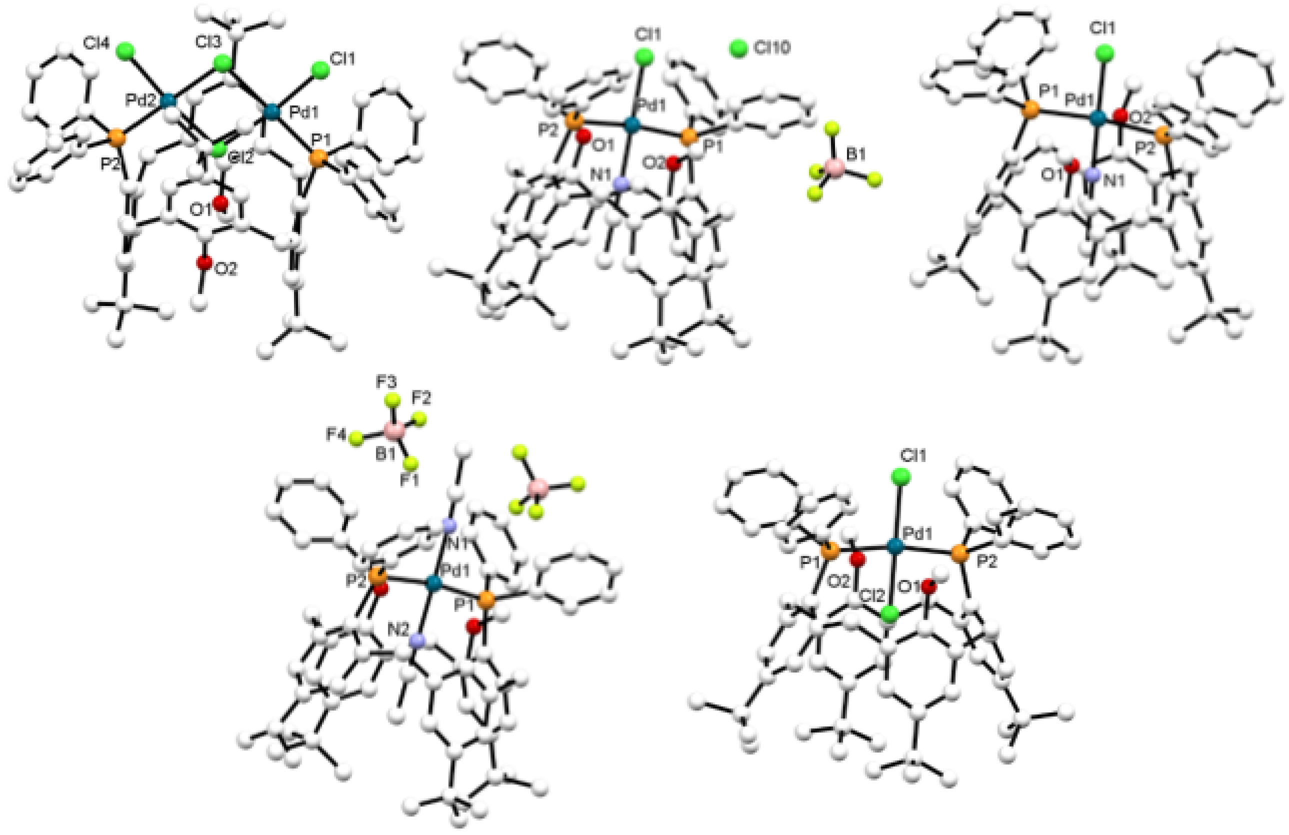

Figure 35. Molecular structures of complex **118** (top left), **119** (top center), **120** (top right), **121** (bottom left) and **122** (bottom right) [112].

The complexes were tested as catalysts in the coupling of phenylboronic acid with 4-chloroacetophenone in refluxing 1,4-dioxane and NaH as base. Interestingly, the activity trend was found to be **121** > **120** > **119** > **122** > **118**. The highest activity of the dicationic species was attributed to the easier formation of active Pd^0 by prompt replacement of the two acetonitrile ligands with the aryl moieties of the substrates and further reductive elimination. The two mono-cationic species **119** and **120** exhibited significantly different reactivity (11 and 56% substrate conversion, respectively), suggesting the non-innocence of the counterion. It has been shown that the coordination sites involved in the cross-coupling reactions are in *cis* to each other [113]; hence it was hypothesized that one of the P-Pd bond is dissociated during the catalysis. In this scenario, the ligand would act as a bulky mono-phosphine-calixarene species.

Cross-coupling reactions catalyzed by the well-defined Pd complexes of calix[4]arene-based disphosphites **123**-**127** were disclosed by Krishnamurthy *et al* in 2011 (Figure 36) [114]. With respect to the Suzuki-Miyaura coupling of $PhB(OH)_2$ with substituted aryl halides, the activity trend was found to be **123** > **126** > **125** > **127** > **124**, regardless of the substrate. The highest efficiency of

123 over the other complexes of the series was accounted to a combination of both electronic and steric effects.

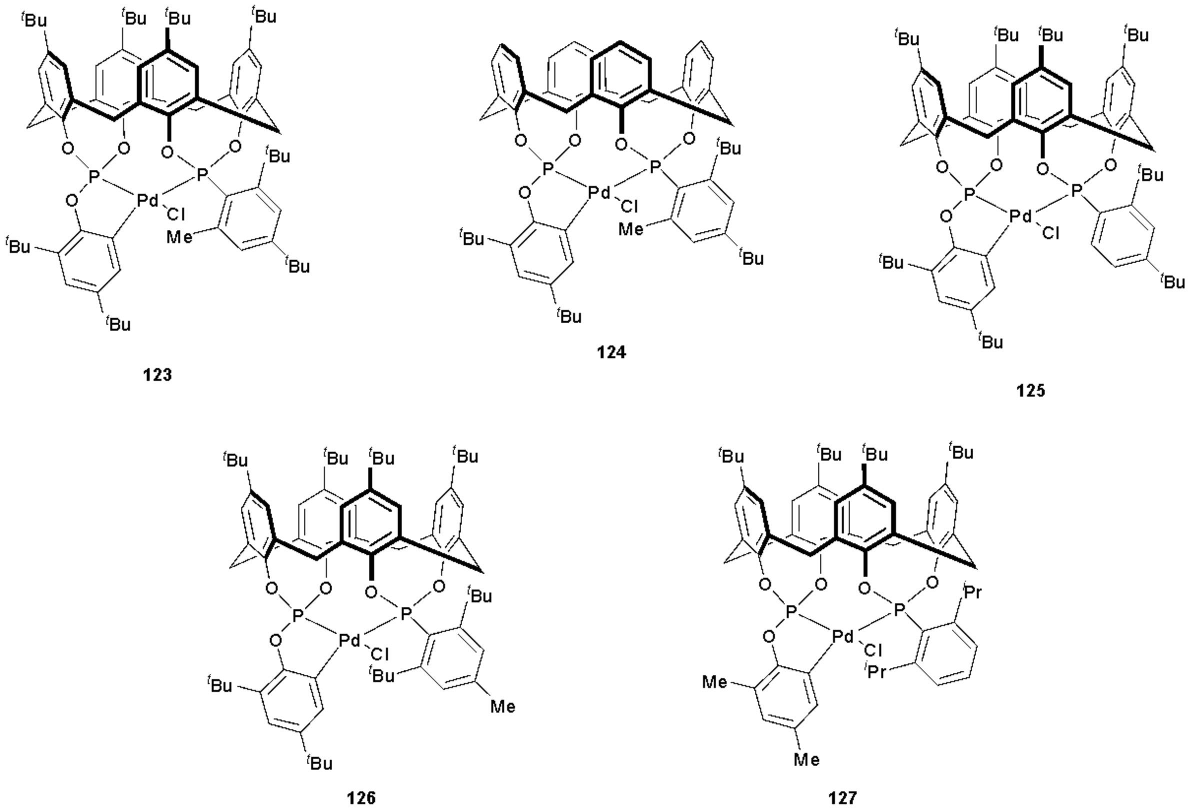

Figure 36. Calix[4]arene-diphosphates Pd complexes **123-127** [114].

Furthermore, the Heck coupling of styrene and PhX (X = Br, I) in the presence of **123-127** and $n\mathrm{Bu_4NBr}$ as co-catalyst was studied (Scheme 13 and Table 11). With respect to iodobenzene, moderate yields were achieved with **123-125** and **127** (runs 1-3 and 5, respectively), while low activity was exhibited by the more sterically hindered complex **126** (9% isolated yield, run 4). Also, in the case of bromobenzene (runs 6-10), complex **123** exhibited the best performance (run 6), while the least active catalyst was **124** (run7); however, the yields achieved with all complexes were found in a rather narrow range (16-24%). In all cases, the only product of the reaction was *trans* stilbene, as determined by ^{1}H NMR spectroscopy.

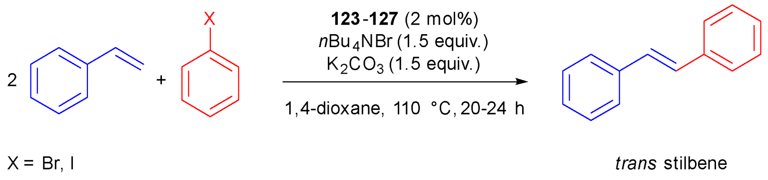

Scheme 13. Heck coupling of styrene and PhX (X = Br, I) catalyzed by **123-127** [114].

Table 11. Heck coupling of styrene and PhI or PhBr catalyzed by Pd-complexes **123-127** [114].

Run	Substrate	Complex	Time (h)	Isolated Yield (%)
1	Iodobenzene	**123**	20	30
2		**124**		24
3		**125**		28
4		**126**		9
5		**127**		27
6	Bromobenzene	**123**	24	24
7		**124**		16
8		**125**		18
9		**126**		22
10		**127**		20

Reaction conditions: Styrene 4 mmol, substrate 2 mmol, K_2CO_3 1.5 equiv., *n*BuNBr 1.5 equiv., [Pd] 2 mol%, 1,4-dioxane 5 mL, 110 °C, 20-24 h.

Palladium complexes of the calixarene-derived mono-iminophosphoranes have also been reported to catalyze Suzuki-Miyaura coupling of bromo- and chloroaryl with phenylboronic acid. The catalysts were prepared *in-situ* by reacting $Pd(OAc)_2$ with compounds **128-129** (Figure 37) and the previously encountered congeners **90-101** (figure 29) [102]. With respect to aryl bromides, all catalytic systems were active, although the efficiency trend was highly dependent on the substrate. Overall, systems based on **100** and **129** were generally more efficient than the others with the former slightly less performing than the latter. However, the opposite trend was observed upon screening these two systems in the reaction involving aryl chlorides.

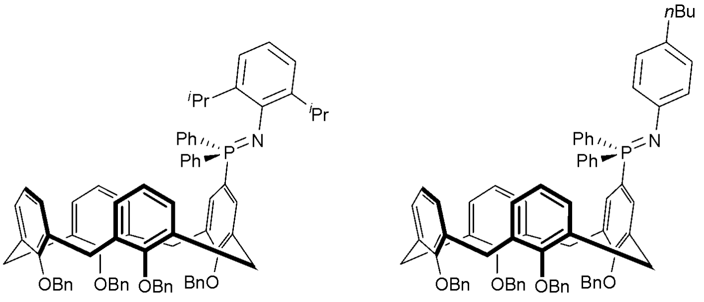

128

129

Figure 37. Calixarene-derived mono-iminophosphoranes **128** and **129** [102].

Finally, Wu *et al.* disclosed the Suzuki-Miyaura reaction catalyzed by $Na_2Pd_2Cl_6$ in aqueous media in the presence of tetraethyl *p*-*tert*-butyl-calix[4]aryl tetraacetate [115]. Rather than acting as ligand for Pd, the role of the calixarene in this case was the sequestration of Na ions form aqueous solutions of the metal precursor, affording a highly catalytically active Pd_2Cl_6 unit.

With respect to larger calixarenes, three novel NHC-calix[8]arene Pd complexes have been recently disclosed by Martini, Huc *et al* (figure 38) [116-118]. In both compounds **130** and **131**, the upper rim is functionalized with a benzyloxy group, while a *tert*-butyl moiety is found in **132**. Moreover, while the NHC fragment of **130** and **132** features an *N*-mesityl group, the bulkier 2,6-diispropylphenyl- (Diip) substituent is found in **131**. All complexes were tested in the Suzuki-Myiaura coupling of $PhB(OH)_2$ and several ArBr substrates in ethanol in the presence of potassium phosphate as a base. Although the complexes were insoluble in alcohol (rendering this an example of heterogeneous catalysis), high conversions of 4-bromotoluene (85-97%) were achieved at 80 °C with catalyst loading as low as 0.005 mol%. The catalytic activity of these complexes was affected by their structural features. In fact, the activity trend was found to be **131** ≈ **130** > **132**, suggesting that both the benzyloxy group at the calixarene as well as a bulkier substituent on the NHC moiety are beneficial. In fact, when screening different bromoaryls, **131** was slightly better performing than its mesityl-substituted congener, especially in the case of less reactive substrates, such as electron-rich or sterically hindered ones. Interestingly, these heterogeneous catalysts were as active as their homogeneous versions, in which the NHC part is not bound to a calixarene scaffold. Nevertheless, the products isolated in the presence of the heterogeneous catalysts contained only traces (10 ppm) of residual palladium, while amounts of metal up to 500 ppm were found in the case of the homogenous systems.

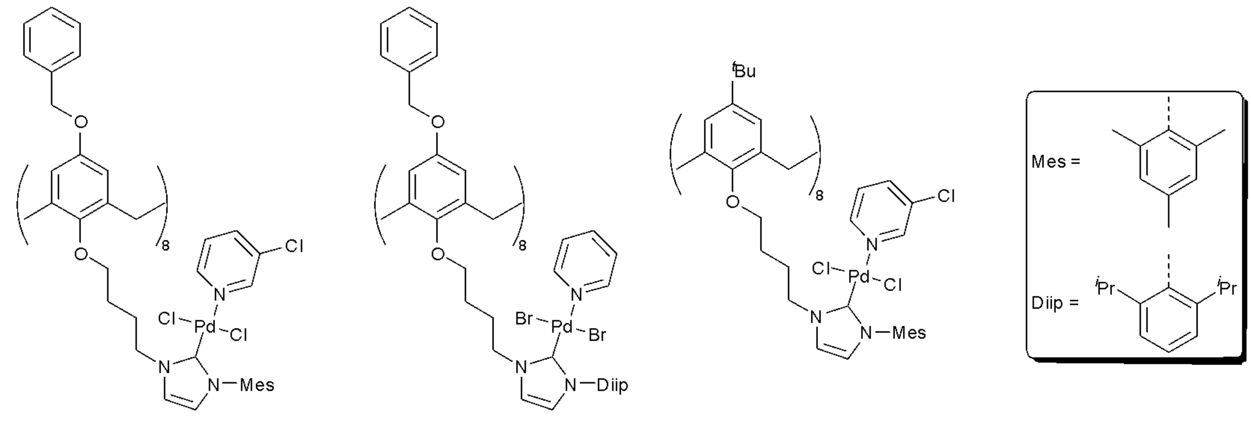

130 131 132

Figure 38. NHC-calix[8]arene Pd complexes **130-132** [116].

Analogous supported catalysts, obtained from the immobilization of Pd(X)(cinnamyl)(NHC) (X = Cl, I) on calix[8]arene scaffolds, have been recently tested in several Buchwald-Hartwig couplings [119]. Initial studies performed on the benchmark coupling between 4-chlorotoluene and morpholine revealed that the more hindered the NHC ligand, the more active the catalyst. Although

Cl- and I-derivatives proved equally performing in terms of substrate conversion (>99%), the former exhibited slightly faster kinetics. Under the optimized reaction conditions (1,4-dioxane, 100 °C in the presence of 1.5 equiv. of KO*t*Bu), the coupling of substituted aryl halides with various primary and secondary amines was efficiently performed with catalyst loadings as low as 0.03 mol%. The results were comparable to that achieved in the presence of homogeneous systems bearing very bulky NHC ligands. Leaching studies indicated that the coupling products contained less than 1% of the initial Pd employed in the reaction. Moreover, the catalysts could be recycled at least once, albeit with a significant drop of activity.

5.7.2 Allylic Alkylation

The allylic alkylation (also called Tsuji-Trost reaction) is a palladium-catalyzed nucleophilic substitution reaction in which the substrate presents a leaving group in an allylic position [120]. Reports concerning the use of calixarene-Pd catalysts in this transformation are rather scant. In 2008, Krishnamurthy *et al.* studied the allylic substitution of crotyl acetate and crotyl chloride with sodium diethyl methylmalonate in the presence of complex **133** (Scheme 14) [121]. The *trans* linear alkene was the main reaction product, regardless of the substrate (70 and 65%, for crotyl- acetate and chloride, respectively), while only 10% of *cis* product was recovered. Interestingly, the formation of a moderate amount of branched product (*ca.* 20%) was observed. This is remarkable, since lower amount of this species (*ca.* 10%) can be produced by most of the catalytic systems employed for allylic substitution, limiting the application of this transformation for asymmetric synthesis. The particular regioselectivity of the catalyst was attributed to the presence of electron-withdrawing phosphorus atoms making the allylic carbon more prone to nucleophilic attack, hence favoring the formation of the branched product.

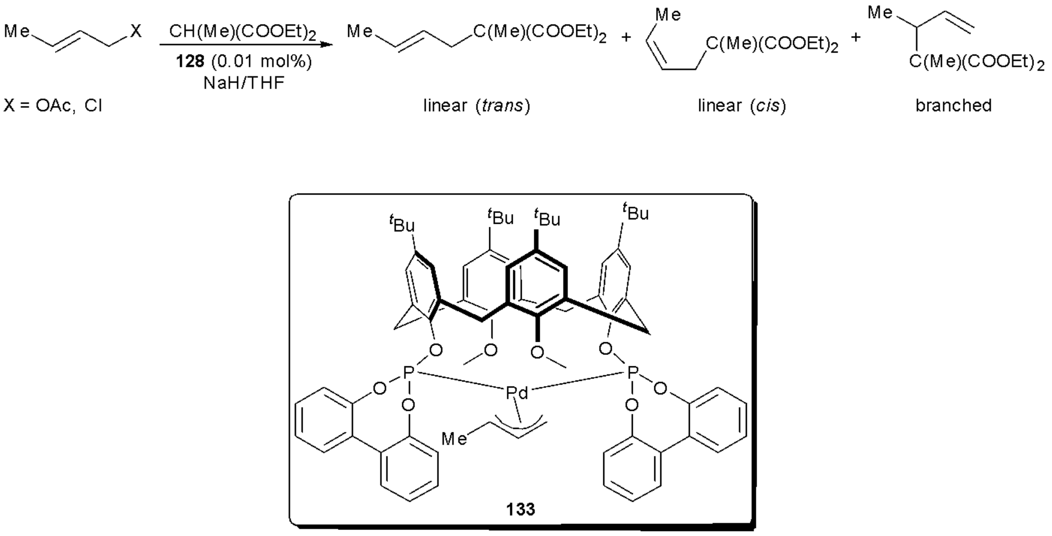

Scheme 14. Allylic substitution catalyzed by complex **133** [121].

Concomitantly, Kamer *et al.* reported the allylic alkylation of cinnamyl acetate with diethyl methylmalonate catalyzed by the [Pd(allyl)Cl]$_2$/**134** system (Scheme 15) [87]. Quantitative substrate conversion was achieved after 20 h at room temperature, affording a mixture of *trans* linear isomer (56%) and branched product (44%). Such regio- and stereoselectivity was found to be consistent to previously reports concerning Pd complexes of mixed P/N ligands [122]. Finally, optical active Pd-catalysts based on the P-chiragenic calix[4]arene mono- and diphosphines **135-140** were used for the enantioselective alkylation of (E)-(±)-1,3-diphenylprop-2-en-1-yl acetate with dimethyl malonate (Scheme 16) [123]. The catalysts were prepared *in-situ* by reacting the ligand with [Pd(allyl)Cl]$_2$ whilst the nucleophile was generated by reacting dimethyl malonate with a base. Selected results are reported in table 12.

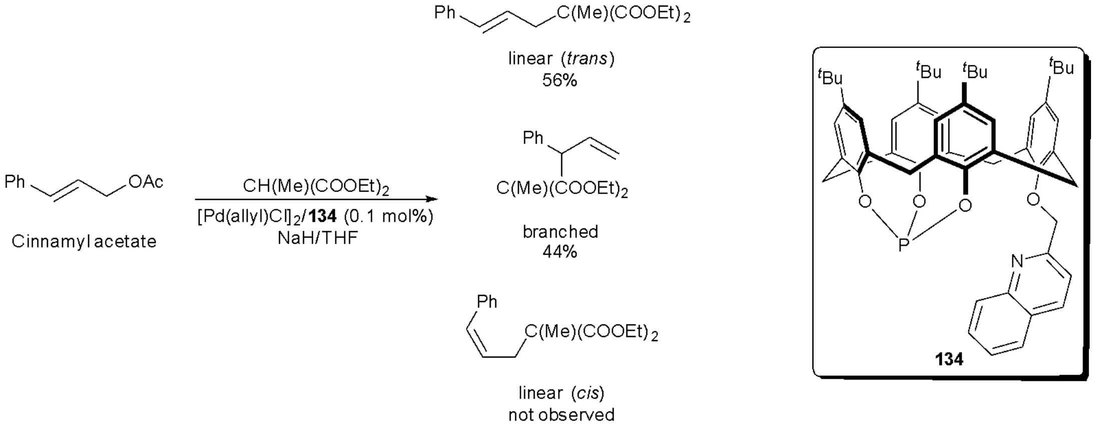

Scheme 15. Allylic substitution of cinnamyl acetate with a mixed P/N-palladium catalyst [87].

Complete conversion was observed within 1-20 h in dichloromethane with BSA (*N*,*O*-bis(trimethylsilyl)acetamide) as a base, regardless of the catalytic systems, affording the product as the (*S*)-isomer. Poor enantioselectivity was observed in the presence of **135** and **140** (5 and 16% *ee*, runs 1 and 6, respectively). Moderate selectivity was achieved with **138** at room temperature and 0 °C (70 and 73% *ee*, runs 2 and 3, respectively). Finally, 82% enantiomeric excess was reached upon using *n*BuLi as a base at 0°C in THF (run 4). In the case of benzylamine, the product was isolated as the (*R*)-isomer and the catalysts selectivity trend was found to be similar to that malonate reaction. Interestingly, good selectivity (*ee* 76%) was achieved with the mono-phosphine **136**, whilst a racemic mixture was isolated upon using **139**. In order to explain the higher selectivity of the [Pd]/**138** system, the optimized geometry of the complex was computed. The calculations showed a clear dissymmetry of both the HOMO and the LUMO, compatible with a complexes η^1-allyl moiety, thought to play a key role in the regio- and stereoselectivity of the nucleophilic attack.

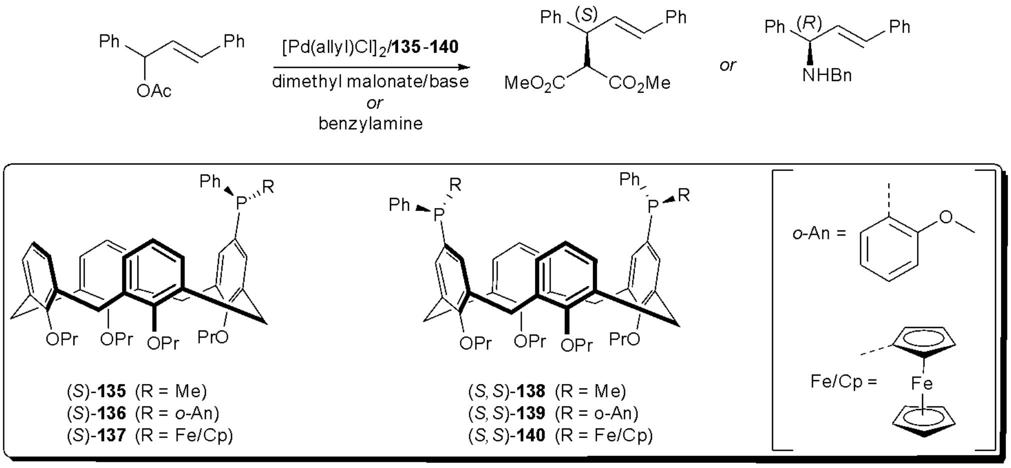

Scheme 16. Enantioselective Pd-catalyzed alkylation of (E)-(±)-1,3-diphenylprop-2-en-1-yl acetate [123].

Table 12. Enantioselective Pd-catalyzed alkylation of (E)-(±)-1,3-diphenylprop-2-en-1-yl acetate [123].

Run	Ligand	Base	Temperature (°C)	Solvent	Conversion (%)[a]	*ee*[b,c]
1	**135**	BSA	25	CH_2Cl_2	>99	5
2	**138**	BSA	25	CH_2Cl_2	>99	70
3	**138**	BSA	0	CH_2Cl_2	>99	73
4	**139**	*n*BuLi	0	THF	>99	82
5	**139**	BSA	25	CH_2Cl_2	>99	40
6	**140**	BSA	25	CH_2Cl_2	>99	16

Reaction conditions: 0.008 mmol of $[Pd(allyl)Cl]_2$, 0.016 mmol of ligand **138**-**140** (or 0.032 mmol of **135**), 0.8 mmol of (*E*)-(±)-1,3-diphenylprop-2-en-1-yl acetate, 1.6 mmol of dimethyl malonate and 1.6 mmol of base (and a catalytic amount of KOAc in the case of BSA) in 6 mL of dry solvent. Reaction times: 1-20 h. [a] Determined by ^1H NMR spectroscopy of the crude mixture. [b] Determined by HPLC. [c] (*S*) absolute configuration. BSA = *N*,*O*-bis(trimethylsilyl)acetamide.

5.8 Platinum

5.8.1 Cross-Coupling Reactions

Reports concerning calixarene-Pt catalysts are scarce. The Suzuki-Miyaura coupling of phenylboronic acid with different aryl halide promoted by complex **141** has been recently described by Krishnamurthy *et al.* (Figure 39 and table 13) [114]. In the case of iodobenzene, high yield was obtained with of 3 mol% of Pt (run 1) while moderate activity was shown with loadings as low as 1 and 0.5 mol% (runs 2 and 3, respectively). The catalyst was moderately active also in the case of bromobenzene (run 4), whilst a low yield was obtained with the more challenging substrate chlorobenzene (12% conversion, run 5).

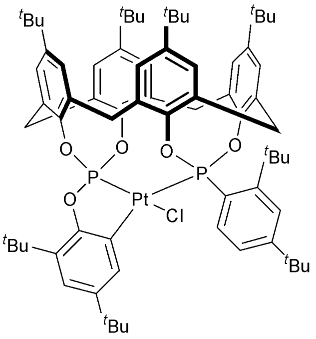

141

Figure 39. Cycloplatinated complex **141** [114].

para-Substituted bromo-benzenes were also tolerated, affording the corresponding bi-aryl products in *ca*. 50% isolated yield (runs 6 and 7). Remarkably, **141** proved to be better performing than its Pd-analogue **125** (Figure 36) under the same reaction conditions.

Table 13. Pt-catalyzed Suzuki-Miyaura coupling of phenylboronic acid and aryl halides [114].

Run	Substrate	Catalyst loading (mol%)	Isolated Yield (%)
1	Iodobenzene	3	88
2		1	76
3		0.5	67
4	Bromobenzene	1	51
5	Chlorobenzene	1	12
6	4-Bromotoluene	1	53

7	4-bromoanisole	1	47

Reaction conditions: $PhB(OH)_2$ 1.5 mmol, aryl halide 1 mmol, K_3PO_4 2 mmol, toluene 4 mL, T = 100 °C, 20 h.

5.8.2 Hydrogen Oxidation

Pt electrodes layered with the *S*-functionalized calixarene **142** (Figure 40) have been used in polymer electrolyte membrane fuel cells (PEMFCs) technology for the hydrogen oxidation reaction (HOR) [124]. Indeed, this type of chemical modification proved to limit the cathode degradation occurring during the shutdown/startup of the device yet with the same activity of conventional Pt-catalysts.

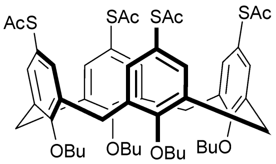

142

Figure 40. Upper rim functionalized calix[4]arene used in chemically modified electrodes for polymer electrolyte membrane fuels cells [124].

5.9 Copper

5.9.1 Oxidation Reactions

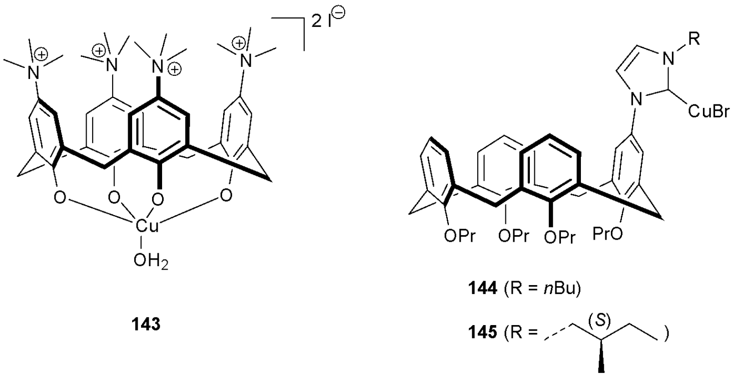

143

144 (R = *n*Bu)

145 (R =)

Figure 41. Copper complexes supported by calixarene-based ligands [125-128, 130].

In 2012, Lang *et al.* developed the zwitterionic Cu^{II} complex **143** (Figure 41), bearing a water soluble calix[4]arene scaffold [125]. The compound was tested as a catalyst in the aerobic oxidative polymerization of 2,6-dimethylphenol (DMP) in water (Scheme 17).

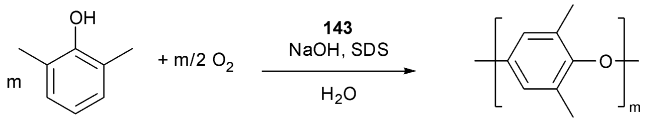

SDS = Sodium *n*-dodecyl sulfate

Scheme 17. Oxidative polymerization of 2,6-dimethylphenol in water catalyzed by **143** [125].

The reaction required a phase transfer agent (sodium *n*-dodecyl sulfate, SDS) to dissolve the monomer in water. The catalyst was found to be particularly active at 70 °C, affording polymers with M_n up to 10 kDa and polydispersities narrower than that achieved with previously reported copper catalysts [126]. Moreover, the complex was shown to be reusable several times without significant loss of activity.

Later, **143** was employed in the catalytic oxidation of benzyl alcohol to benzaldehydes in water with H_2O_2 as oxidant (Scheme 18) [127]. Higher conversions (90-98%) were obtained for substrates bearing electron-donating groups, while slightly lower activity was observed in the case of electron-poor aromatic rings. Moreover, the position of the substituent was found to affect the reactivity of the substrates (*para* > *meta* > *ortho*). Heteroatom-containing aromatic alcohols were also readily converted into their corresponding aldehydes, albeit in lower yield, while aliphatic and secondary alcohols remained almost unreacted. The reusability of the catalyst was considered also in this case. Nevertheless, a drop of activity of *ca*. 30% was observed already after the second cycle.

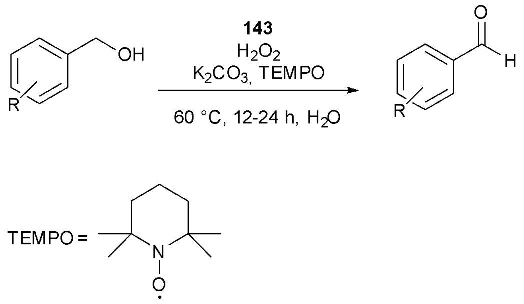

Scheme 18. Oxidation of benzyl alcohols with H_2O_2 in water catalyzed by **143** [127].

Finally, complex **143** was tested in the catalytic synthesis of quinoxalines via oxidative cyclization of deoxybenzoins with 1,2-phenylenediamines (Scheme 19) [128]. During the optimization of the reaction conditions, the catalyst proved to be effective both in the one-pot procedure and in the two-step approach (oxidation of the deoxybenzoins to benzyl followed by its condensation with the diamine). However, higher yields were achieved in the first case. Electron-withdrawing groups at the deoxybnezoin unit were well tolerated, while lower conversions were observed in the case of methoxy-substituted substrates. In the case of functionalized diamines, the opposite trend was observed. Indeed, low conversions (spanning from 30 to 45%) were obtained for *meta* substituted halide or nitro-diamines. Moreover, complete inactivity was observed in the case of *ortho*-substituted substrates, regardless of the electronic nature of the substituent. Unlike the previous examples, catalyst **143** could not be separated from the reaction mixture and reused due to the partial oxidation of the diamine.

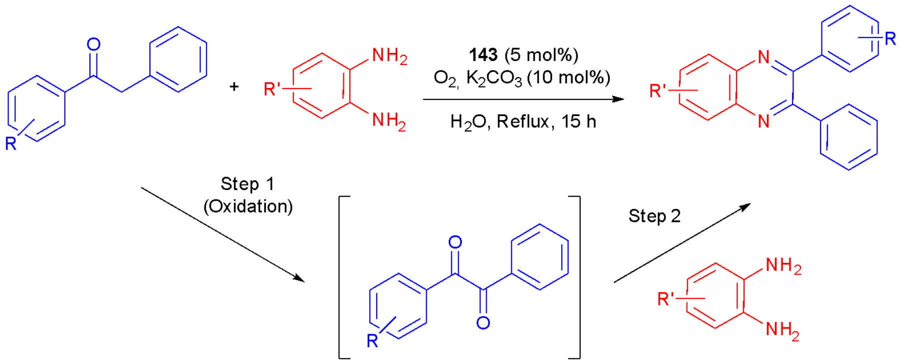

Scheme 19. Copper-catalyzed synthesis of quinoxalines [128].

5.9.2 Cycloaddition of Azides and Alkynes

The Cu^I-catalyzed cycloaddition of azides and alkynes (CuAAC) affording triazoles is undoubtedly the most common example of a Click-reaction [129]. In this scenario, copper complexes supported by *NHC*-functionalized calix[4]arene ligands (**144-145**, Figure 41) have recently been studied (Scheme 20) [130]. High functional group tolerance with respect to both azide and alkyne parts was observed. In fact, almost quantitative yield was achieved in all cases at room temperature with 1 mol% of **144**. Depending on the alkyne, the reaction time spanned from minutes to 4 hours. Only the reaction between phenylacetylene and 2-(azidomethyl)-1,3-dioxolane was unsuccessful. The optically active complex **145** was tested in the kinetic resolution of a racemic azide in order to prove its efficiency in asymmetric catalysis. Unfortunately, no selectivity was exhibited by the compound, since the reaction between phenylacetylene and (1-azidoethyl)benzene led to a racemic mixture of the corresponding triazole, as observed by chiral HPLC analysis.

In terms of heterogeneous systems, the copper polyoxometalate-based organic–inorganic hybrid was recently employed as catalyst in the CuAAC reaction [131]. High conversion and functional group tolerance were exhibited by the compound at 70 °C in methanol, affording variously substituted triazoles in almost quantitative yield within 10 h. Moreover, the catalyst could be reused up to five times maintaining its original activity.

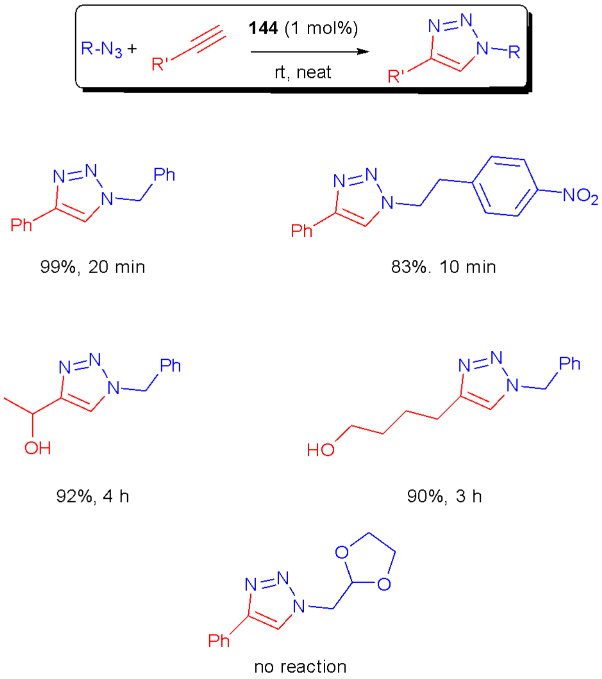

Scheme 20. Selected results for the cycloaddition of azides and alkynes (CuAAC) catalyzed by **144** [130].

5.10 Zinc

5.10.1 Ring Opening Polymerization of Cyclic Esters and Alcohol Acylation

Our group recently developed a series of zinc complexes based on calix[4]- and oxacalix[*n*]arenes (*n* = 3, 6) scaffolds (**146-148** and **149-150**, respectively, Figure 42) and their activity as catalysts for the ROP of ε-caprolactone was tested (Table 14) [70, 132].

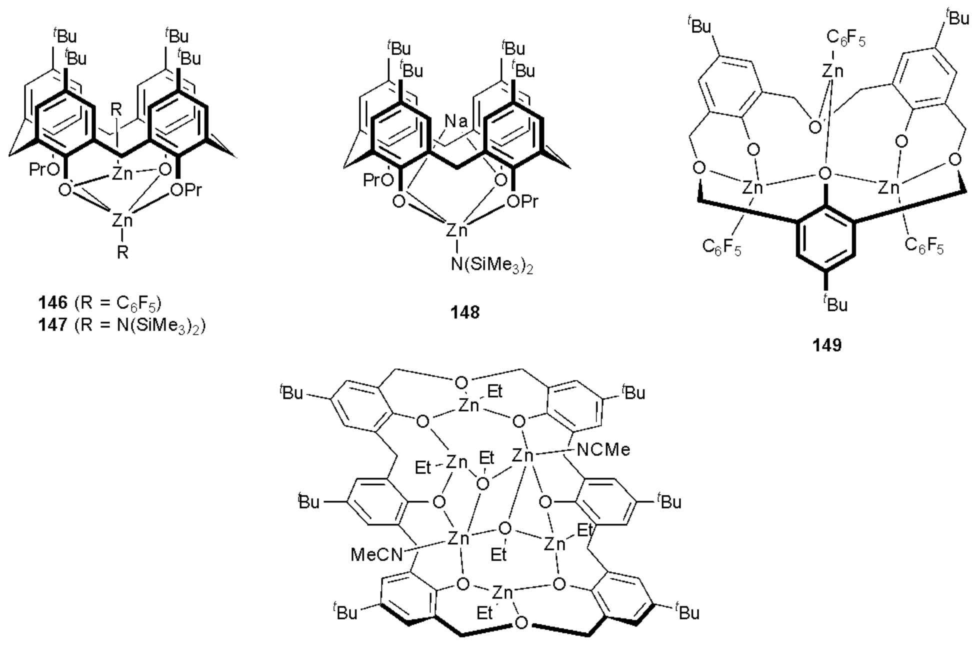

Figure 42. Zinc calixarene complexes used in the ROP of cyclic esters [70, 132].

Table 14. Selected date for the ROP of ε-CL catalyzed by Zn complexes **146-150** [70, 132].

Run	Complex	T (°C)	ε-CL:BnOH	Time (h)	Conv. (%)[a]	$M_{n\text{(obs.)}}$[b, c] (kDa)	$M_{n\text{(calc)}}$[d] (kDa)	M_w/M_n[b]
1	**146**	20	25:1	24	none	-	-	-
2		100	25:1	1	98	6.75	2.91	1.31
3		100	100:1	3	85	4.76	9.82	1.06
4	**147**	20	100:2	4	49	4.74	2.91	1.27
5	**148**	20	100:1	24	21	-	-	-
6	**149**	100	100:1	1	95	2.97	11.0	1.11
7	**150**	20	500:1	24	10	2.62	5.72	1.20
8		60	300:2	24	99	7.43	17.0	1.30

Reaction conditions: Toluene, BnOH taken from toluene solution. [a] Determined by ^{1}H NMR spectroscopy. [b] From GPC. [c] Values corrected using the Mark-Houwink factor of 0.56 from PS standards in THF. [d] Calculated from $M_{w(CL)}$ × $[CL]_0/[BnOH]_0$ × conversion + $M_{W(BnOH)}$.

Complex **146**, bearing a pentafluorophenyl ancillary ligand was inactive at room temperature, even with a low monomer:catalyst ratio (run 1). However, by increasing the temperature to 100 °C, almost complete monomer conversion was achieved in 1h, affording a polymer whose M_n was higher than the expected value (run 2). Under the same reaction conditions and by increasing the monomer:catalyst ratio to 100, 85% conversion was obtained in 3 h. The molecular weight of the polymer isolated in this run was *ca.* half of the calculated value, albeit with a narrow polydispersity (1.06, run 3). Interestingly, the *bis*-trimethylsilylamido derivative **147** proved active already at room temperature (run 4). On the other hand, the Na-containing complex **148** exhibited poor performances, allowing for only 21% conversion after 24 h at room temperature (run 5). The oxacalix[3]arene-based catalyst **149** was highly active (95% conversion in 1 h), generating a polymer with M_n lower than the calculated value, albeit with rather good control (run 6). Finally, the larger oxcalixarene-derivative **150** proved poorly active at room temperature with a high CL:catalyst ratio (500, run 7). Nevertheless, by performing the reaction at 60 °C with a higher catalyst loading and an additional equivalent of co-activator (BnOH), full conversion was observed after 24 h. The polymer exhibited M_n lower than expected, with a polydispersity index of 1.3 (run 8). Finally, complexes **146**, **147** and **149** were also tested in the ROP of *rac*-lactide; while **146** was active at room temperature, the remaining catalysts allowed for monomer conversion only at 100 °C. The syndiotactive bias (P_r) of the polymers isolated was found to be in the range of 0.64-0.62, suggesting the formation of heterotactic PLA.

Based on the promising results obtained with Ti-complexes bearing oxo-depleted mixed-*N*,*O*-butylcalix[4]arene [42], the corresponding Zn compound **151-152** was recently synthesized by Rawat *et al.* and tested as catalysts in the acylation of alcohols (Scheme 21) [133].

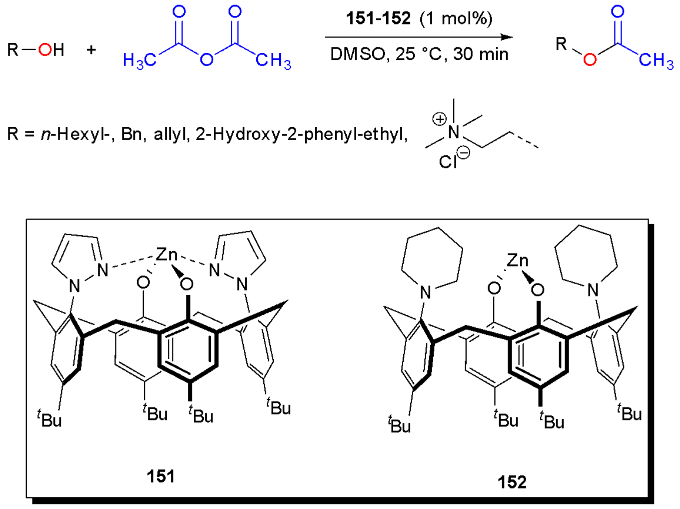

151

152

Scheme 21. Acylation of alcohols catalyzed by Zn complex bearing a 1,3-bis(pyrazole)-p-*tert*-butylcalix[4]arene ligand [133].

Complex **151** was found to be suitable for the conversion of all the investigated substrates, albeit requiring the presence of 1 equiv. (with respect to the substrate) of tetramethylammonium chloride in order to achieve complete conversion. On the other hand, **152** proved active only in the acylation of choline chloride in the absence of the additive. Finally, both complexes were tested in the ROP of *rac*-lactide. While the piperidine derivative **152** was inactive, its pyrazole congener allowed for complete monomer conversion in refluxing toluene with 1 mol% catalyst loading, affording a polymer with M_n of 16 kDa and rather broad polydispersity (1.78).

6. Rare Earth Metals

6.1 Ring Opening Polymerization of Cyclic Esters and Epoxides

Very recently, we have synthesized 8 novel multinuclear Sc-calix[*n*]arene (n = 4, 6 ,8) complexes by treating the parent calix[*n*]arene with either Sc(O*i*Pr)$_3$ or Sc(OTf)$_3$ [134,135]. Preliminary studies indicated these species were suitable as catalysts for the ROP of cyclic esters (ε-CL, δ-VL and *r*-LA) and cyclohexene oxide (CHO). In particular moderate monomer conversions (77 and 70% for ε-CL and CHO, respectively) towards low molecular weight oligomers were achieved with a mixed Sc/Na-calix[4]arene adduct under solvent free conditions within 24 hours. The larger calix[8]arene-based analogue proved inactive in the ROP of ε-CL. On the other hand, it allowed for 65% conversion towards a poly-cyclohexene oxide having a M_n of *ca*. 6 kDa and a M_w/M_n of 1.6. MALDI-ToF analysis of the samples suggested the formation of both linear and cyclic species.

To the best of our knowledge, this is the sole recent example of rare earth metal-calixarene complexes employed in catalytic reactions. Other recent reports concern the use calix[*n*]arenes in the selective extraction of rare earth metal ion from a number of different matrixes [136], while well-defined complexes have been mainly investigated in terms of their structural/luminescent features and coordination behavior [137,138].

In terms of catalytic applications, rare earth complexes of ligands related to calixarenes (calix[4]pyrroles) have been reported to promote the ROP of *L*-lactide [139] and the hydrophosphonylation of aldehydes and unactivated Ketones [140]. Nevertheless, all of the above subjects are beyond the scope of the present review and will not be further discussed.

7. Main Group Metals

7.1 Aluminum

7.1.1 Meerwein-Ponndorf-Verley (MPV) reduction of ketones

The Meerwein-Ponndorf-Verley (MPV) reduction of ketones to their corresponding alcohols promoted by Al-calix[4]arene complexes (Scheme 22) has been extensively investigated by the group of Katz [141]. The catalytically active species is generated *in-situ* by the reaction of the aluminocalixarene-Me precursors **153a-f** with the sacrificial alcohol under the reaction conditions. Compound **154**, featuring the Al-*i*Pr group, proved extremely versatile in the reduction of variously substituted ketones, exhibiting high functional group tolerance. Kinetic investigations highlighted a *zero-order* dependence of rate on ketone concentration.

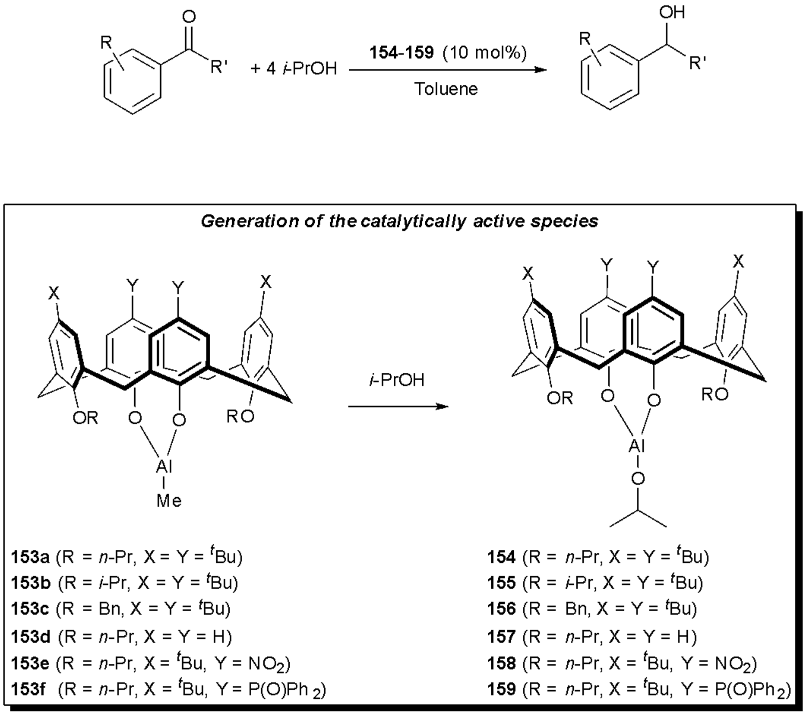

Scheme 22. Meerwein-Ponndorf-Verley (MPV) reduction of ketones catalyzed by **154-159** [141].

The effect of the calixarene structure on the reaction rate of the 2-chloroacetophenone reduction with *i*PrOH was next studied. By comparing the 1,3-substituents at the lower rim, the reaction rate followed the trend **154** > **156** > **155**, suggesting that increasing the size of the group is detrimental for the reaction. Nevertheless, it has to be noted that the reaction catalyzed by **156** is only 20% slower than that in the presence of the *n*Pr-analogues, while a 2-fold lower rate is observed upon using **155**. This is remarkable, since the *i*Pr- and Bn-groups have similar steric bulk. The higher activity of **156** compared to that of **155** was ascribed to π-interactions between the Al center and the aromatic rings of the Bn-substituents that would favor a more rigid catalyst structure, enhancing its activity. With respect to the substituents at the upper rim, replacement of all *tert*-butyl groups with H atoms (**157**) led to an increase of reaction rate by *ca*. 40%, while the nitro and phosphine-oxide congeners (**158** and **159**, respectively) proved poorly active and completely inactive, respectively. This was explained in terms of the possible coordination of these substrates to the metal center. Furthermore, the catalytic species generated by reacting **153** with secondary alcohols were found more active than those generated from primary ones. With respect to the ketone, enhanced reactivity was observed in the case of benzophenones bearing *ortho*- and *para* halide substituents.

The asymmetric version of this reaction was later disclosed. In this case, the reaction was promoted by Al catalysts based on chiral 1,3-phosphite substituted calixarenes **160**-**164** (Scheme 23) [142]. When using **160** for the reduction of *o*-fluorobenzophenone, high enantioselectivity (>99%) was observed during the early stages of the reaction, while a drop of *ee* (80%) was achieved at higher conversions. Better performance, both in terms of conversion and enantioselectivity, were exhibited by **161**. This was attributed to the extended π-delocalization in its (*S*)-VANOL group compared to that of the (*S*)-BINOL moiety of **160**. On the other hand, low activity and almost no selectivity were achieved with **162**. This suggested that further extension of π-delocalization is detrimental for the reaction. The important role of such electron-delocalization was confirmed by the poor selectivity of complexes **163** and **164**. Both compounds lack of direct bonding between the P-atoms and the aromatic rings of the phosphite group, hence no electron delocalization can occur. This was thought to limit the transmission of chiral information causing a decrease of enantioselectivity. Steric effects also proved relevant. In fact, the reduction of the less hindered substrate *o*-chloroacetophenone, only 40% enantiomeric excess was obtained in the presence of catalyst **160**.

Finally, the same group investigated the behaviour of silica-grafted Al-calixarene complexes in the MPV reduction of 2-chloroacetophenone with isopropanol as reducing agent [143]. Depending on the approach followed for the synthesis of these heterogeneous catalysts, species having "open" and "closed" active sites were isolated. As expected, "open-site" catalysts performed as good as the corresponding homogeneous systems, while no activity was observed in the case of the "closed-site" counterparts. In contrast, both types of catalysts were found to be active in the oxidation of cyclohexene to cyclohexene oxide with *tert*-butyl hydroperoxide. This suggested that, unlikely the MPV reductions, the formation of a covalent bond between the accessible Al centers and the substrate is not required for the olefin epoxidations with organic peroxides.

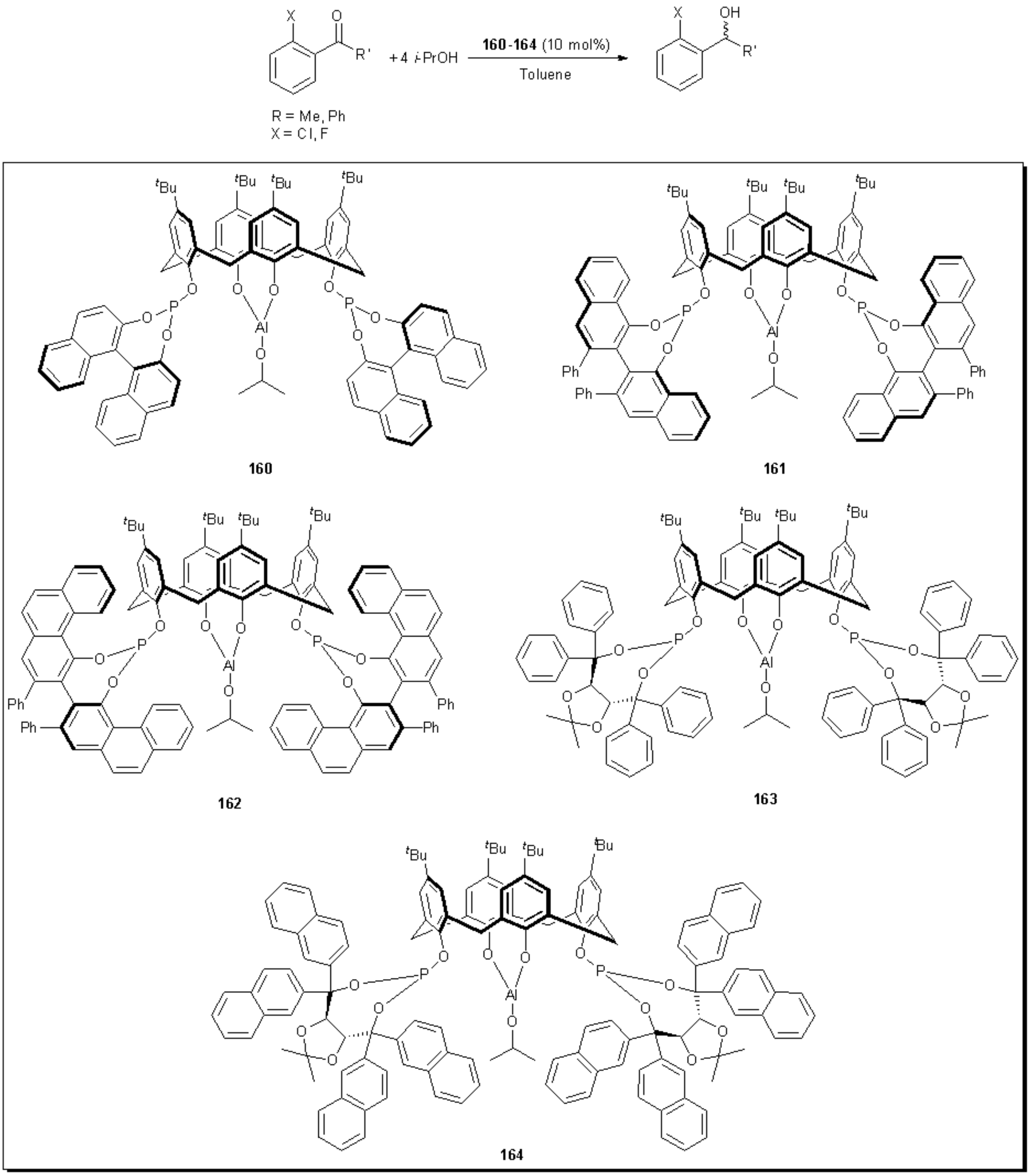

Scheme 23. Enantioselective Meerwein-Ponndorf-Verley (MPV) reduction of ketones catalyzed by chiral Al-calixarene complexes **160-164** [142].

8. Concluding Remarks

The outputs described in this review underline the efficiency of metallocalix[*n*]arene complexes in numerous catalytic reactions. A summary of these transformations is shown below in Chart 2. Cross-coupling reactions, olefin oxidation and polymerization processes are the most studied fields. Remarkably, while olefin polymerization was the most investigated topic in our 2008 review, over the past 12 to 13 years, the interest in this area has been gradually dropping. On the other hand, increasing attention has been dedicated to the ROP of cyclic esters. This is in line with the growing demand for biodegradable polymers derived from renewable sources that should limit the use of single-use petroleum-based polyolefins with the intent of reducing plastic pollution.

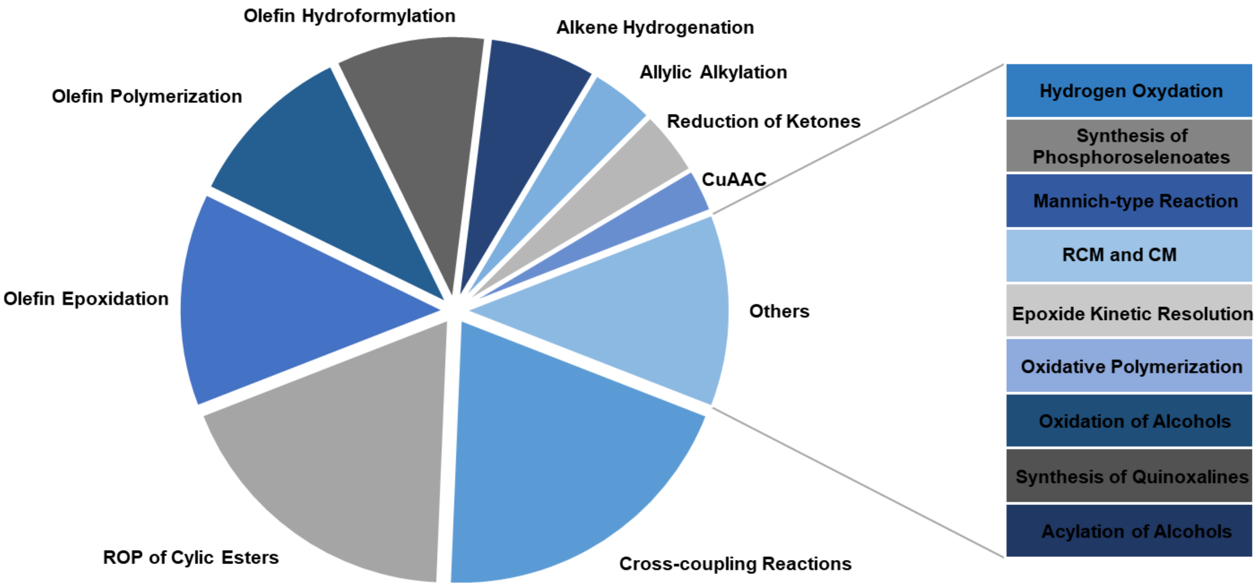

Chart 2. Breakdown of the reactions catalyzed by metallocalix[*n*]arene complexes described in this review.

Although general trends cannot be drawn due to the breadth of the systems/reactions discussed, some considerations can still be made. For instance, Ti-based complexes bearing larger calix[*n*]arenes (n = 6 or 8) were shown to be less efficient catalyst for the ROP of cyclic esters than their smaller congeners; similarly, the presence of multiple metal centers onto the calixarene scaffold also proved detrimental, especially in terms of polymerization control (*cf.* refs. 32 and 35]. Interestingly, the opposite behaviour was observed for the Ti-catalyzed olefin polymerization [25].

The nature of the ancillary ligands was also shown to affect the efficiency of the metallocalixarene catalysts, albeit such influence was also dependent on the system/process investigated. In fact, while the presence of a labile ligand (I, Br or MeCN) proved beneficial for the titancalixarene-catalyzed ROP of lactones [32, 37], the opposite was observed for the Buchwald-Hartwig coupling promoted by Pd(X)(cinnamyl)(NHC-calix[8]arene) (X = Cl, I) species [119] or in the Ni-catalyzed electrolytic CO_2 reduction [105].

Remarkably, metallocalixarenes displayed higher efficiency compared to other benchmark systems. Indeed, Ni-calix[4]arene-iminophosphorane and Pd-calix[4]arene-monophosphine complexes displayed turn over frequencies up to 6 orders of magnitude higher than conventional phosphine-based systems in cross-coupling reactions [102, 111]. Moreover, in the case of asymmetric transformations, the presence of the calixarene cavity allowed for enhanced enantioselectivity [123, 142].

Heterogeneous systems featuring metallocalixarenes grafted onto inert supports have emerged as an interesting class of class of practical and reusable catalysts for several transformations, such as olefin epoxidation [43, 46], three-component- [73] and cross-coupling reactions [119]. Notably, in the latter example, the calixarene scaffolds serve also as support for the actual catalyst.

The majority of the reports concerned the use of calix[4]arene scaffolds, while limited attention has been dedicated to the larger congeners. These systems remain attractive since, along with the positive features of their smaller analogues, offer the possibility to coordinate multiple metal centers, allowing for cooperative effects enhancing the activity of the catalysts. Moreover, the larger calix[*n*]arenes have increased conformational flexibility and can therefore adapt more readily to the energy requirements of a catalytic process. In this field, the development of homo- and hetero-multimetallic complexes based on larger calix[*n*]arenes (n >4) is currently ongoing in our laboratory. In fact, heterbimetallic systems often exhibited enhanced activity compared to that of their homometallic analogues [17, 135]. This is probably due to cooperative effects between the different metal centers.

9. Acknowledgements

We thank the UKRI Creative Circular Plastic grant (EP/S025537/1) for support.

10. References

[1] R. Kumar, A. Sharma, H. Singh, P. Suating, H. S. Kim, K. Sunwoo, I. Shim, B. C. Gibb and J. S. Kim, Chem. Rev. 119 (2019), 9657-9721.

[2] B. Mokhtari, K. Pourabdollah and N. Dallali, J. Radioanal. Nucl. Chem., 287 (2011) 921–934.

[3] S. J. Dalgarno, P. K. Thallapally, L. J. Barbour and J. L. Atwood, Chem. Soc. Rev., 32 (2007) 236–245.

[4] C.D. Gutsche, Calixarenes, Royal Society of Chemistry, Cambridge, 1989.

[5] D. M. Roundhill, Prog. Inorg. Chem. 43 (1995) 553-592.

[6] C. Wieser, C. B. Dielman, D. Matt, Coord. Chem. Rev. 165 (1997) 93-161.

[7] A. Ikeda, S. Shinkai, Chem. Rev. 97 (1997) 1713-1734.

[8] C. D. Gutsche, Calixarenes Revisited, Royal Society of Chemistry, Letchworth, 1988.

[9] J. L. Atwood, L. J. Barbour, M. J. Hardie, C. L. Raston, Coord. Chem. Rev. 222 (2001) 3-32.

[10] Z. Asfari, V. Bo¨hmer, J. Harrowfield, J. Vicens (Eds.), Calixarenes 2001, Kluwer, Dordrecht, 2001.

[11] P. D. Harvey, Coord. Chem. Rev. 233/234 (2002) 289-309.

[12] C. Redshaw, Coord. Chem. Rev. 244 (2003) 45-70.

[13] C. D. Gutsche and L. J. Bauer, J. Am. Chem. Soc. 1985, 107, 6052-6059.

[14] D. M. Homden and C. Redshaw, Chem. Rev. 108 (2008) 5086-5130.

[15] O. Santoro, M. R. J. Elsegood, S. J. Teat, T. Yamato and C. Redshaw, RSC Adv. 11 (2021) 11304-11317.

[16] For more information concerning the concepts of *living* and *immortal* polymerization please see the following review: N. Ajellal, J.-F. Carpentier, C. Guillaume, S. M. Guillaume, M. Helou, V. Poirier, Y. Sarazin and A. Trifonov, Dalton Trans. 39 (2010) 8363-8376.

[17] T. Xing, C. Jiang, M. R. J. Elsegood and C. Redshaw *Unpublished Results.*

[18] R. McLellan, J. Rezé, S. M. Taylor, R. D. McIntosh, E. K. Brechin and S. J. Dalgarno, Chem. Commun. 50 (2014) 2202-2204.

[19] S. Chen, J. Chen, X. Xu, Y. He, R. Yi, R. Qiu, J. Organomet. Chem. 818 (2016) 123-127.

[20] Y. Li, H. Zhao, X. Mao, X. Pan and J. Wu, Dalton Trans. 45 (2016) 9636-9645.

[21] S. M. Kang, C. H. Kim, K. C. Lee and D. W. Kim, Org. Lett. 21 (2019) 3062-3066.

[22] M. J. Walton, S. J. Lancaster and C. Redshaw, ChemCatChem 6 (2014) 1892-18098.

[23] C. Ludwig and M. R. Viant, Phytochem. Anal. 21 (2010) 22-32.

[24] The terms *iso-* and *heterotactive* as well as the parameters P_r and/or P_m refer to the PLA microstructure. For further information please see: O. Santoro, X. Zhang and C. Redshaw, Catalysts 10 (2020) 800-848.

[25] O. Santoro and C. Redshaw, Catalysts 10 (2020) 210-238.

[26] O.V. Ozerova, N. P Rathb, and F. T Ladipo, J. Organomet. Chem. 586 (1999) 223–233.

[27] M. Frediani, D. Sémeril, A. Comucci, L, Bettucci, P. Frediani, L. Rosi, D. Matt, L. Toupet, and W. Kaminsky, Macromol. Chem. Phys. 208 (2007) 938–945.

[28] J. Espinas, U. Darbost, J. Pelletier, E. Jeanneau, C. Duchamp, F. Bayard, O. Boyron, J.-P. Broyer, J. Thivolle-Cazat, J.-M. Basset, M. Taoufik and I. Bonnamour, Eur. J. Inorg. Chem. (2010) 1349-1059.

[29] A. Proto, F. Giugliano and C. Capacchione, Eur. Polym. J. 45 (2009) 2138-2141.

[30] M. Frediani, D. Sémeril, A. Mariotti, L. Rosi. P. Frediani, L. Rosi, D. Matt and L. Toupet, Macromol. Rapid Commun. 29 (2008) 1554-1560.

[31] M. Frediani, D. Sémeril, D. Matt, L. Rosi, P. Frediani, F. Rizzolo and A. M. Papini, Int. J. Polym. Sci. (2010) Article ID 490724, 6 pages.

[32] Z. Sun, Y. Zhao, O. Santoro, M. R. J. Elsegood, E. V. Bedwell, K. Zahra, A. Walton and C. Redshaw, Catal. Sci. Technol. 10 (2020) 1619-1639.

[33] K. Rodgers, W. Mayes, O. Santoro, C. Redshaw, R. Mccumskay and D. R. Parsons, Mar. Pollut. Bull. 167 (2021) 112272.

[34] J. D. Ryan, K. J. Gagnon, S. J. Teat and R. D. McIntosh, Chem. Commun. 52 (2016) 9071-9073.

[35] O. Santoro, M. R. J. Elsegood, E. V. Bedwell, J. A. Pryce and C. Redshaw, Dalton Trans. 49 (2020) 11978-11996.

[36] T. Xing, Z.-Y. Wang, Y.-C. Sun, Z.-H. He, K. Wang, Z.-T. Liu, M. R. J. Elsegood, E. V. Bedwell and C. Redshaw, J. Appl. Polym. Sci. 138 (2021) 50513.

[37] T. Xing, T. J. Prior, K. Chen and C. Redshaw, Dalton Trans. 50 (2021) 4396-4407.

[38] T. Katsuki and K. B. Sharpless, J. Am. Chem. Soc., 102 (1980) 5974-5976.

[39] K. Matsumoto, Y. Sawada, B. Saito, K. Sakai and T. Katsuki, Angew. Chem., Int. Ed., 44 (2005) 4935-4939.

[40] Y. Sawada, K. Matsumoto and T. Katsuki, Angew. Chem., Int. Ed., 46 (2007) 4559-4561.

[41] A. Berkessel, T. Guther, Q. Wang and J.-M. Neudorfl, Angew. Chem., Int. Ed., 52 (2013) 8467-8471.

[42] V. Rawat, K. Press, I. Goldberg and A. Vigalok, Org. Biomol. Chem. 13, (2015) 11189-11193.

[43] N. E. Thornburg, A. B. Thompson and J. M. Notestein, ACS Catal. 5 (2015) 5077-5088.

[44] N. A. Grosso-Giordano, C. Schroeder, A. Okrut, A. Solovyov, C. Schöttle, W. Chassé, N. Marinković, H. Koller, S. I. Zones and A. Katz, J. Am. Chem. Soc. 140 (2018) 4956-4960.

[45] N. A. Grosso-Giordano, A. S. Hoffman, A. Boubnov, D. W. Small, S. R. Bare, S. I. Zones and A. Katz, J. Am. Chem. Soc. 141 (2019) 7090-7106.

[46] L. Winner, G. Daniloff, R. V. Nichiporuk, A. Solovyov and A. Katz, Top Catal. 58 (2015) 441-450.

[47] X. Wang, Y. Yu, Z. Wang, J. Zheng, Y. Bi and Z. Zheng, Inorg. Chem. 59 (2020) 7150-7157.

[48] X.-X. Yang, W.-D. Yu, X.-Y. Yi and C. Liu, Inorg. Chem. 59 (2020) 7512-7519.

[49] X.-X. Yang, W.-D. Yu, X.-Y. Yi, L.-J. Li and C. Liu, Chem. Commun. 56 (2020) 14035-14038.

[50] N. Li, J.-J. Liu, J.-W. Sun, B.-X. Dong, L.-Z. Dong, S.-J. Yao, Z. Xin, S.-L. Li and Y.-Q. Lan, Green Chem. 22 (2020) 5325-5332.

[51] R. Lapenta, N. A. De Simone, A. Buonerba, C. Talotta, C. Gaeta, P. Neri, A. Grassi and S. Milione, Catal. Sci. Technol. 8 (2018) 2716-2727.

[52] C. Redshaw, L. Clowes, D. L. Hughes, M. R. J. Elsegood and T. Yamato, Organometallics 30 (2011) 5620-5624.

[53] S. Gambarotta, Coord. Chem. Rev. 237 (2003) 229-243.

[54] C. Redshaw, M. A. Rowan, L. Warford, D. M. Homden, A. Arbaoui, M. R. J. Elsegood, S. H. Dale, T. Yamato, C. P. Casas, and S. Matsui, Chem. Eur. J. 13 (2007) 1090-1107.

[55] I. E. Soshnikov, N. V. Semikolenova, A. A. Shubin, K. P. Bryliakov, V. A. Zakharov, C. Redshaw, and E. P. Talsi, Organometallics 28 (2009) 6714-6720.

[56] L. Clowes, C. Redshaw and D. L. Hughes, Inorg. Chem. 50 (2011) 7838-7845.

[57] C. Redshaw, M. J. Walton, D. S. Lee, C. Jiang, M. R. J. Elsegood and K. Michiue, Chem. Eur. J. 21 (2015) 5199-5210.

[58] T. Xing, T. J. Prior, M. R. J. Elsegood, N. V. Semikolenova, I. E. Soshnikov, K. Bryliakov, K. Chen and C. Redshaw, Catal. Sci Tech. 11 (2021) 624-636.

[59] R. L. Meyer, P. Miró, W. W. Brennessel and E. M. Matson, Inorg. Chem. DOI: 10.1021/acs.inorgchem.1c00887.

[60] N. E. Thornburg, S. L. Nauert, A. B. Thompson and J. M. Notestein, ACS Catal. 6 (2016) 6124-6134.

[61] N. Morlanés and J. M. Notestein, App. Catal. A – Gen., 387 (2010) 45-54.

[62] N. Morlanés and J. M. Notestein, J. Catal. 275 (2010) 191-201.

[63] C. Redshaw, D. Homden, D. L. Hughes, J. A. Wright and M. R. J. Elsegood, Dalton Trans. (2009) 1231-1242.

[64] S. Acharya and T. A. Hanna, Polyhedron 107 (2016) 113-123.

[65] Z. Sun, Y. Zhao, T. J. Prior, M. R. J. Elsegood, K. Wang, T. Xing and C. Redshaw, Dalton Trans. 48 (2019) 1454-1466.

[66] Y. Li, K.-Q. Zhao, C. Feng, M. R. J. Elsegood, T. J. Prior, X. Sun and C. Redshaw, Dalton Trans. 43 (2014) 13612-13619.

[67] L.-L. Liu, H.-X. Li, L.-M. Wan, Z.-G. Ren, H.-F. Wang and J.-P. Lang, Chem. Commun. 47 (2011) 11146-11148.

[68] C. Bonaccorso, G. Brancatelli, F. P. Ballistreri, S. Geremia, A. Pappalardo, G. A. Tomaselli, R. M. Toscano and D. Sciotto, Dalton Trans. 43 (2014) 2183-2193.

[69] R. V. Patel, J. G. Panchal, B. R. Mistry and S. K. Menon, Incl. Phenom. Macrocycl. Chem. 74 (2012) 473-480.

[70] A. Arbaoui, C. Redshaw, M. R. J. Elsegood, V. E. Wright, A. Yoshizawa and T. Yamato, Chem. Asian J. 5 (2010) 621-633.

[71] O. Dechy-Cabaret, B. Martin-Vaca, D. Bourissou, Chem. Rev. 104 (2004) 6147-6176.

[72] A. Crochet and K. M. Fromm, Polyhedron 52 (2013) 610-616.

[73] S. Sayin and M. Yilmaz, RSC Adv. 7 (2017) 10748-10756.

[74] T. Brendgen, T. Fahlbusch, M. Frank, D. T. Schuhle, M. Seßler and J. Schatza, Adv. Synth. Catal. 351 (2009) 303-307.

[75] A. K. Chatterjee, J. P. Morgan, M. Scholl, R. H. Grubbs, J. Am. Chem. Soc. 122 (2000) 3783-3784.

[76] S. B. Garber, J. S. Kingsbury, B. L. Gray, A. H. Hoveyda, J. Am. Chem. Soc. 122 (2000) 8168-8179.

[77] N. Noll and F. Werthner, Chem. Eur. J. 27 (2021) 444-450.

[78] R. V. Patel, J. G. Panchal and S. K. Menon, Incl. Phenom. Macrocycl. Chem. 67 (2010) 63-71.

[79] I. Abdellah, C. Martini, A. Dos Santos, D. Dragoe, V. Guérineau, V. Huc and E. Schulz, ChemCatChem 10 (2018) 4761-4767.

[80] A. Ignaszak, N. Patterson, M. Radtke, A. True, M. R. J. Elsegood, T. J. Prior and C. Redshaw *Unpublished Results*

[81] W. Seiche, A. Schuschkowski, B. Breit, Adv. Synth. Catal. 347 (2005) 1488 – 1494.

[82] D. Sémeril, C. Jeunesse, D. Matt, L. Toupet, Angew. Chem. Int. Ed. 45 (2006) 5810 – 5814.

[83] D. S. Meril, D. Matt, L. Toupet, Chem. Eur. J. 14 (2008) 7144 – 7155.

[84] C. J. Cobley, D. D. Ellis, A. G. Orpen, P. G. Pringle, J. Chem. Soc. Dalton Trans. (2000) 1109 – 1112.

[85] C. K. Brown, G. Wilkinson, J. Chem. Soc. A (1970) 2753 – 2764.

[86] D. Sémeril, D. Matt, L. Toupet, W. Oberhauser and C. Bianchini, Chem. Eur. J. 16, (2010) 13843-13849.

[87] A. Marson, J. E. Ernsting, M. Lutz, A. L. Spek, P. W. N. M. van Leeuwen and P. C. J. Kamer, Dalton Trans. (2009) 621-633.

[88] L. Monnereau, D. Sémeril, D. Matt and L. Toupet, Adv. Synth. Catal. 351 (2009) 1629-1636.

[89] C. J. Cobley and P. G. Pringle, Catal. Sci. Technol. 1 (2011) 239-242.

[90] N. A. Drigo, A. N. Gorbunov, D. N. Gorbunov, M. Y. Talanova, Y. S. Kardasheva, V. V. Kovalev, A. L. Maximov, I. M. Vatsouro, Chem. Heterocycl. Comp. 52 (2016) 1042-1053.

[91] F. Elaieb, D. Sémeril, D. Matt, M. Pfeffer, P.-A. Bouit, M. Hissler, C. Gourlaouen and J. Harrowfield, Dalton Trans. 46 (2017) 9833-9845.

[92] J. M. Brown, in: E. N. Jacobsen, A. Pfaltz, H. Yamamoto (Eds.), Comprehensive Asymmetric Catalysis, vol. 1, Springer, Berlin, 1999, (Chapter 5.1).

[93] T. Ohkuma, M. Kitamura, R. Noyori, in: I. Ojima (Ed.), Catalytic Asymmetric Synthesis, 2nd ed., Wiley–VCH, New York, 2000 (Chapter 1).

[94] J. G. de Vries, in: C. J. Elsevier (Ed.), The Handbook of Homogeneous Hydrogenation, vols. 1–3, Wiley–VCH, Weinheim, 2007.

[95] S. Liu and C. A. Sandoval, J. Mol. Catal. A: Chem. 325 (2010) 65-72.

[96] N. Khiri, E. Bertrand, M. -J. Ondel-Eymin, Y. Rousselin, J. Bayardon, P. D. Harvey and S. Jugé, Organometallics 29 (2010) 3622-3631.

[97] L. Monnereau, D. Sémeril, D. Matt, L. Toupet, Polyhedron 51 (2013) 70-74.

[98] A. Palermo, A. Solovyov, D. Ertler, A. Okrut, B. C. Gates and A. Katz, Chem. Sci. 8 (2017) 4951-4960.

[99] C. Schöttle, E. Guan, A. Okrut, N. A. Grosso-Giordano, A. Palermo, A. Solovyov, B. C. Gates and A. Katz, J. Am. Chem. Soc. 141 (2019) 4010-4015.

[100] L. Monnereau, D. Sémeril, D. Matt, L. Toupet and A. J. Mota, Adv. Synth. Catal. 351 (2009) 1383-1389.

[101] L. Monnereau, D. Sémeril and D. Matt, Chem. Commun., 47 (2011) 6626–6628.

[102] L. Monnereau, D. Sémeril and D. Matt, Adv. Synth. Catal. 355 (2013) 1351-1360.

[103] L. Monnereau, D. Sémeril, D. Matt and C. Gourlaouen, Eur. J. Inorg. Chem. (2017) 581-586.

[104] L. Alouia, R. Abidi, M. J. Chetcuti, Inorg. Chim. Acta 505 (2020) 119494-119499.

[105] C. A. Reyes-Mata and I. Castillo, Inorg. Chim. Acta 507 (2020) 119607-119613.

[106] T. A. Al-Attas, H. Zahir, S. A. Ali, S. A. Al-Bogami, Z. Malaibari, S. A. Razzak, and M. M. Hossain, Fuel Process. Technol. 185 (2019) 158-168.

[107] T. Fahlbusch, M. Frank, G. Maas and J. Schatz, Organometallics 28 (2009) 6183-6193.

[108] E. Brenner, D. Matt, M. Henrion, M. Tecia and L. Toupet, Dalton Trans. 40 (2011) 9889-9898.

[109] H. Ren, Y. Xu, E. Jeanneau, I. Bonnamour, T. Tu and U. Darbost, Tetrahedron 70 (2014) 2829-2837.

[110] E. K. Bullough, M. A. Little and C. E. Willans, Organometallics 32 (2013) 570-577.

[111] L. Monnereau, D. Sémeril, D. Matt and L. Toupet, Chem. Eur. J. 16 (2010) 9237-9247.

[112] K. Hirasawa, S. Tanaka, T. Horiuchi, T. Kobayashi, T. Sato, N. Morohashi and T. Hattori, Organometallics 35 (2016) 420-427.

[113] M. A. Zuideveld, B. H. G. Swennenhuis, M. D. K. Boele, Y. Guari, G. P. F. van Strijdonck, J. N. H. Reek, P. C. J. Kamer, K. Goubitz, J. Fraanje, M. Lutz, A. L. Spek, P. W. N. M van Leeuwen, J. Chem. Soc., Dalton Trans. (2002) 2308−2317.

[114] P. Maji, L. Mahalakshmi, S. S. Krishnamurthy and M. Nethaji, J. Organomet. Chem. 696 (2011) 3169-3179.

[115] B. Mua, J. Li, Z. Han and Y. Wu, J. Organomet. Chem. (700) 2012 117-124.

[116] I. Abdellah, P. Kasongo, A. Labattut, R. Guillot, E. Schulz, C. Martini and V. Huc, Dalton Trans. 47 (2018) 13843-13848.

[117] A. Labattut, S. A. Fayssal, J. Buendia, I. Abdellah, V. Huc, C. Martini and E. Schulz, React. Chem. Eng., 5 (2020) 1509-1514.

[118] A. Peramo, I. Abdellah, S. Pecnard, J. Mougin, C. Martini, P. Couvreur, V. Huc and D. Desmaële, Molecules 25 (2020) 1459-1472.

[119] S. Abi Fayssal, T. Naret, V. Huc, J. Buendia, C. Martini and E. Schulz Catal. Sci. Technol. 11 (2021) 5223-5231

[120] I. G. Rios, A. Rosas-Hernandez and E. Martin, Molecules 2011, 16, 970-1010.

[121] A. Sarkar, S. S. Krishnamurthy, M. Nethaji, Tetrahedron 65 (2009) 374-382.

[122] R. J. van Haaren, C. J. M. Druijven, G. P. F. van Strijdonck, H. Oevering, J. N. H. Reek, P. C. J. Kamer and P. W. N. M. van Leeuwen, J. Chem. Soc., Dalton Trans., (2000) 1549-1554.

[123] N. Khiri-Meribout, E. Bertrand, J. Bayardon, M. -J. Eymin, Y. Rousselin, H. Cattey, D. Fortin, P. D. Harvey and S. Jugé, Organometallics 32 (2013) 2827-2839.

[124] B. Genorio1, D. Strmcnik, R. Subbaraman, D. Tripkovic, G. Karapetrov, V. R. Stamenkovic, S. Pejovnik and N. M. Markovic, Nature Mater. 9 (2010) 998-1003.

[125] L.-M. Wan, H.-X. Li, W. Zhao, H.-Y. Ding, Y.-Y. Fang, P.-H. Ni, J.-P. Lang, J. Polym. Sci. A Polym. Chem. 50 (2012) 4864-4870.

[126] C. Gu, K. Xiong, B. Q. Shentu, W. L. Zhang and Z. X. Weng, Macromolecules 43 (2010) 1695-1698.

[127] J. Gao, Z.-G. Ren and J.-P. Lang, J. Organomet. Chem. 792 (2015) 88-92.

[128] J. Gao, Z.-G. Ren and J.-P. Lang, Chinese Chem. Lett. 28 (2017) 1087-1092.

[129] L. Liang and D. Astruc, Coord. Chem. Rev. 255 (2011) 2933-2045.

[130] B. Ourri, O. Tillement, T. Tu, E. Jeanneau, U. Darbost and I. Bonnamour, New J. Chem. 40 (2016) 9477-9485.

[131] L.-J. Yue, Y. -Y. Liu, G. -H. Xu and J. -F. Ma, New J. Chem. 43 (2019) 15871-15878.

[132] M. J. Walton, S. J. Lancaster, J. A. Wright, M. R. J. Elsegood and C. Redshaw, Dalton Trans. 43 (2014) 18001-18009.

[133] A. K. Sinha, A. Vigalok, V. Rawat, Tetrahedron Lett. 60, (2019) 796-799.

[134] Although Scandium is a d-block element, it is historically considered a rare earth element.

[135] A. F. A. Alshamrani, O. Santoro, T. J. Prior, M. Alamri, G. Stasiuk, M. R. J. Elsegood and C. Redshaw, Dalton Trans. 50 (2021) 8302-8306.

[136] S. R. Menon and J. A. R. Schmidt, Tetrahedron, 72 (2016) 767-774.

[137] A. S. Ovsyannikov, I. V. Khariushin, S. E. Solovieva, I. S. Antipin, H. Komiya, N. Marets, H. Tanaka, H. Ohmagari, M. Hasegawa, J. J. Zakrzewski, S. Chorazy, N. Kyritsakas, M. W. Hosseini and S. Ferlay, RSC Adv., 10 (2020) 11755-11765.

[138] R. S. Viana, C. A. F. Oliveira J. Chojnacki, B. S. Barros, S. Alves-Jr and J. Kulesza, J. Solid State Chem. 251 (2017) 26-32.

[139] S. Zhou, S. Wu, H. Zhu, S. Wang, X. Zhu, L. Zhang, G. Yang, D. Cuia and H. Wang, Dalton Trans., 40 (2011) 9447-9453.

[140] S. Zhou, H. Wang, J. Ping, S. Wang, L. Zhang, X. Zhu, Y. Wei, F. Wang, Z. Feng, X. Gu, S. Yang and H. Miao, Organometallics 31 (2012) 1696-1702.

[141] P. Nandi, Y. I. Matvieiev, V. I. Boyko, K. A. Durkin, V. I. Kalchenko and A. Katz, J. Catal. 284 (2011) 42-49.

[142] P. Nandi, A. Solovyov, A. Okrut and A. Katz, ACS Catal. 4 (2014) 2492-2495.

[143] P. Nandi, W. Tang, A. Okrut, X. Kong, S.-J. Hwang, M. Neurock and A. Katz, Proc. Natl. Acad. Sci. U.S.A, 110 (2013) 2484-2489.